TÉCNICO LISBOA

Technological Assessment of Commercial Ammonia Synthesis Methods in Coastal Areas of Germany

Shahmir Ali Nosherwani

Thesis to obtain the Master of Science Degree in

Energy Engineering and Management

Supervisors: Dr. Rui Pedro da Costa Neto

Prof. Carlos Augusto Santos Silva

Examination Committee

Chairperson: Prof. Susana Isabel Carvalho Relvas

Supervisor: Dr. Rui Pedro da Costa Neto

Member of the Committee: Prof. Francisco Manuel de Silva Lemos

October 2020

I declare that this document is an original work of my own authorship and that it fulfils all the requirements of the Code of Conduct and Good Practices of the *Universidade de Lisboa*

Acknowledgements

I would like to start in the name of Allah, the Most Beneficent and the Most Merciful. I would like to express my deepest gratitude for all the blessings.

I would take this opportunity to thank my supervisor, Prof. Rui Carlos Neto, for his constant and continuous support and his mentorship. Moreover, I would like to appreciate and thanks InnoEnergy in granting me admission and scholarship in this program.

Finally, a very special thanks to my parents (Dr. Waqar and Rukhsana Waqar), family, teachers, relatives and friends for their support and motivation.

Abstract

The study covers the techno economic environmental analysis of conventional ammonia synthesis via fossil fuels and green ammonia synthesis via renewable energy technology. The basis for comparison to check the economic feasibility of different ammonia plants is levelized cost of ammonia production. The conventional ammonia synthesis plant uses Steam Methane Reforming and Haber Bosch Process plants that requires natural gas as a source of hydrogen and air as a source of nitrogen. Similarly, the green ammonia plant uses water electrolysers (Alkaline/PEM electrolysers), Air Separating Unit, Water Desalination and Haber Bosch Process plants that are all powered by onshore wind farm.

It has been found out that the current cost of ammonia production using onshore wind farms is expensive than the conventional ammonia synthesis. This poses a barrier in using green ammonia synthesis methods as the product is not able to compete in the market. However, future development and decreased capital cost of water electrolyser in 2030 show that ammonia production costs will compete with conventional ammonia synthesis given that carbon tax and natural gas prices increase in the future.

Keywords

Ammonia Synthesis, SMR, HBP, Water Electrolysers, Onshore wind.

Resumo

O trabalho debruça-se sobre a análise ambiental técnico-económica da síntese convencional de amónia por meio de combustíveis fósseis e da síntese de amónia verde (eletrólise para produção do hidrogénio) por meio de tecnologia de energia renovável. A base de comparação para verificar a viabilidade económica de diferentes fábricas de amónia centra-se no o custo nivelado de produção de amónia. A fábrica de síntese de amónia convencional utiliza o processo de reformação de metano com vapor para a produção de hidrogénio no processo Haber Bosch, que requerem gás natural como fonte de hidrogénio e ar como fonte de azoto. Da mesma forma, a fábrica de amónia verde utiliza eletrolisadores de água (eletrolisadores alcalinos / PEM), unidade de separação de ar, dessalinização de água e uma fábrica com o processo Haber Bosch, todas alimentadas por parques eólicos onshore.

Foi descoberto que o custo atual de produção de amónia recorrendo a parques eólicos onshore é mais dispendioso do que a síntese de amónia convencional. Isso representa uma barreira no uso de métodos de síntese de amónia verde, pois o produto não é capaz de competir no mercado. No entanto, o desenvolvimento futuro e a redução do custo de capital do eletrolisador de água em 2030 mostram que os custos de produção de amónia competirão com a síntese de amónia convencional, visto que o imposto sobre as emissões de carbonos e os preços do gás natural aumentam no futuro.

Palavras-chave

Síntese de amónia verde, SMR, HBP, eletrolisadores de água, energia eólica onshore.

Table of Contents

List of Figures

List of Tables

List of Acronyms

ARPAE	Advanced Research Project Agency-Energy
ASU	Air Separation Unit
CEPCI	Chemical Engineering Plant Cost Index
CS	Carbon Steel
DMC	Direct Manufacturing Cost
EHBP	Electric Haber Bosch Process
EHBP-HR	Electric Haber Bosch Process with Heat Recovery Unit
EU	European Union
FC	Fuel Cells
FCI	Fixed Capital Investment
FMC	Fixed Manufacturing Cost
FOB	Free-on-Board
GE	General Expenses
GHG	Green House Gases
HBP	Haber Bosch Process
HTS	High Temperature Shift
IPCC	InterGovernmental Panel on Climate Change
LCOA	Levelized Cost of Ammonia
LCOE	Levelized Cost of Electricity
LMTD	Log Mean Temperature Difference
LTS	Low Temperature Shift
MVC	Mechanical Vapour Compression
NG	Natural Gas
PEM	Polymer Electrolyte Membrane/Proton Exchange Membrane
PSA	Pressure Swing Absorption
RES	Renewable Energy Source
SMR	Steam Methane Reforming
SMR-HR	Steam Methane Reforming with Heat Recovery Unit
SS	Stainless Steel
SSAS	Solid State Ammonia Synthesis
TDS	Total Dissolved Solids
UN	United Nations
WGS	Water Gas Shift

List of Symbols

Roman Symbols

A_{EX}	Heat Exchange Area
A_P	Surface Density of Plate-Fin Heat Exchanger
C_{BM}	Bare Module Cost
C_P	F.o.b costs
C_{GR}	Grass Root Costs
C_{OL}	Cost of Labour
C_{OM}	Cost of Manufacturing
c_p	Specific Heat Capacity
C_{RM}	Cost of Raw Material
C_{TM}	Cost of Total Module
C_{UT}	Cost of Utilities
C_{WT}	Cost of Waste Treatment
Dv	Diameter of Separator Vessel
F_{BM}	Bare Module Factor
F_M	Material Factor
F_P	Pressure Factor
F_T	Superheat Correction Factor
G	Gibbs Free Energy
K_{EQ}	Equilibrium Constant
Lh	Liquid Depth in Separator Vessel

h	Enthalpy
$\dot{m}$	Mass Flowrate
N_{OL}	Number of Operators per shift
N_{NP}	Number of Non-particulate steps
P	Pressure
Q_{in}	Heat gained
Qc	Heat produced by combusting natural gas
Q_{EX}	Heat exchanged
Qw	Heat gained by fluid in a Boiler
R	Ideal Gas Constant
T	Temperature
u_T	Settling velocity
V	Volume
W_{el}	Electric Work
W_{fl}	Fluid Work
W_{sh}	Shaft Work

Greek Symbols

ρ	Density
Δ	Change in a specific property
Γ	Specific Weight
η	Efficiency of a System

1. Introduction

1.1 Motivation

The nineteenth century industrial revolution coupled with growth of population resulted in an increase demand for nitrogen-based fertilizers. Moreover, the use of nitrogen in explosives in World War 1 and use of ammonia in buses in Belgium during World War 2 made ammonia a major topic of research in the nineteenth and twentieth century [1] [2].

In twentieth century, ammonia was produced at a very high cost because of very high energy requirements. One process was researched for ammonia production using 1000°C and atmospheric pressure but very little ammonia was produced. But as research continued, it become clear that ammonia production can be made viable by using lower temperature and higher pressures in presence of a suitable catalyst. In 1913, Haber developed a commercial ammonia plant at BASF with a capacity of 30 tonnes per day [1].

Currently, ammonia plants having capacities of producing over 3000 tons per day and ammonia is one of the commonly synthesized chemicals with a global production of 180 million tons (2017) [1] [3]. With a growth rate of around 2% annually for the last two decades, ammonia is projected to reach 360 million tons in 2030 [4]. Ammonia produced is majorly consumed by fertilizer industry. Fertilizer industry consumes around 80% of global ammonia production [5].

Moreover, approximately all of the hydrogen, required for ammonia production, is produced from fossil fuels and majorly from natural gas as shown in figure 1 [6]. The production of ammonia consumes about 1.8 – 3.0 % of global energy production and is responsible for emitting 1% of carbon emissions (around 290 mega tons) annually around the globe [2]. Natural gas release around 2.7 metric tons, while coal release 3.4 tons of greenhouse gases (GHG) for every ton of ammonia produced [7].

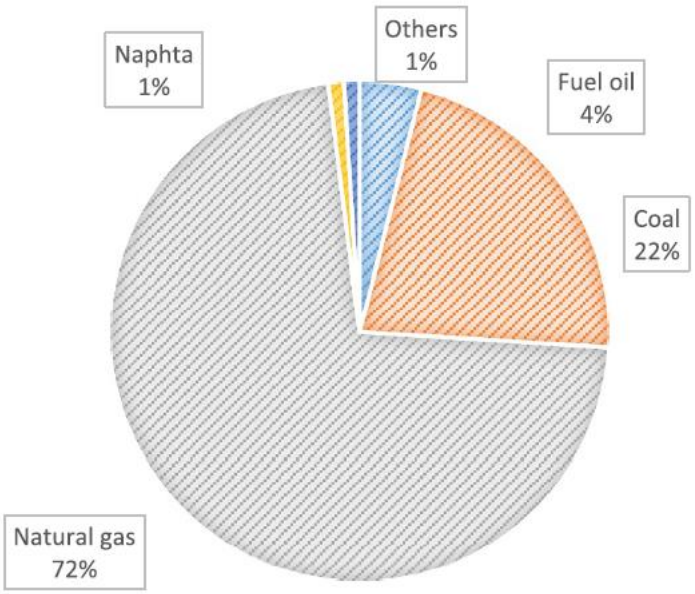

Figure 1: Raw material for hydrogen production for ammonia synthesis - 2018 [6]

The growing levels of carbon emissions, also called as greenhouse gases (GHG), has led to increase in increase global temperatures (global warming). This has been studied and proved [8]. To counter the impact of increased GHG emissions, policies like Paris Agreement 2015 and European Union policy have been formulated to decrease the dependence on fossil fuels. Moreover, the prices of natural gas are expected to increase in the future and increase in carbon tax in developed nations may disrupt the fertilizer industry in the future [9] [10]. This could also adversely impact world population.

To decrease the dependence of ammonia production on fossil fuels, ammonia industry can also incorporate renewable energy technology to provide energy for air separation, water electrolysis and ammonia synthesis loop [9]. The feasibility of using renewable energy technology for ammonia production has been studied recently by the demonstration plants in Oxford, UK and Fukushima, Japan. The former used wind energy and the latter used solar energy to obtain green hydrogen from water via electrolysis, nitrogen from air separation and to power the Haber Bosch process to make green ammonia [11] [12].

Similarly, in the last two decades several research groups have been studying electrochemical formation of ammonia using the solid-state ammonia synthesis (SSAS). The recent interest in electrochemical route is due to the prediction of having less environmental impacts, less energy requirements and more economically viability [13].

Moreover, this interest in synthesis of green ammonia can be attributed to the application of ammonia in power generation and automobiles sectors [2]. This application is currently is under study. Ammonia synthesized, using renewable energy technology, can be used as a chemical energy storage [2]. The stored ammonia can then be later used as a fuel in a gas turbine, car engine, direct ammonia fuel cell (DAFC), or cracked to form hydrogen, which can then be used in a hydrogen fuel cell [2].

Furthermore, the market for ammonia is estimated to be at $91-225 billion per year and 1% shift from fossil fuel generation to renewable energy technology is estimated to be around $1.5 billion per year globally and reducing 1.8 kg of CO_2 per ton ammonia if green electricity is used. The market of ammonia shows the profitability of the interested companies working on ammonia-related technologies [2].

Hence, this thesis will discuss the business feasibility of green ammonia production and compare it with existing ammonia production method using steam methane reforming (SMR) and Haber Bosch Process (HBP). Green ammonia will be synthesized using water electrolyser, HBP and ASU systems, which in turn are powered by onshore wind technology.

1.2 Previous Work

Morgen et. al [14] investigated, in 2014, the feasibility producing ammonia from diesel generator and wind power with a back-up diesel generator for a remote island of USA called Monhegan. The energy

produced from the wind farm was used to run cryogenic air distillation for air separation, alkaline electrolysers for electrolysis of water, mechanical vapour compression for desalination of water and Haber-Bosch synthesis loop. The levelized cost of ammonia (LCOA) was estimated to be $1224/ton of ammonia.

Similarly, Nayak-Luke et. al [15] investigated, in 2018, the feasibility of producing ammonia from solar and wind farm for a remote island of Scotland, Lerwick. A MATLAB code was developed to use the renewable energy profiles to optimize the size of alkaline electrolysers, air separation unit (ASU), HBP and hydrogen storage. A proton exchange membrane (PEM) fuel cell is used to consume hydrogen and meet any power deficit.

Using estimates from 2025 and 2030, LCOA was estimated at £588 per ton of ammonia, with a levelized cost of electricity (LCOE) at £45.7 per MWh, renewable energy mix of 90% wind and 10% solar technology, electrolyser capital at £308 per kW and ASU/HBP process minimum power is taken 20% of rated power.

Moreover, Bartels et. al [16] investigated, in 2008, ammonia production costs from natural gas, coal, nuclear, solar, wind, ocean thermal energy conversion (OTEC) and biomass. The highest cost for ammonia production is incurred while using solar energy with the estimated ammonia production costs range from $830-5951/ ton of ammonia, while ammonia production cost from wind energy range from $660–2342/ton of ammonia. Furthermore, the cheapest source was found to be coal with cost estimation in the range of $147- 432/ton of ammonia.

A similar approach is used in research and studies conducted on ammonia synthesis using renewable energy by Morgen et. al [17] , Song et. al [18], Sánchez et. al [19] and Grundt et. al [20].

1.3 Objective

The objective of this work is to study the potential of producing ammonia in a sustainable way. Techno-economic studies compares the existing SMR – HBP with alkaline electrolyser technology and PEM electrolyser technology. Using DWSIM, a steady-state chemical process simulator, ASU, SMR, and HBP are simulated for small scale ammonia (300 tons per day of ammonia) [21]. The small scale is considered in this work as the electrolysis technology is developed but scale of manufacturing is undersized when compared large scale SMR-HBP plants [22].

The economics studies use capital costs and operating costs to calculate the levelized cost of ammonia (LCOA). LCOA will be a basis to compare conventional SMR-HBP with alkaline electrolyser-HBP and PEM electrolyser-HBP. Moreover, the economics study focuses on Germany as it is one of the leading European Union (EU) countries with renewable energy generation of around 42% [23].

1.4 Thesis

The thesis work will consist of four chapters, along with this introductory chapter. Chapter 2 is a literature review of different methods existing commercially to produce hydrogen, nitrogen and ammonia. Chapter 3 is system selection, system economics and LCOA calculations. Chapter 4 includes discussion and comparison of LCOA calculated in this work with already published works. Moreover, Chapter 4 will include future work and recommendations in improving the thesis work.

2. Literature Review

2.1 Hydrogen Production

Hydrogen is one of the most abundant elements in nature but not readily available. It is usually bonded to other molecules that can be found naturally (like water or fossil fuels). There are a lot of process available to produce hydrogen but the availability of technology on commercial scale and the economics have favoured the production of hydrogen from fossil fuels [24]. The share of global hydrogen production from natural gas is 48% (through SMR), followed by heavy oils 30% and coal is 18% [24]. The remaining 4% of hydrogen is produced through water electrolysis [24].

Natural gas is converted into hydrogen using SMR process [25]. The process converts natural gas and steam into hydrogen and oxides of carbon [24]. It is a catalysed process that requires high temperatures and pressures and is discussed in detail in section 2.1.1.

Heavy oils and coal can be converted into hydrogen through partial oxidation, autothermal reforming or gasification (of coal) [24] [26]. Partial oxidation involves conversion of hydrocarbon, steam and oxygen into hydrogen and oxides of carbon [26]. The catalytic process takes place around 950°C and the non-catalytic process takes place around 1150-1310°C [24].

Autothermal reforming combines two method mentioned above [24]. The exothermic energy from partial oxidation provides energy for endothermic steam reforming. Reforming and oxidation take place simultaneously as steam or oxygen is injected into the reformer [24].

Gasification converts coal into gas at temperatures >800°C by using a gasification medium [26]. There are two gasification mediums; steam (steam-coal gasification) and hydrogen (hydrogasification). Typically, the process involves partial burning of coal by injecting air or oxygen to provide energy for autothermal reactions [26].

The splitting of water to produce hydrogen is an established method. The types of electrolyser and technology will be discussed in detail in section 2.1.2.

2.1.1 Steam Methane Reforming (SMR)

SMR process is utilized to produce hydrogen from methane and steam. The process is highly developed and mature technology in industrial sector for hydrogen production. It produces approximately 48% of the world hydrogen production [27] and 72% of hydrogen for global ammonia production [6].

In SMR, steam and natural gas are mixed in a proper ratio and fed into a reactor with a suitable catalyst. The reaction is a hi0000000000ghly endothermic reaction and reforming reactions takes place at elevated temperature (800-1000ºC) and pressure (10-30 bars). The heat of endothermic reaction is provided through external means by burning natural gas or some gaseous fuel, and product stream from SMR may contain 5-10% of unconverted methane [27] [28]. Figure 2 shows the process of SMR and

described in the sub-sections below.

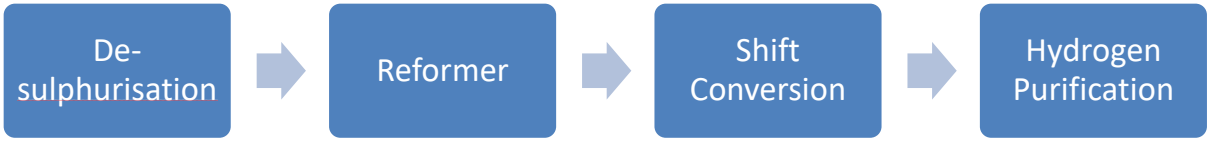

Figure 2: Block diagram of SMR process [28]

2.1.1.1 De-sulphurization

For steam methane reforming (SMR), natural gas is first de-sulphurized because of sensitivity to catalysts to sulphur containing compounds. Chlorides, halides and mercury are considered poisonous for SMR catalysts [27]. A de-sulphurization unit is utilised to remove all poisonous compounds from the natural gas. This is achieved by heating to 350 - 400ºC and passing it over a cobalt molybdenum catalyst and passed over zinc oxide. The following reactions takes place and reduce the sulphur concentration to less than 0.1 ppm [28];

$$\mathbf{R - SH + H_2 \rightarrow H_2S + RH} \qquad \textbf{(A.1)}$$

$$\mathbf{ZnO + H_2S \rightarrow H_2O + ZnS} \qquad \textbf{(A.2)}$$

2.1.1.2 Reforming Section

The purified natural gas is mixed with steam and heated to 500-600ºC and feed into a primary reformer at 25 - 40 bars. In new or revamped SMR plants, the heated mixture is first passed through an adiabatic pre-reformer at 300-525ºC. The aim of pre-reforming is to convert higher hydrocarbons to methane, carbon monoxide and hydrogen, and to avoid any coke deposition in reformers [27].

After pre-reforming, the mixture is heated to around 500ºC and fed to the reformer with nickel-containing reforming catalyst. The heat for endothermic reaction is provided by combusting a part of feed (natural gas) to raise the temperature to 700-950ºC at the reformer outlet. This stage achieves around 95% conversion of methane and contains 12 to 15% of carbon monoxide (dry gas base) [27] [28].

The production of hydrogen takes place in two sets of reactions, steam reforming and water shift, as shown below [28];

Steam reforming: $\mathbf{CH_4 + H_2O \leftrightarrow CO + 3H_2;\ \Delta H^{\circ}_{298} = 206 kJ/mol}$ **(A.3)**

Water shift reaction: $\mathbf{CO + H_2O \leftrightarrow CO_2 + H_2;\ \Delta H^{\circ}_{298} = -41 kJ/mol}$ **(A.4)**

2.1.1.3 Shift Conversion

The carbon monoxide is converted into carbon dioxide and hydrogen in shift section of the process. The reaction is exothermic and thermodynamically favoured at low temperature. The water gas shift (WGS) is taken place in two reactors in series; high temperature shift (HTS) and low temperature shift (LTS) [27] [28].

The process gas is first cooled down to around 400ºC and fed to HTS reactor. In HTS reactor, CO is conversion takes place in the presence of iron oxide/chromium oxide catalyst at approximately 400ºC. The process gases are then further cooled to around 200- 220ºC and fed to LTS. In LTS reactor, residual CO conversion takes place in the presence of copper oxide/zinc oxide - based catalyst. The process gas leaving LTS usually contains about 0.05% to 0.5% of CO [27] [28].

2.1.1.4 Hydrogen Purification

The process gas is cooled to condense the excess steam and subsequently, removing condensate from the process gas. Hydrogen purification can be achieved using pressure swing absorption (PSA) or through CO_2 scrubber – methanation [27] [28].

The conventional scrubber absorbs carbon dioxide by using a chemical solvent (amine solutions) or a physical solvent (glycol dimethylethers). Methanation is next step after CO_2 scrubber, where trace amounts of carbon dioxide and carbon monoxide are converted to methane as shown in reaction below. This is to avoid any catalytic poisoning in ammonia synthesis. The reaction takes place around 300ºC with nickel as a catalyst. Purity of hydrogen is around 97-99% with traces of methane and steam. Methane is an inert gas for ammonia synthesis loop but moisture is removed before the gases are feed to ammonia synthesis loop [27] [28].

$$\mathbf{CO + 3H_2 \rightarrow CH_4 + H_2O} \quad \textbf{(A.5)}$$

$$\mathbf{CO_2 + 4H_2 \rightarrow CH_4 + 2H_2O} \quad \textbf{(A.6)}$$

2.1.2 Electrolysis of Water

Water can be split into hydrogen at cathode and oxygen at anode electrochemically using electricity. This is an alternate route to produce high purity hydrogen other than the conventional SMR to produce hydrogen from natural gas for ammonia production as shown in figure 3 [9]. However, the production of hydrogen using water electrolysis accounts for 0.5% of global ammonia production [2].

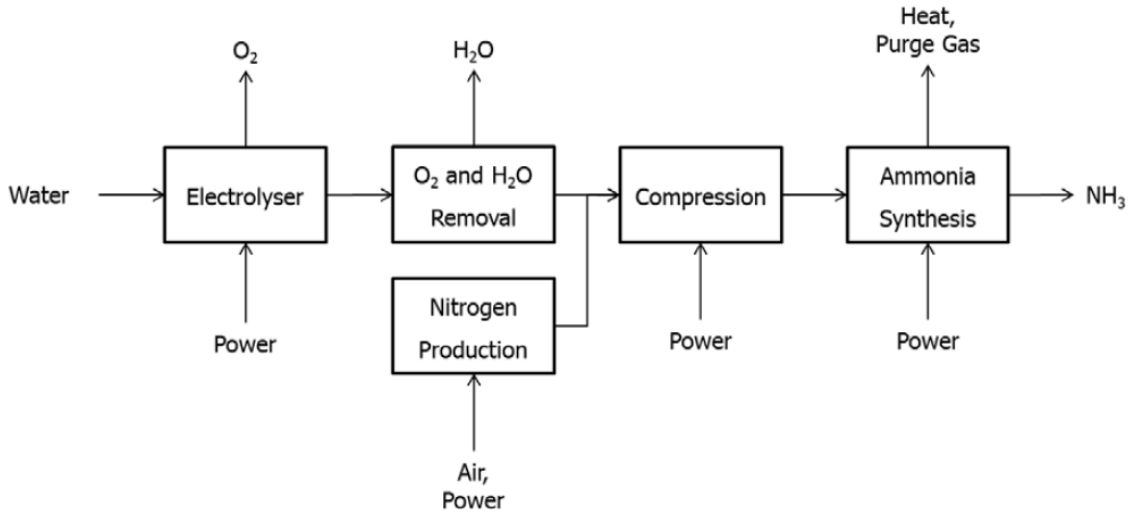

Figure 3: Synthesis of Ammonia using water electrolysis [9]

The production of hydrogen using electrolysis of water for ammonia production has been used by Norsk Hydro since 1928. [20] In the past, main plants that were using alkaline water electrolysis to produce hydrogen for ammonia were [20];

- Rjukan (Norway) – 165 MW producing 27,900 Nm^3 H_2/hour
- Glomjford (Norway) – 160 MW producing 27,100 Nm^3 H_2/hour
- Aswan (Egypt) – 100 MW producing 16,900 Nm^3 H_2/hour
- Reykjavik (Iceland) – 20 MW producing 3000 Nm^3 H_2/hour
- Cusco (Peru) – 24 MW

However, currently there no commercial plants are operational due two reasons. Firstly, the very high energy requirements to overcome the thermodynamic barrier, 39.4 kWh/kg of hydrogen (ideal), to produce hydrogen water. Secondly, the electrolysis technology is developed but scale of manufacturing is undersized when compared to commercial SMR-HBP producing 1000-1500 tonnes of ammonia per day. This can be observed in figure 4, where the slope of line 4 and line 5, representing electrolysis of water, is flat beyond 400 Nm^3/hr [29] [30].

Considering the discussion above, the water electrolysis technology coupled with HBP is not competitive for large scale ammonia production. However, the predicted increase in natural gas prices, carbon emission tax, reduction in investment cost of electrolysers and improved efficiency of electrolysers could change the future of hydrogen production [9] [29] [31].

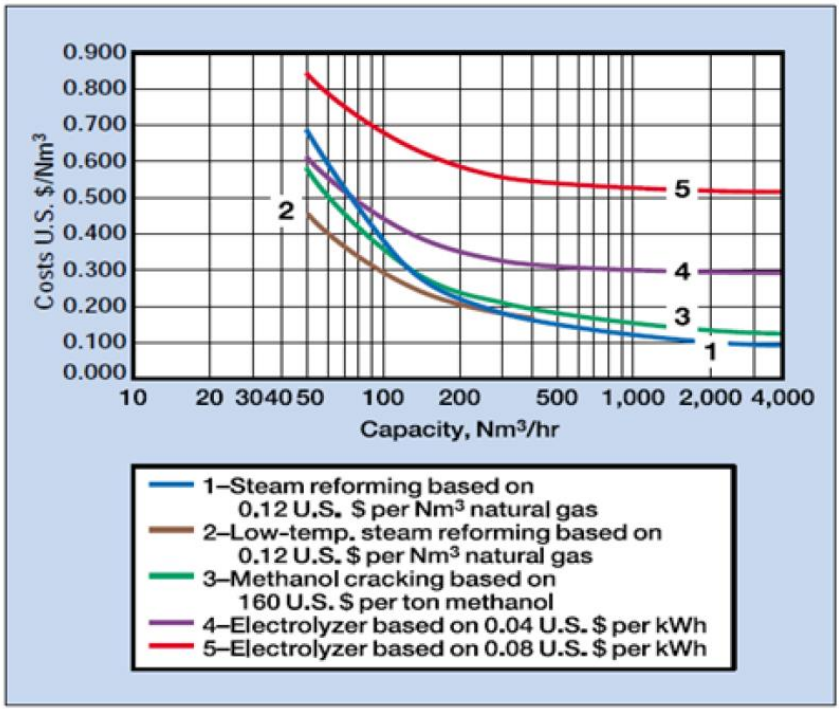

Figure 4: Hydrogen production costs for different technologies – 2000 [30]

Currently, there are three types of electrolyser available; alkaline electrolyser, solid oxide electrolyser

and PEM electrolyser. Solid oxide electrolyser are not discussed in this work because it is currently under development and have no commercial availability in the market, while both alkaline and PEM electrolyser are commercially available [32] [33]. The technical and economical specifications of commercial PEM and alkaline water electrolysis systems is shown in table 1.

The commercial low pressure alkaline electrolysers have a system efficiency between 63 – 70% as shown in table 1, this could be increased up to 80 – 85 % with developments of better electrodes and diaphragms [26]. Alkaline electrolyser operates in the range of 10% to full design capacity, with the ability to operate with high hydrogen production rate and have large stacks compared to PEM electrolyser systems [10]. Alkaline electrolyser produces high purity hydrogen, but it contains trace amounts of oxygen. Oxygen is poisonous to the catalyst in HBP and is removed using a catalytic converter. Oxygen is reacted with hydrogen to produce water, which is later removed through a drier [29]. The purity of gas and the low current density (200 - 600 mA cm^{-2}) are the main drawbacks of the technology. High levels of purity can be obtained using auxiliary purification unit [29] [26]. Furthermore, alkaline electrolysers are developed to work with intermittingly using renewable energy technology like wind or solar [26].

PEM electrolyser are considered as an alternative to alkaline electrolyser with a high current density of 1500 – 2000 mA cm^{-2} [29]. PEM systems are relatively small with a compact design and can be operated at higher pressures and higher temperature [26]. They have a wider operating range from 0 to 160% (The electrolyser can be operated in overload conditions for some time, if the plant and power electronics are designed accordingly), this offers flexibility in decentralized production and storage of hydrogen using renewable energy technology [10]. Although PEM system have an efficiency around 50%, this is compensated by reduced energy requirements for compression and no need for auxiliary purification (hydrogen produced is already 99.998% pure) [26]. When compared to alkaline electrolyser, PEM system have shorter lifetime, expensive electrode catalysts and membrane materials, and small size of stacks. These are main drawbacks of the PEM systems [10] [26].

The following subsections discuss alkaline electrolysis and PEM electrolysis processes. Both processes have an ideal thermodynamic energy requirement of 39.4 kWh/kg of hydrogen and a high purity requirement of water. A mechanical vapor compression (MVC) unit can be employed to purify water as discussed in sub-section below [29].

Table 1: Techno-economical specifications of commercial electrolysers [10] [33]

Specifications	PEM	Alkaline
Cell Temperature (ºC)	50 – 80	60 – 80
Operating Pressure (bar)	30 – 80	1 – 30
Electrical Efficiency (% LHV)	56-60	63 – 70
Stack Lifetime (Operating Hours)	30,000 - 90,000	60,000 - 90,000
Capital Expenditure (USD / kW_e)	1100 – 1800	500 – 1400
Rated power (kW)	1.8 – 174	2.8 – 3534
Rated production (N m^3h^{-1})	0.265 – 30	1 – 760
Specific energy consumption (kWh/ N m^{-3})	5.8 – 7.3	4.5 – 7.5

2.1.2.1 Alkaline Electrolysis

Alkaline technology is the most mature and commercial compared to other water electrolyser systems. It has been in use for commercial application since 1920s as discussed above making it one of the oldest technologies among other water electrolysis systems. Moreover, it is economical to manufacture compared to other water electrolysers as the electrodes are made from simple iron or nickel steel electrodes, that are abundant and are inexpensive [10] [34].

The alkaline electrolysis process has an anode and a cathode compartment immersed in 20-40 % alkaline solution, like NaOH or KOH as shown in figure 5 [26]. The anode and cathode compartments are separated by membrane to aid in transporting positive or negative ions across it. Electric energy splits the water in hydrogen at cathode and oxygen at anode in a stoichiometric ratio of 2:1 as shown in the reactions below [27] [29]. Hydrogen gas produced is purified before feeding it to HBP. Depending on the type of auxiliary purification technology, hydrogen gas purity ranges between 99.9-99.9998%, while oxygen purity is in the range of 99.2-99.993% [26].

Anode: $$2OH^- \rightarrow 1/2O_2 + H_2O + 2e^- \quad \textbf{(A.7)}$$

Cathode: $$2H^+ + 2e^- \rightarrow H_2 \quad \textbf{(A.8)}$$

Overall: $$H_2O \rightarrow 1/2O_2 + H_2 \quad \textbf{(A.9)}$$

The operating temperatures are less than 150ºC with an ideal thermodynamic energy of 39.4 kWh/kg of hydrogen and with an ideal cell potential of 1.229 V at 25ºC [29] [26]. However, To maintain the operating temperature of alkaline electrolyser and to account for irreversible processes in the reaction mechanism, that is gas expansion at electrodes, the typical cell voltages ranges from 1.85V to 2.05V corresponding to electrical energy requirement of 4-4.5 kWh/Nm^3 of hydrogen with a efficiency of around 80% [26]. Moreover, the electrolyser operates using DC current, so the overall energy efficiency should consider the efficiency of the transformer (commonly taken as 95%) [29].

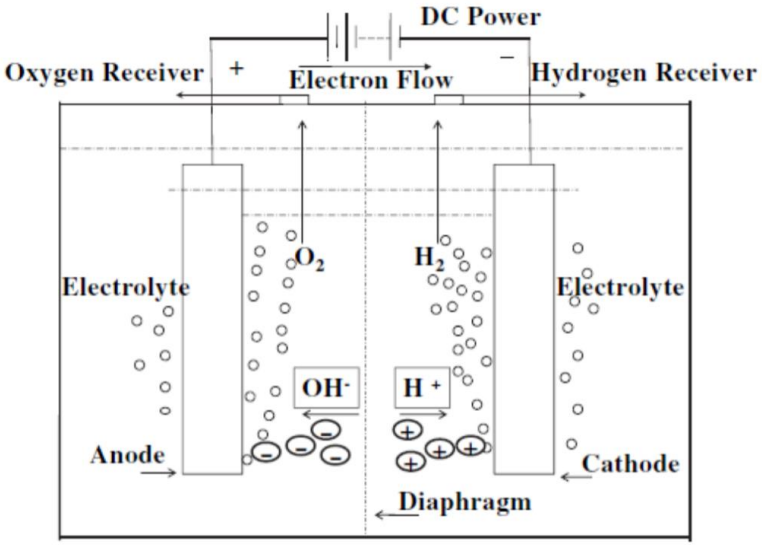

Figure 5: Schematic view of water electrolysis using an alkaline electrolyte cell [35]

2.1.2.2 PEM Electrolysis

The development of PEM electrolyser dates to 1950s, when membranes were developed by the US space program for PEM fuel cells [26]. However, the first PEM electrolyser were introduced by General Electric in 1960s to overcome operation difficulties associated with the operation of alkaline electrolysers [10]. PEM electrolyser uses a solid polymer electrolyte membrane or proton exchange membrane as show in figure 6. The electrolyte is made of a thin (20-300 micro-meter thick) solid ion-conducting membrane (usually Nafion) [29] [33]. This membrane system doesn't require additional electrolyte like potassium hydroxide nor it requires the recovery and recycling of electrolyte like in alkaline electrolyser [10] [26].

PEM electrolyser system operates at 30 bars, has an anode and a cathode compartment immersed in deionized water [29]. The anode and cathode compartments are separated by membrane to aid in transferring proton from anode side to cathode side [33]. Electric energy splits the water in hydrogen at cathode and oxygen at anode in a stoichiometric ratio of 2:1 as shown in the reactions below [36]. Moreover, this membrane separates hydrogen and oxygen gas limiting crossover of gases [33] [36]. Thus, high purity of gases is obtained as discussed above and requiring no further purification of gases.

Anode: $$\mathbf{H_2O \rightarrow 1/2O_2 + 2H^+ + 2e^-}$$ **(A.10)**

Cathode: $$\mathbf{2H^+ + 2e^- \rightarrow H_2}$$ **(A.11)**

Overall: $$\mathbf{H_2O \rightarrow 1/2O_2 + H_2}$$ **(A.12)**

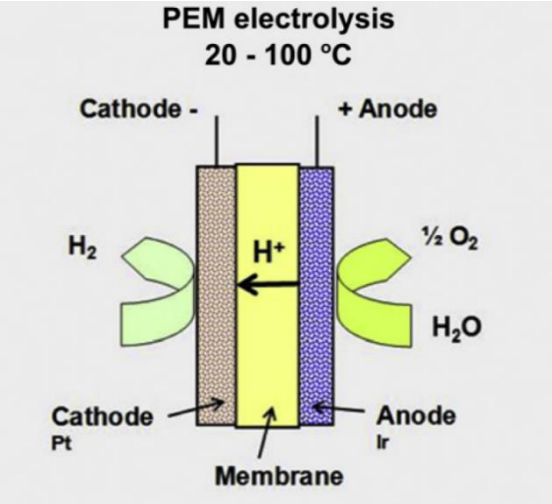

Figure 6: Schematic view of water electrolysis using a PEM electrolyte cell - edited [36]

2.1.2.3 Mechanical Vapor Compression

The water must be purified and desalinated before feeding to alkaline electrolyser or PEM electrolyser. The high-water purity or total dissolved solids (TDS) requirements for alkaline electrolyser is less than 10ppm and for PEM electrolyser, it is less than 0.5 ppm [17] [37]. While the electrolyser units have a water purification section (reverse osmosis modules), they are not designed for desalination.

Sea water has a TDS range of 10,000-45,000 ppm with an average TDS of 35,0000. Considering the TDS of sea water, operation on electric energy only and for medium scale units, a single effect mechanical vapor compression (MVC) desalination is the considered attractive as per studies conducted by Morgen et.al [17] and Alcantara et.al [29]. MVC system is compact, does not require external heating and operates on electricity. The output water has a ppm limit of less than 20 [17] and less than 10 ppm [38].

MVC system as shown in figure 7 has 5 major components, namely; compressor, evaporator, preheaters, brine and product pumps (not shown in figure 7) [39]. The seawater is fed in the evaporator and sprayed on the horizontal tubes forming a film. The thin film over the tubes increases the surface area, enhancing the heat transfer and making evaporation process efficient. The vapours, formed in the evaporator section, are transferred to the compressor through a vapor suction tube. The vapor suction tube has a mist eliminator to avoid carry-over of brine and water droplets in vapor stream, which could damage the compressor rotor blades. The vapor is pressurized and is superheated in compressor unit. The vapours are passed inside the horizontal tubes of evaporator, where condensation takes place and latent heat is transferred to the brine film [39].

Since product stream and rejected brine stream are at a higher temperature, the feed seawater is heated in MVC by exchanging heat between the product stream and rejected brine stream in Distillate Feed Preheater, and by exchanging heat between the rejected brine stream and seawater feed in Brine Feed Preheater [39].

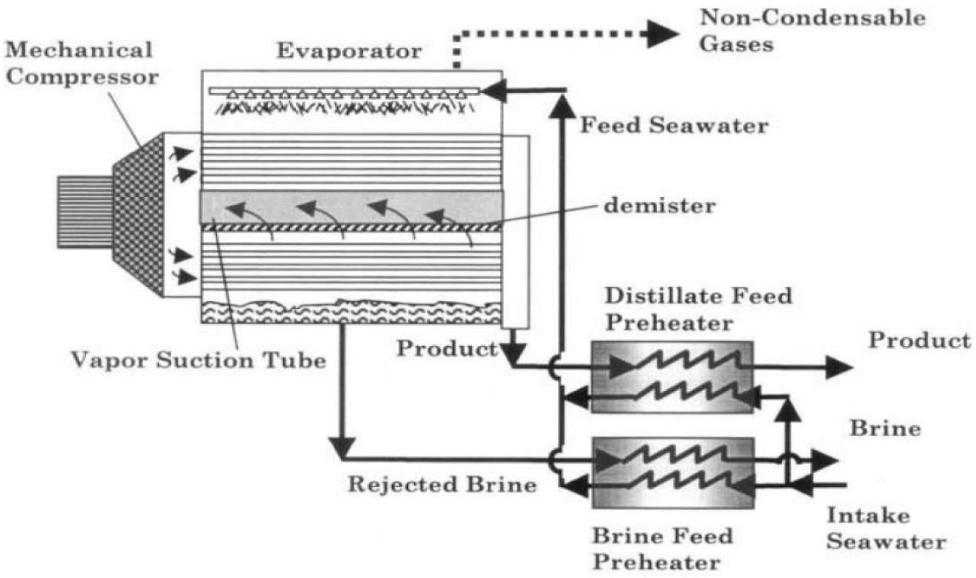

Figure 7: Schematic view of a mechanical vapor compression unit – edited [39]

MVC is operated entirely using electric power making it suitable for remote population that has access to electric power. Other advantages include; [39]

- Simple operation and compact system
- Moderate investment cost
- Proven commercial viability for small and medium scale system
- Less problems associated with scaling and minimum thermal insulation requirement as the operation takes place at a low temperature of 60°C.
- High water purity can be achieved.

2.2 Nitrogen Production

The air is composed majorly from nitrogen, oxygen and argon as shown in table 2. They have a wide variety of applications in steel, chemical, semiconductor, aeronautical, medical, food and refining industries. Nitrogen exists as a diatomic gas molecule at standard temperature and pressure (STP) which is used in industries as a flame-retarder and as a preservative [17] [40].

To obtain these valuable fractions especially nitrogen, air can be separated using cryogenic distillation, pressure swing absorption (PSA) or membrane separation technique [17] [40]. The process of cryogenic air distillation will be discussed in section 2.2.1, while PSA and membrane separation technique will be

briefly discussed in this section.

Table 2: Composition of air [40]

Component	Chemical Symbol	Volume (%)
Nitrogen	N_2	78.1
Oxygen	O_2	20.95
Argon	Ar	0.93
Carbon Dioxide	CO_2	0.033
Rare Gases	-	0.002

PSA, as shown in figure 8, is a simple separating technique in which air is passed through an absorber bed (carbon molecular sieve) in horizontal or vertical cylindrical vessel at a high pressure (5-12 bar) and then desorbed at a lower pressure (atmospheric pressure) [41] [42] [43]. The binding force for nitrogen and oxygen with Carbon molecular sieve (CMS) is not significant however the pores and cavities in CMS allows faster diffusion of oxygen than nitrogen [43]. This allows oxygen to be absorbed by CMS absorber bed and the process in accelerated with increased pressure during the absorbing phase [17] [41]. The nitrogen is separated in the absorption phase which lasts 40-60s, after which the system is depressurized and opened to atmosphere [43]. During depressurizing stage, oxygen and waste gases are released, and the system is prepared for the next cycle. Each cycle takes approximately 1 minute [41]. Moreover, there are two absorbing beds as shown in figure 8, this is to minimize any fluctuations in the flow [41].

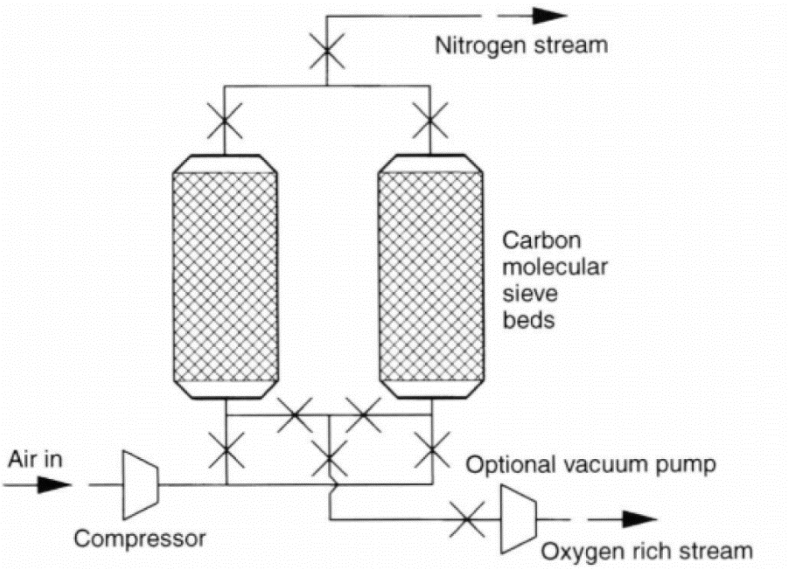

Figure 8: Schematic view of a two bed PSA air separator for Nitrogen [42]

Membrane separation technique involves compressing the air to 6-15 bars and heated (to avoid water condensation) before introducing the air in the hollow membrane [41] [43]. The principle working of this technology is absorbing of gases in air on high pressure side, diffusion through the membrane to low pressure side and desorbing on the low pressure side [41] [43]. The gases in air behave differently when passing through this non-porous hollow membrane and this ability is called permeability [17] [41].

Oxygen, carbon dioxide and water vapor are more permeable through the membrane, leaving nitrogen with traces of oxygen and argon as a retentate on high pressure side [41] [43]. A membrane separation system, as shown in figure 9, has a pre-treatment skid and a group of membrane modules with a life expectancy of 5-10 years [41].

These three methods for air separation are discussed in table 3 in terms of production capacity and gas purity for nitrogen. The purity of nitrogen for membrane separation system is less than required for HBP as shown in table [41] [43], so in order to achieve higher levels of purity a downstream catalytic deoxygenation system is required making the membrane system less economical and high energy intensive [17] [41] [43].

Meanwhile, PSA can achieve high levels of purity, as shown in table 3, for a small nitrogen output. This makes PSA viable for a micro-scale ammonia plant [17].However, if the nitrogen production volume is increased, the purity of nitrogen decreases (a 30% increase in production capacity, increases the oxygen content in the product from 0.5-2%) [17] [41] [43]. This problem of impurity can be countered by using a catalytic deoxygenation system, but this makes PSA less economical with high energy requirements [17].

Moreover, PSA and membrane system techniques are modular systems that will achieve no economies of scale and loss of space to fulfil the volume and purity requirement of medium and large scale ammonia plants [17]. This makes both techniques not suitable for medium and large scale

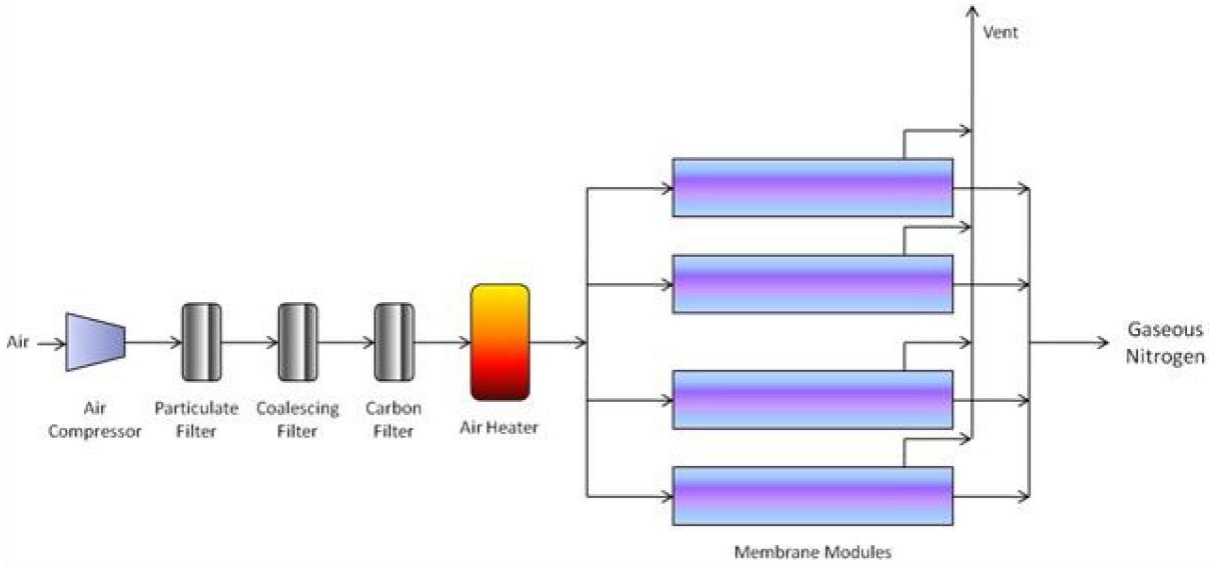

Figure 9: Schematic view of a membrane separation system for Nitrogen [17]

Table 3: Application range of air separation techniques for nitrogen [43]

Method	Typical Purity (%)	Production Capacity (m_n^3/hr)	Load Range (%)
Membrane	<99.5	1-1000	30-100
PSA	<99.99	5-5000	30-100
Cryogenic distillation	Residual concentrations are in ppb range	200-400000	60-100

ammonia production [17]. On the other hand, cryogenic air distillation is a low-cost technology that delivers high purity nitrogen and high volume of nitrogen output. Moreover, it has lower energy requirements as it operates on low pressures, this makes it a highly attractive technology for medium to large scale ammonia plants [17] [41] [43]. The technology is a commercial success as cryogenic distillation accounts for 90% commercial nitrogen production, while the remainder is supplied through either PSA or membrane separation techniques [41].

2.2.1 Cryogenic Air Separation

Cryogenic air distillation separates the air into different gases by exploiting the difference in liquefaction temperatures of nitrogen (77.4 K), oxygen (90.2 K) and argon (87.3K) [43]. Although the process is complex and with numerous fluid flow as shown in figure 10, this process can supply high purity nitrogen, oxygen and argon with high product output [17] [41] [43]. Although the principle of cryogenic air separation is the same, the process has a lot of variation [43]. The process typically uses two or three distillation columns separate the gases in the air [29]. The second and third column are required for argon purification and will incur extra costs [29].

The plant has of a cold section and a warm section [43]. The warm section consists of compression, pre-cooling, drying and purification processes; while the cold section consists of heat exchanger and distillation columns [43]. All equipment in cold section or cryogenic equipment are housed inside a “coldbox”. This is to reduce cold losses by having container like steel structure filled with insulating material [43].

The ambient air is first fed to a mechanical filter to remove dust particles and then, compressed to about 6 bars using an intercooled staged compressor [40] [43] [44]. The compressed air is pre-cooled with chilled water (between 5°C -20°C) in a direct contact cooler [40] [43] [44]. This results in reduction of the moisture content of the compressed air. The chilled water is supplied by an evaporative cooler, where it exchanges heat with residual nitrogen-rich gas from the separation [40] [43] [44]. The cold and compressed air is finally fed into molecular sieve absorber, that is periodically loaded/regenerated, of

warm section [40] [43] [44]. This results in removal of remaining water content, carbon dioxide and dilute amounts of numerous hydrocarbons before feeding into cold section of cryogenic air distillation [43] [44].

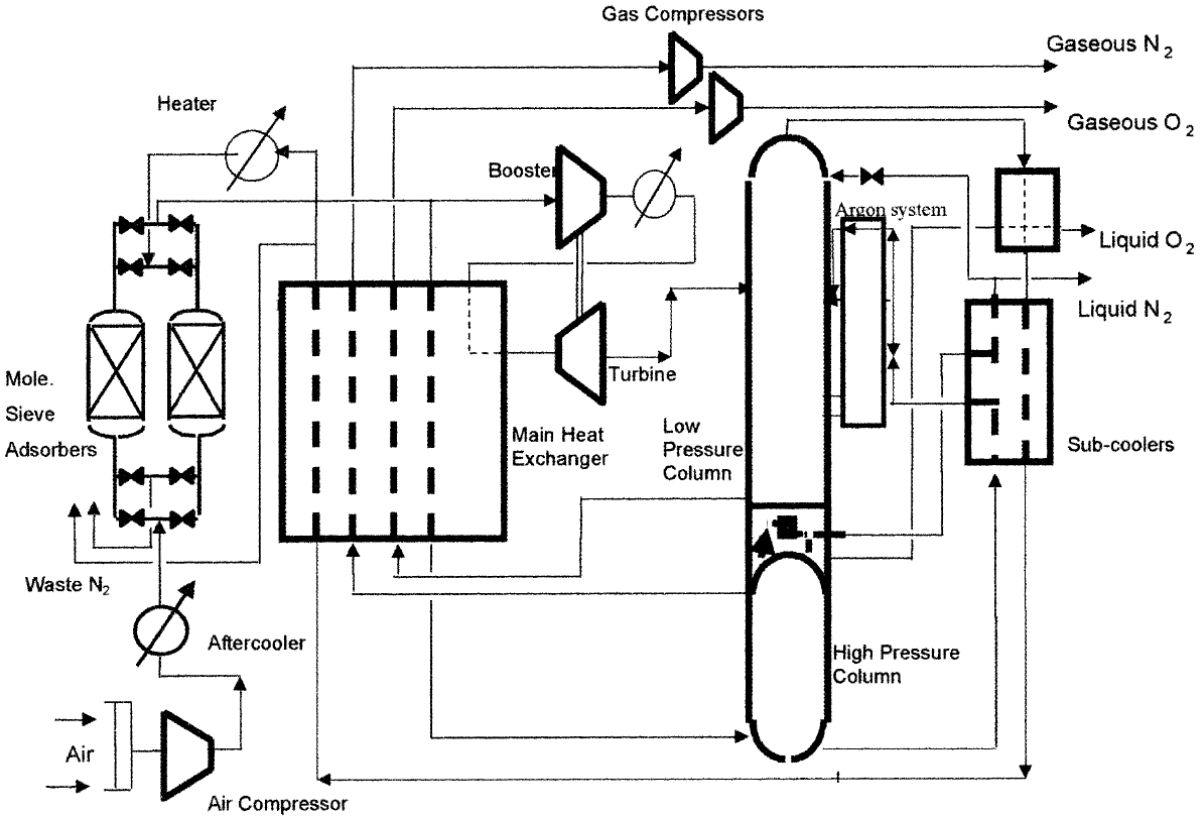

Figure 10: Schematic of a simplified flowsheet of cryogenic air separation plant [45]

The cold air is further cooled to approximately liquefaction temperature in heat exchangers. The heat is exchanged from gas and liquid streams from the rectification process to incoming air. A fraction of the air is expanded in the turbine/throttling system to account for any thermal irreversibility in the process. The air is subsequently fed to high pressure column (pressure is between 5-6 bars) where nitrogen collects at the top while oxygen at the bottom due to difference in the volatilities of the components. Nitrogen, from high pressure column, is condensed and cooled by liquid oxygen sump from low pressure column in a combined condenser-evaporator. A fraction of the liquid nitrogen is used as a reflux for high pressure column and the rest is expanded and fed as reflux onto to the top of low pressure column. Moreover, the gases are separated further in low pressure column with typical pressure between 1.3-1.5 bars [43] [44].

The impure liquid oxygen is then fed to crude argon column. In this column, oxygen is removed from the bottom of the column and fed back to low pressure column, while argon, with nitrogen impurities, is taken from the top and fed into pure argon column [40] [43] [44]. In pure argon column, nitrogen is released into the atmosphere along with small quantities of waste gases from the top, while pure argon is collected at the bottom [40] [43] [44]. The liquified rich oxygen mixture from high pressure column sump is expanded and evaporated in condenser-evaporator of both crude argon and pure argon columns [43]. This ensures necessary cooling for the reflux of these columns. Similarly, the liquified rich

oxygen mixture from high pressure column sump is used to provide heat for the sump of pure argon column [43].

2.3 Ammonia Production

Ammonia is among the most common synthesized chemical, with a global production of 180 million tonnes (2017). The global ammonia production is increasing by 2% annually for the last two decades and it is projected to reach 360 million tonnes in 2030. The favourable chemical and physical properties of ammonia, along with its ease of storage in tanks (liquefies by compressing it to 0.8 MPa at atmospheric temperature or by lowering the temperature to -33°C at atmospheric pressure) makes it viable in wide variety of application [2] [5].

Ammonia is a vital raw material for fertilizer and agriculture industry, it is consumed around 80 % from total ammonia consumption in 2016 as shown in figure 11 [5]. The consumption by weight of ammonia in fertilizer industry was 143 million tonnes in 2017 [3]. Apart from fertilizer synthesis, ammonia is used to manufacture nitric acid, which is post processed to make explosives, fibres, plastics, dyes, pharmaceutical drugs and ammonium nitrate [5]. The other commercial uses of ammonia also include the production of chemicals for SCR systems, refrigeration units, wastewater treatment, metal treatment, leather, rubber, paper, household cleaning, food and beverage industries [46] [47].

The pathways for production of ammonia that are discussed in this thesis are depicted in figure 12 and compared in table 3. The systems/processes include HBP (section 2.3.1), solid state ammonia synthesis (section 2.3.2), air separation units (section 2.2), SMR (section 2.1.1) and electrolysis of water (section 2.1.2).

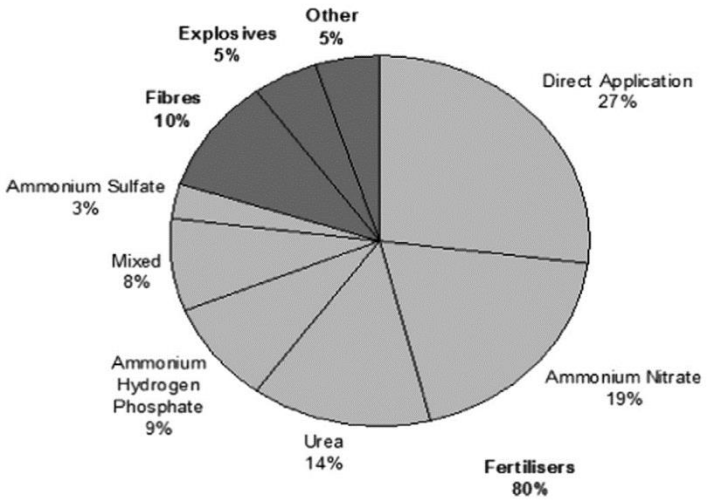

Figure 11: Applications of ammonia, by percentage [5]

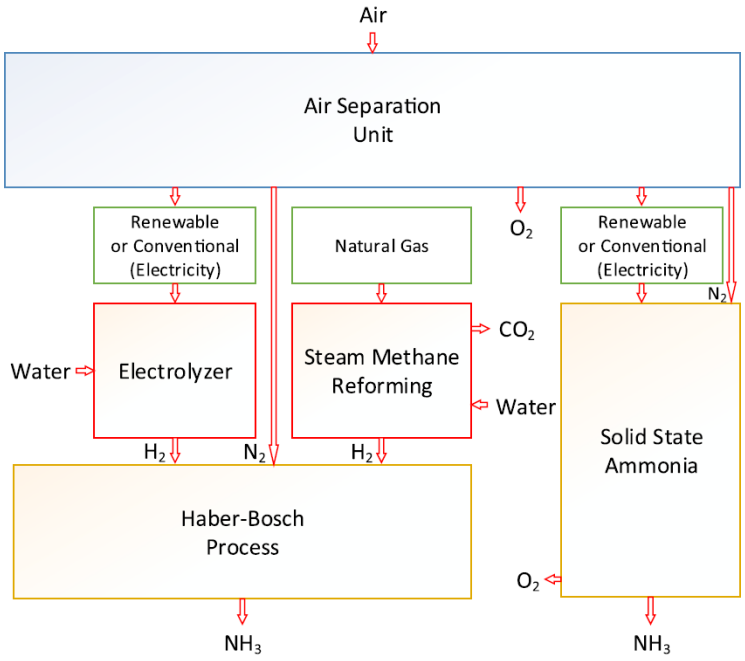

Figure 12: Ammonia production routes from conventional or renewable energy sources [6]

Table 4: Comparison of ammonia synthesis technologies [13] [47] [16] [48]

Production method	**Energy consumption (kWh/ton NH3)**	**CO2 (kg/kg NH3)**	**Efficiency**
SMR + Haber-Bosch	9,500	1.7-2.1	61-66%
Water Electrolysis + Haber-Bosch	12,000	-	Approx. 54 %
SSAS	7,000 – 8,000	-	65-70 %

2.3.1 Haber Bosch Process

HBP is the most common and commercial process for ammonia synthesis. Most of the ammonia is produced globally by utilization of HBP on an industrial scale. Figure 13 below shows a schematic diagram of ammonia synthesis via HBP. Although the HBP may have different configurations in every industry, the basic process flow and features are the same and well established. It involves compressors, a reactor, a flash drum and a network of heat exchangers [29].

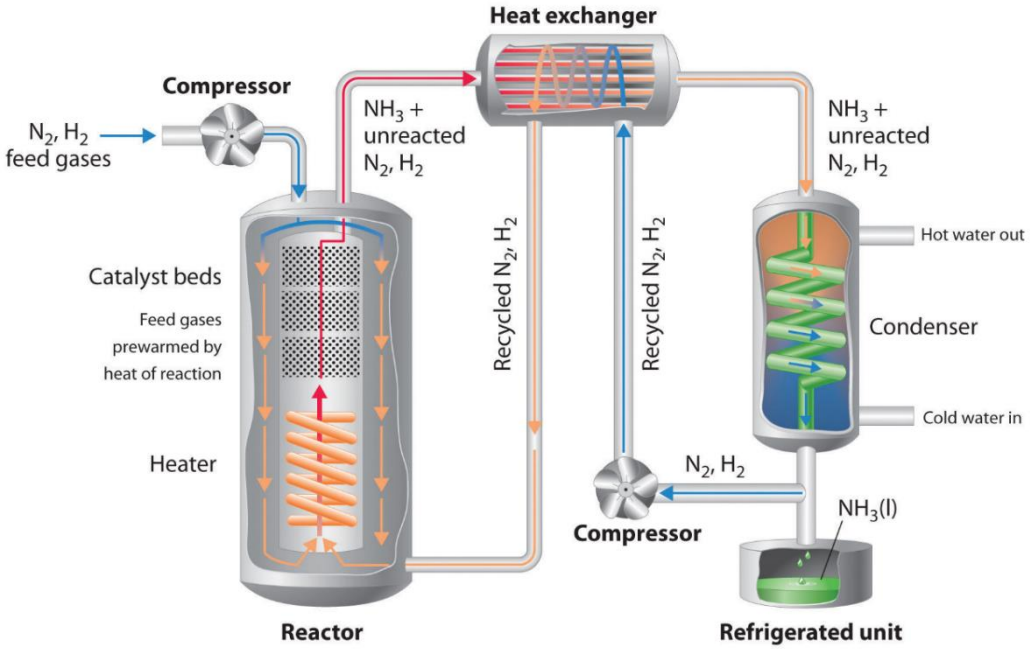

Figure 13: Simplified HBP loop for ammonia synthesis [49]

The feed gases, with a purity of 99.99% for both nitrogen and hydrogen, are compressed to the required pressure using intercooled staged compressors. The feed gases are heated to a required temperature and fed to catalyst beds, where nitrogen and hydrogen are reacted to form ammonia. The gases are then transferred to a condenser, where ammonia is separated from unreacted nitrogen and hydrogen. The unreacted hydrogen and nitrogen are compressed and recycled into the main feed stream. Moreover, to avoid the build-up of inert gases and having an adverse impact on efficiency, the gases are purged periodically [17] [29].

The synthesis of ammonia is an exothermic reaction (-92 kJ/mol) involves mixing of hydrogen and nitrogen in a ratio of 3:1 as shown in the equation below. Additionally, the process includes iron-based catalyst with temperature and pressure ranging from 450–600 °C and 100–250 bar, respectively. The high operating parameters are a trade-off between the Le Chatelier's principle and the fast reaction rates. This converts 20-30 % of hydrogen into the final product, so in order to increase the yield to 98 % a recycle loop is used [6] [9].

$$\mathbf{3H_2 + N_2 \leftrightarrow 2NH_3} \qquad \textbf{(A.13)}$$

2.3.2 Solid State Synthesis of Ammonia

Electrochemical ammonia synthesis is relatively new process to ammonia directly through electrolytic cells [13]. It is alternative to HBP that combines nitrogen, from air, with hydrogen or any hydrogen-containing compound (like water) in an electrolytic cell [50]. Using of water as a hydrogen carrier, if commercial success is achieved, will save capital costs, energy consumption and reduce carbon footprint to produce hydrogen for ammonia synthesis [29]. However, this process is currently under

research and development and there is no commercial system available in the market [50].

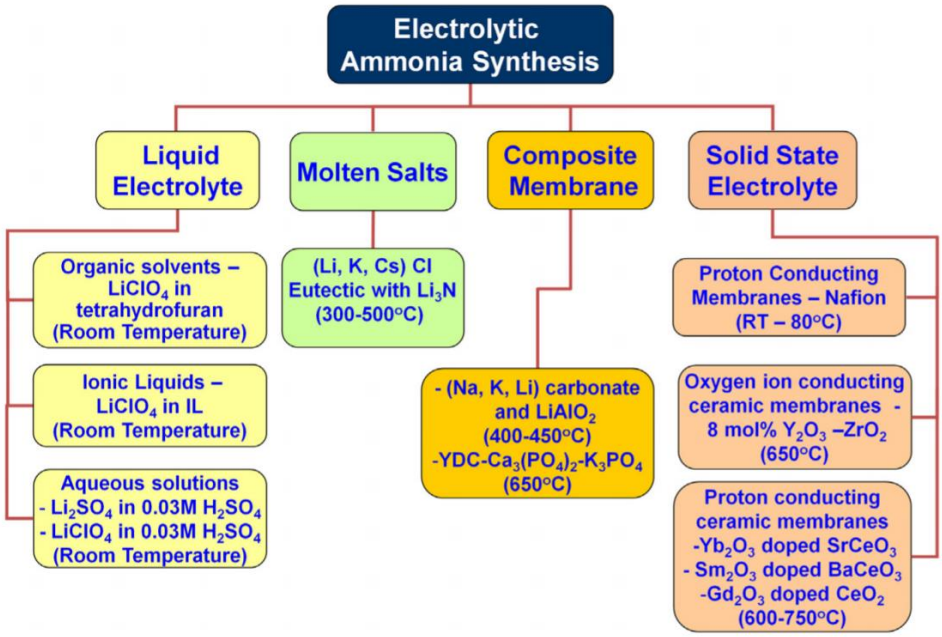

Figure 14: Electrolytes for ammonia synthesis [13]

Currently, there are different types of electrolytes, that are categorized by Giddey et. al, as shown in figure 14 that can be used for electrochemical synthesis of ammonia [13]. Solid state electrolyte systems or SSAS can be further divided, by Kyriakou et. al [50], into high temperature (greater than 500°C), intermediate temperature (between 100°C and 500°C), and low temperature (less than 100°C) systems. For high temperature systems, the highest ammonia synthesis rate reported is 9.5 x 10^{-9} mol s^{-1} cm^{-2} at 500°C. Similarly, for low temperature systems, the highest ammonia synthesis rate reported is 1.13 x 10^{-8} mol s^{-1} cm^{-2} at 80°C [50]. However, the required ammonia production rate is in the range of 4.3-8.7 x 10^{-7} mol s^{-1} cm^{-2} for electrochemical systems to be commercially viable [13]. Thus, the current research data is still 1 to 2 orders of magnitude too low [50]. The devices, operating on low temperature and pressure, can save capital costs, energy costs and material costs compared to conventional HBP in the future [29].

2.4 Wind Energy - Onshore

The onshore wind turbine dates back to 1888 in Cleveland, Ohio. Charles Bush developed a multi-bladed rotated that was 17m in diameter. The wind turbine drove a 12-kW dynamo which was connected to a battery bank. The battery bank was used to feed different motors and lights around his house. The development, research and investment over the years have tested different turbine designs and configuration including two-bladed rotors and vertical axis designs. However, the recent designs of large

turbines are dictated by three-bladed, horizontal axis wind turbine with typical heights more than 80m (utility scale). This upwind wind turbine is supported by a housing called nacelle. The housing contains the controlling mechanism, gear box and electrical generator [51].

The wind turbine simply operates by converting kinetic energy of the wind into mechanical energy by rotating the turbine blades [52]. The rotating blades drive the main shaft within nacelle. This shaft is connected to a gearbox which is connected to a generator, hence converting wind energy to electric energy [53]. The yaw control within the turbine helps in orienting the wind turbine in the direction of winds, while the pitch control optimise energy capture by changes the angle of the blades [52]. The collection of wind turbine on land are called onshore wind farms, while the turbines in sea or oceans are called offshore wind farms [54]. A typical wind turbine starts generating electricity when wind speed reaches around 6-9 mph (cut-in speed) and will shut down if the wind is blowing too strong (cut-off speed) to save wind turbine from any damage [52].

Onshore wind energy technology is considered fully developed and commercially available renewable energy technology [55]. It is economically attractive, clean and readily available (depending upon location) [56]. Onshore wind energy has following advantages;

- Relatively cheap and cost effective in many regions. In UK, LCOE for onshore wind costs around 7-9 p/kWh, which is cheaper when compared to offshore wind technology and nuclear technology [53] [54] [57].
- Relatively clean energy technology that does not contribute to GHG emissions. Some GHG emissions (approximately 9 gCO_2/kWh) are involved in the process of manufacturing, transporting and installation of wind turbines, while gas generators emit 450 gCO_2/kWh and coal power plants emit 1,050 gCO_2/kWh. As per ADEME (the French Agency for the Environment and Energy Management) in 2017, each kWh of energy produced from wind farm results in avoiding 500-600 grams of carbon emissions. Moreover, it has been estimated that, by 2020, onshore wind technology can prevent 975 million of carbon emissions annually [54] [56] [58].
- Readily available as it takes less than a year to be constructed and start operating. This results in faster return on investment [59].
- It has smaller footprints by less than 1% where they are erected. Hence, farming and other activities can take place simultaneously with power generation [59].

However, the disadvantages include;

- Production of onshore wind energy is intermittent. This leads to power production when the wind is blowing at certain speeds, so in order to produce power as per demand, a fossil fuel plant is needed as a back-up [54].
- Onshore wind farms have been criticised for its visual impact. Although other power plants have a similar impact, wind farms occupy a larger area as wind turbines are more spread out [54].
- The rotating blades can result in a bird/bat fatality. However, the number of accidents is

very low. Moreover, the risk can be mitigated by carefully selecting a site [54].

Considering the advantages of the onshore wind technology, the demand for onshore wind increased over the years as the installed capacity has increased from 148 GW in 2009 to 540 GW in 2018 [60]. Onshore wind was supplying approximately 4% of global electric production, and it is predicated to provide around 19.6-26.9% of global electricity with a reduction in GHG emissions by 47-147 gigatons by 2050 [59]. This could be attributed to the potential of power production of wind is around 20,000-50,000 TWh/yr [55].

3. System Selection and Economics

3.1 Cost Estimation Methods

The equipment cost estimation methods are based on Morgan et. al [17], Turton el. al [61] and Feng et. al [62]. The approach is module costing technique which is used for making preliminary cost estimated for new chemical plants. The purchase cost of equipment is evaluated using for some base conditions (carbon steel equipment operating at ambient pressure). However, the cost of equipment is adjusted by multiplying factors if the equipment working at different conditions, other than base conditions. This usually depends upon the specific type of equipment, pressure and material of the equipment. Module costing technique will be applied for SMR, HBP and cryogenic ASU.

Note: Prices calculated in this thesis are in US dollars ($).

3.1.1 Capital Cost Estimation

The capital costs include direct costs, indirect costs, contingency costs and auxiliary costs. The direct costs is comprised of equipment free-on-board (f.o.b) cost (the cost of equipment at manufacturer's site), cost of materials for installing the equipment (this includes piping, fireproofing, support, electrical and painting work associated with equipment) and labour cost for installing the equipment. The indirect costs includes the transportation costs (this includes freight charges, insurance costs and taxes), construction overhead costs (this includes all fringe benefits for supervisory personnel) and contractor engineering expenses (this includes costs for managing the project) [61].

3.1.1.1 Free-on-board Costs

The cost of equipment at manufacturer's site or f.o.b costs, operating at ambient pressure and made from carbon steel, can be calculated using equation 1.

$$\mathbf{log_{10}C_P^{\circ} = K_1 + K_2 log_{10}(A) + [K_3 log_{10}(A)]^2} \qquad \textbf{(1)}$$

Where A is capacity or size of equipment to be purchased and K1, K2 and K3 are equipment specific constants mention in table 5.

The prices mentioned in [61] are from 2001 in US dollars, so inflation must be taken into account in order to accurately depict these prices in present time. Chemical Engineering Plant Cost Index (CEPCI) is used in this work to account for inflation as previously done by Morgan et. al [17], Turton el. al [61] and Feng et. al [62].

CEPCI index in 2001 was 397, while in 2019 it was 607.5 [63]. Equation 2 can used to convert prices from 2001 to 2019, where C_1 represents the purchase cost in 2001, C_2 represents the purchase cost in 2019, I_1 represents CEPCI index in 2001 and I_2 represents CEPCI index in 2019.

$$\mathbf{C_2 = C_1 \left[\frac{I_2}{I_1}\right]} \quad \textbf{(2)}$$

Table 5: Cost parameter of equipment used in this work [61]

Equipment Type	K1	K2	K3	Capacity, Units	Minimum Size	Maximum Size
Heat Exchanger (shell in tube)	4.8306	-0.8509	0.3187	Area, m^2	10	1000
Compressor	2.2987	1.36040	-0.1027	Fluid Power, kW	450	3000
Enclosed Electric Drive	1.956	1.7142	-0.2282	Shaft Power, kW	75	2600
Reactor	3.4974	0.4485	0.1074	Volume, m^3	0.3	520
Demister Pad	3.2353	0.4838	0.3434	Area, m^2	0.7	10.5
Furnace	7.3488	-1.166	0.2028	Duty, kW	1000	100000
Pump (centrifugal)	3.3892	0.0536	0.1538	Shaft Power, kW	1	300
Tower	3.4972	0.4485	0.1074	Volume, m^3	0.3	520
Tank (fixed roof)	4.8509	-0.3973	0.1445	Volume, m^3	90	30000
Trays (sieve)	2.9949	0.4465	0.3961	Area, m^2	0.07	12.3
Steam Boiler	6.9617	-1.48	0.3161	Duty, kW	1200	9400

3.1.1.2 Pressure Cost Factor

The operation of equipment above ambient pressure increases the risk of equipment failure. To avoid that, the equipment undergoes various mechanical design procedures. To accommodate the increase in the cost of equipment due to increase in operating pressure, pressure cost factor (F_P) is calculated. For equipment, other than pressurized vessels, equation 3 can used to calculate the F_P.

$$\log_{10}F_P = C_1 + C_2\log_{10}(P) + [C_3\log_{10}(P)]^2 \quad (3)$$

Where, P is the design pressure in bar gauge (barg), and C1, C2 and C3 are equipment specific constants shown in table 6. It should be noted that some equipment doesn't have pressure ratings and have values of C1, C2 and C3 equal to zero.

Table 6: Pressure cost factor of equipment used in this work [61]

Equipment Type	C1	C2	C3	Pressure Range (barg)
Heat Exchanger (shell in tube)	0	0	0	P<5
	0.03881	-0.11272	0.08183	P>5
Compressor	0	0	0	-
Enclosed Electric Drive	0	0	0	-
Tank	0	0	0	P<0.07
Furnace	0	0	0	P<10
	0.1405	-0.2698	0.1293	10<P<200
Tray (sieve)	0	0	0	-
Steam Boiler	0	0	0	P<20
	2.594072	-4.23476	1.72204	20<P<40

For cylindrical pressure vessels operating above ambient pressure, the F_P can be calculated using equation 4.

$$F_{P,vessel} = \frac{\frac{(P+1)D}{2(850-0.6(P+1))}+CA}{t_{min}} \quad (4)$$

Where, t is wall thickness in metres (m) taken as 0.0063m, P is the design pressure in bar gauge (barg), D is the diameter of the vessel in metres (m), and CA is corrosion allowance in metres (m) taken as 0.00315m.

Note: Equation 4 is used for reactors, towers and separators.

3.1.1.3 Material Cost Factor and Bare Module Factor

The changes in working condition, including changes in operating pressures, temperatures or pH, from base conditions results in the utilization of different material for construction of equipment. The material in this thesis is selected as per material compatibility mentioned in [17], [61] and [64]. Material cost factor, F_M, is used to accommodate the changes in equipment cost due to change in construction material as shown in equation 5.

$$\mathbf{C_{BM} = C_P^{\circ} F_{BM} = C_P^{\circ}[B_1 + B_2 F_P F_M]} \quad \textbf{(5)}$$

Where, F_{BM} represents the factor to install an equipment on site made of specific material and specific operating pressure, F_P represents pressure factor, F_M represents material factor, and B1 and B2 are equipment specific constants (shown in table 7).

Table 7: B1 and B2 equipment specific constants [61]

Equipment Type	B1	B2
Heat Exchanger	1.63	1.66
Vertical Reactors (including Towers)	2.25	1.82
Pumps (Centrifugal and Reciprocating)	1.89	1.35

Note: Bare module cost of equipment, C_{BM}^{O}, operating at ambient pressure and made of carbon steel have F_M and F_P equal to unity.

3.1.1.4 Grass Root Cost

The grass root cost, C_{GR}, refers to installing a new equipment or developing a project from scratch. This includes costs other than direct and indirect costs. The additional costs are contingency and fees, and auxiliary facilities cost.

The contingency helps to avoid any hinderance in project due to unforeseen events like unpredicted rise in the prices of equipment or delay in project due to storms. The contingency and fees cost is taken at 18% of module cost. The total module cost can be calculated by adding contingency and fees cost as shown in equation 6. This value represents expansions or alteration of small to medium scale to an existing facility.

$$\mathbf{C_{TM} = 1.18 \sum_{i=1}^{n} C_{BM,i}} \quad \textbf{(6)}$$

The auxiliary facility costs are for developing the site (for e.g. purchasing the land, excavation of the site, and construction of internal road), auxiliary buildings (for e.g. office rooms, cafeteria, and maintenance rooms), off-site and utilities (for e.g. handling raw material and final product, control facilities and process utilities). This cost is not affected by construction material and material of construction of the equipment or process, hence is taken as 50% of bare module cost. C_{GR} can now be calculated by adding this cost to C_{TM} as shown in equation 7.

$$\mathbf{C_{GR}} = \mathbf{C_{TM}} + \mathbf{0.50} \sum_{\mathbf{i=1}}^{\mathbf{n}} \mathbf{C_{BM,i}^{\circ}} \quad \textbf{(7)}$$

3.1.2 Manufacturing Cost Estimation

The economic feasibility of a project must include daily and routine operating cost of plant before assessing the project. The manufacturing is classified broadly into three categories;

- Direct Manufacturing Cost (DMC): This is depended and proportional to the rate of production. It includes cost of raw material, operating labour, waste treatment, operating supplies, maintenance and repairs, laboratory charges, patents and royalties.
- Fixed Manufacturing Cost (FMC): These costs are independent of rate of production. It includes cost of depreciation, taxes, insurance and plant overhead costs.
- General Expenses (GE): These costs are not directly related to production activities. It includes cost of distribution, administration and, research and development.

The cost of manufacturing (C_{OM}) is the sum of DMC, FMC and GE as shown in equation 8.

$$\mathbf{C_{OM}} = \mathbf{DMC} + \mathbf{FMC} + \mathbf{GE} \quad \textbf{(8)}$$

C_{OM} can be estimated when following cost components are known;

- Fixed Captial Investment (FCI) taken as C_{GR}
- Cost of Operating Labour (C_{OL})
- Cost of Raw Material (C_{RM})
- Cost of Utilities (C_{UT})
- Cost of Waste treatment (C_{WT})

Each of these costs can be used to calculate the individual items of DMC, FMC and GE as shown in table 8. C_{OM}, without depreciation, can be obtained by solving equation 9 and equations listed in table 8 for DMC, FMC and GE as shown in equation 9.

$$\mathbf{C_{OM}} = \mathbf{0.146\ FCI} + \mathbf{2.215\ C_{OL}} + \mathbf{C_{UT}} + \mathbf{C_{WT}} + \mathbf{C_{RM}} \quad \textbf{(9)}$$

Note: Depreciation will be added separately to the cost of manufacturing. Using a straight-line depreciation model with a 10% salvage value or scrap value of the initial capital investment of the unit at the end of project life.

Table 8: Cost items of manufacturing cost and their respective factors [61]

S.no.	Cost Item	Multiplying Factor
1.	**DMC**	-
a.	Raw material (C_{RM})	-
b.	Waste Treatment (C_{WT})	-
c.	Utilities (C_{UT})	-
d.	Operating Labour (C_{OL})	-
e.	Direct Supervisory and Clerical Labour	$0.18C_{OL}$
f.	Maintenance and Repairs	0.06FCI
g.	Operating Supplies	0.009FCI
h.	Laboratory Charges	$0.15C_{OL}$
Total DMC = $C_{RM} + C_{WT} + C_{UT} + 1.33\ C_{OL} + 0.069$ FCI		
2.	**FMC**	-
a.	Depreciation	*Separately
b.	Taxes and Insurance	0.032FCI
c.	Plant Overhead	$0.708C_{OL}$ + 0.036FCI
Total FMC = $0.708C_{OL}$ + 0.068FCI + depreciation		
3.	**GE**	-
a.	Administration	$0.177C_{OL}$ + 0.009FCI
Total GE = $0.177C_{OL}$ + 0.009FCI		
Total Costs = $C_{RM} + C_{WT} + C_{UT} + 2.215\ C_{OL} + 0.146$FCI + depreciation		

3.1.2.1 Operating Labour Cost (C_{OL})

To estimate C_{OL}, first the numbers of operators are required to run the process shift need to be estimated. This can be estimated using equation 10.

$$\mathbf{N_{OL}} = (\mathbf{6.29} + \mathbf{31.7}\,\boldsymbol{P^2} + \mathbf{0.23N_{NP}})^{\mathbf{0.5}} \quad \textbf{(10)}$$

Where, N_{OL} represents the number of operators required per shift, P represents the number of steps required in handling of solid, and N_{NP} represents the number of main nonparticulate steps like compression or heating. In this thesis, P is zero as there are no solid handling and N_{NP} can be calculated using equation 11.

$$\mathbf{N_{NP}} = \sum \boldsymbol{Equipment} \quad \textbf{(11)}$$

The number of operators required for a process per shift can be calculated using equation 10. The chemical process plant operates 24 hours/day with three working shifts, and if assumed to operate for a full year, it will require 1095 operating shifts/year. Since a single operator, on average, works for 5 shifts/week and 49 weeks/year (3 weeks are assumed for leaves), this results in 245 shifts/year by an operator. Hence, the plant requires approximately 4.5 operators for every operator needed.

The cost of operating labour can be estimated by knowing the average hourly rate of an operator. This is not a fixed value around the globe but varies geographically.

Note: This estimates the number of operator and does not include any supervisory or support staff.

3.1.2.2 Cost of Utilities (C_{UT})

The cost of utilities can be estimated by energy and mass balances around the equipment. The utilities usually include cooling water, fuel, electricity, steam and refrigeration. However, to simplify the work in this thesis, cost of natural gas (for heating purposes and as a hydrogen source), cost of water (for cooling purposes and steam production) and cost of electricity are included. Similarly, heating load for electrolyser-HBP coupling is assumed to be electric load and water required by electrolyser is desalinated and taken from the sea/ocean.

3.1.2.3 Cost of Raw Material (C_{RM})

The cost of raw material can be estimated using mass balances around the equipment. The main raw material in this thesis is natural gas, water, ocean/sea water and air. The cost of natural gas and water are already taken into cost of utilities, while ocean/sea water and air are assumed to be free.

3.1.2.4 Cost of Waste Treatment (C_{WT})

The disposal of waste from a chemical plant is regulated by local legislations, so chemically hazardous

waste is normally treated before being disposed into the environment. The waste streams from different ammonia plants are mentioned in table 9.

Table 9: Waste streams of different ammonia plants

Plant Coupling	Waste stream
SMR - HBP	Carbon dioxide, leaked ammonia, leaked natural gas, and oxygen/argon stream
Alkaline Electrolyser – HBP	Brine discharge, oxygen/argon stream and leaked ammonia
PEM Electrolyser – HBP	Brine discharge, oxygen/argon stream and leaked ammonia

Brine discharge and oxygen/argon stream are environmentally friendly, while the cost of leaked ammonia and leaked natural gas treatment is assumed to be zero.

Note: The cost of emitting carbon dioxide in Germany will be considered for SMR-HBP plant configuration but will be not considered as cost of waste treatment.

3.2 HBP Production Loop

The scope of thesis includes the study of a 300 metric ton per day of ammonia. This will stoichiometrically require 246.7 tons of nitrogen and 53.3 tons of hydrogen per day. The mass flow rates can be converted to volume flow rates at room temperature and pressure using equation 12.

$$\mathbf{PV = nRT} \qquad \textbf{(12)}$$

Where, P represents pressure in pascals (Pa), V represents volume (m^3), n represents the number of moles (mol), T represents temperature (K) and R represents ideal gas constant (8.314 J mol^{-1} K^{-1}).

HBP loop as mentioned varies from industry to industry as per requirement of that specific plant. However, some equipment are common as per basic process flow. These include multi-staged compressor, recycle compressor, reactor, heat exchanger and separator. The actual HBP cycle of industrial scale is extensive design and beyond the scope of this thesis, so a preliminary analysis will be based on process simulations based on available literature.

The high purity nitrogen is fed from cryogenic air distillation, while high purity hydrogen is fed from either alkaline electrolyser plant, PEM electrolyser plant or SMR plant. After selecting the size and major components of the plant, HBP loop is developed on DWSIM simulation software (steady state). The pressure and temperature specifications of equipment are based on models by Morgen et. al [17] and

Araújo et. al [65].

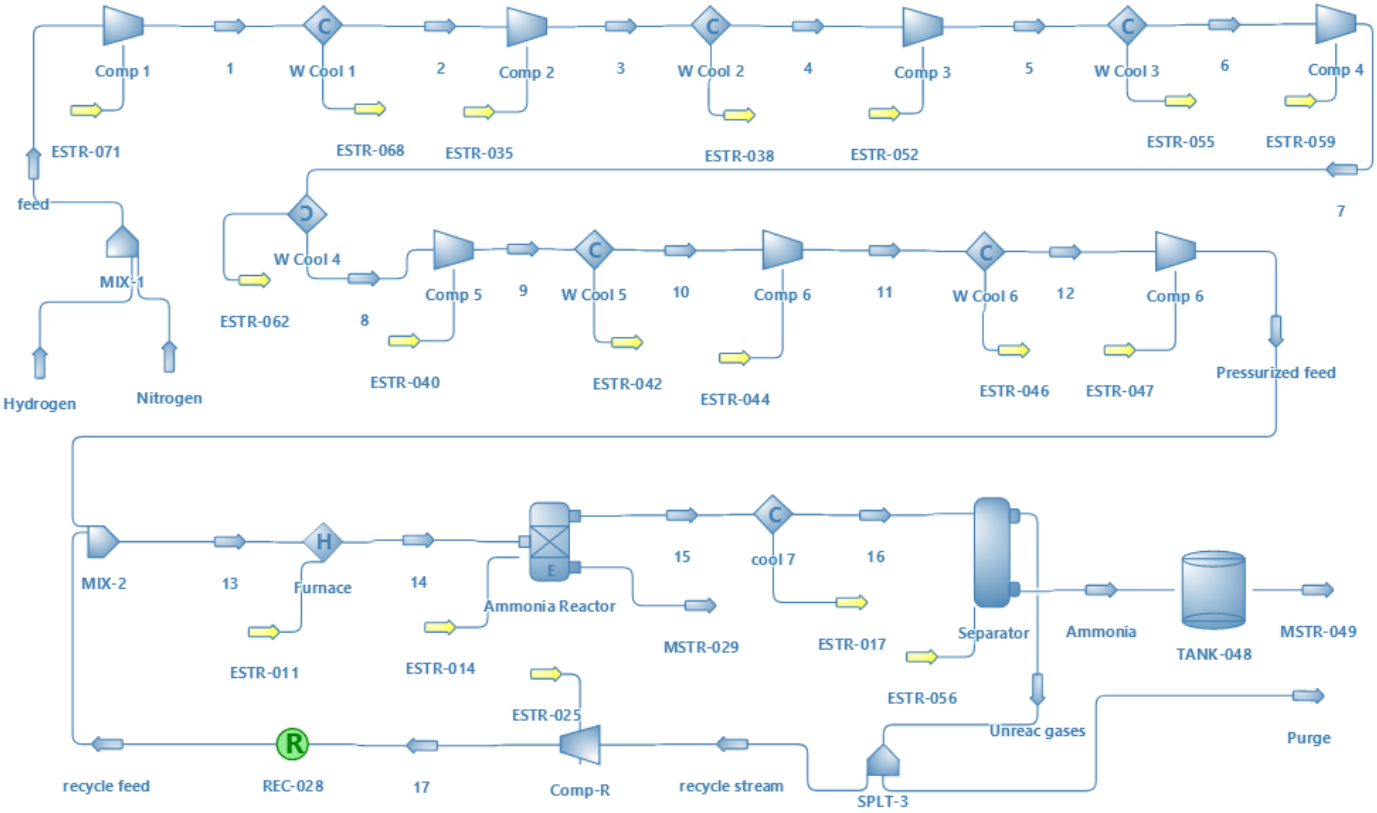

Figure 15: HBP flowsheet generated in DWSIM

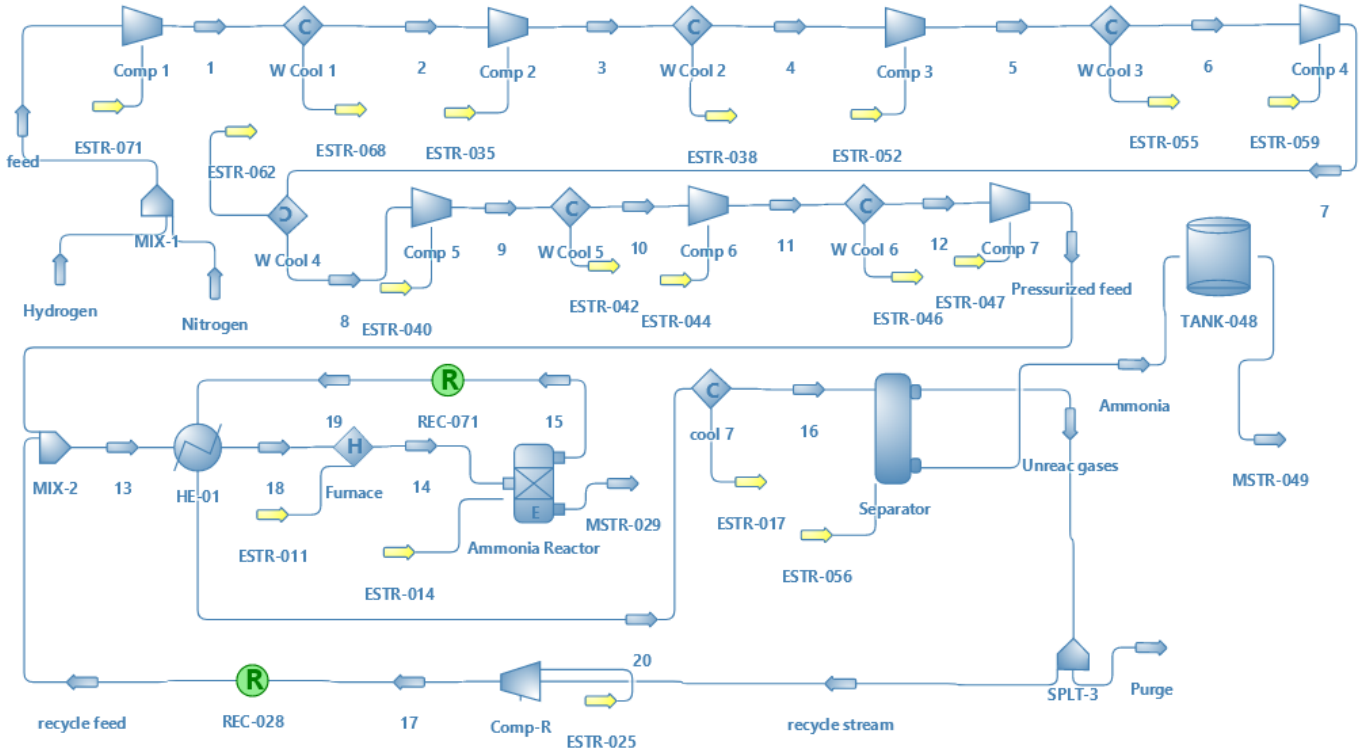

Figure 16: HBP with heat recovery flowsheet generated in DWSIM

Similarly, the equipment are sized and economic estimation is carried out as discussed in section 3.1.

The major equipment are compressors, heat exchangers, reactor and separator. Furnace is used in the case of SMR-HBP coupling, while in the case of alkaline electrolyser and PEM electrolyser, heat load is considered as electric load for simplification purposes.

HBP shown in figure 15 and figure 16 converts high purity nitrogen and hydrogen feed to ammonia. The process takes place at high temperature and pressure shown in stream table A.1-6 in annex 1. The process converts 26.4317% of hydrogen into ammonia, and the unreacted gases are recycled after separating ammonia. In figure 16, the heat exchanger acts as a heat recovery unit and decrease the load on furnace. Although heat recovery is technically feasible, this comparison will help in identifying whether heat recovery is economically feasible or not.

Note: Streams labelled as ESTR-0XX and yellow in colour are energy streams while other streams blue in colour are material streams.

3.2.1 Compressor

Compressor are required to increase the pressure of the feed gases and the unreacted gases in recycle stream. The gases enter compressor 1 at ambient pressure and a temperature of 299.82 K, and they leave compressor 7 and recycle compressor (comp-r) at 158 bars. Since continuous flow and high pressure is required, centrifugal compressors are selected in this thesis (assumed). Moreover, the compressing process is divided into 7 stages with intercooling as shown in figure 15 and 16, this is in order to reduce the work requirements in subsequent compressors. The hot gases are cooled in the intercooler until the last compression stage (compressor 7 in figure 15 and 16). Intercoolers will be covered in section 3.2.2.

The power imparted on the fluid by the compressor can be calculated using equation 13, where h is the specific enthalpy in kJ/kg, ṁ is the mass flow rate in kg/s, c_p is specific heat capacity in kJ/kgK, T_{01} is the stagnation temperature at inlet conditions in K, T_{02} is the stagnation temperature at outlet conditions in K, P is the pressure in Pa, V is the volume in m^3 and k is the index of compression (isentropic process assumed) [66].

$$\boldsymbol{W_{fl}} = \dot{m}(\boldsymbol{h_2} - \boldsymbol{h_1}) = \dot{m}\boldsymbol{c_p}(\boldsymbol{T_{02}} - \boldsymbol{T_{01}}) = \dot{m}\boldsymbol{P_1 V_1}\frac{\boldsymbol{k-1}}{\boldsymbol{k}}\left[\left(\frac{\boldsymbol{P_2}}{\boldsymbol{P_1}}\right)^{\frac{\boldsymbol{k-1}}{\boldsymbol{k}}} - \mathbf{1}\right] \quad \textbf{(13)}$$

Similarly, the increase in temperature as isentropic compression is assumed can be calculated using equation 14 and heat gained by the gases can be calculated using equation 15, where T is temperature of the gases in K and Q_{in}(kW) is the heat gained by gases at every staged of compression [67].

$$\boldsymbol{T_2} = \boldsymbol{T_1}\left(\frac{\boldsymbol{P_2}}{\boldsymbol{P_1}}\right)^{\frac{\boldsymbol{k-1}}{\boldsymbol{k}}} \quad \textbf{(14)}$$

$$\boldsymbol{Q_{in}} = \dot{m}\boldsymbol{c_p}(\boldsymbol{T_2} - \boldsymbol{T_1}) = \dot{m}\boldsymbol{c_p}\Delta\boldsymbol{T} \quad \textbf{(15)}$$

The compressor cost estimation as show in table 5 is based on shaft power. The shaft power required by the compressor is more than power imparted on the fluid, this is attributed to the irreversibility involved

in compression process. The shaft power can be calculated from fluid power (calculated in equation 13) using equation 16, where Ƞ is the isentropic efficiency of the compressor [68]. The isentropic efficiency for compressor 1 is assumed to be 85% while for all other compressors in the loop it is assumed to be 75%.

$$W_{sh} = \frac{W_{fl}}{\eta} \quad \textbf{(16)}$$

Similarly, Electric motor drives, selected to drive the compressor, require more power than the shaft power due to electric power losses. They can be calculated using equation 17, where $Ƞ_e$ is the electric efficiency of the motor. The typical values of electric efficiency of motor is 95% [69] (assumed for this thesis).

$$W_{el} = \frac{W_{sh}}{\eta_e} \quad \textbf{(17)}$$

3.2.1.1 Compressor Cost Estimation

The cost of compressor is depended on material factor of construction and not on pressure factor as it a pressure changing devices that takes high operating pressures into account. The material compatibility is checked from table 4-28 from [64]. Nitrogen gas is inert is compatible with carbon steels (CS) till 600°C and stainless steel (SS) till 800°C, while hydrogen is not compatible with carbon steels and can damage the equipment. Hydrogen is compatible with SS, aluminium based alloy, copper based alloy or nickel based alloy. Moreover, ammonia is compatible with CS, SS, aluminium based alloy or nickel based alloy. Thus, all compressors in HBP loop are assumed to be made from SS as it is relatively cheaper fabrication material compared to other alloys.

After selecting the material and taking power rating of compressors from DWSIM, f.o.b costs are calculated using equation 1. F.o.b costs are converted to operating conditions and base conditions by using equation 5 coupled with appropriate factors in appendix A of [61]. For bare cost module factor made from SS, F_{BM} for compressor is 5.8, and bare cost module operating factor at base condition, F_{BM}^{O} for compressor is 2.8. Moreover, bare module cost factor for enclosed electric drives is 1.5 for both conditions. Finally, the prices are converted to 2019 using the CEPCI index as the prices are in year 2001 from [61]. The capital costs incurred in buying and installing centrifugal compressors and enclosed electric motors are shown in table 10.

Table 10: Capital cost and power rating of compressors and electric motors

Equipment No.	Equipment Type	Rating (kW)	Cost in 2019 ($) for operating conditions	Cost in 2019 ($) for base conditions
Comp 1	Compressor	2856	5267408	2542887
Comp 2	Compressor	1985	4133088	1995284
Comp 3	Compressor	1457	3332149	1608624
Comp 4	Compressor	730	1996322	963742
Comp 5	Compressor	493	1463962	706740
Comp 6	Compressor	459	1382596	667460
Comp 7	Compressor	407	1250695	603784
Comp R	Compressor	82	297057	143407
Comp R with Heat Recovery	Compressor	122	434635	209824
Drive for Comp 1	Electric Motor	3006	329925	329925
Drive for Comp 2	Electric Motor	2089	310948	310948
Drive for Comp 3	Electric Motor	1534	289646	289646
Drive for Comp 4	Electric Motor	769	230799	230799
Drive for Comp 5	Electric Motor	519	194471	194471
Drive for Comp 6	Electric Motor	484	187969	187969
Drive for Comp 7	Electric Motor	428	176784	176784
Drive for Comp R	Electric Motor	86	60126	60126
Drive for Comp R with Heat Recovery	Electric Motor	128	82569	82569

3.2.2 Heat Exchanger

The heat exchanger allows the transfer of heat from a hot fluid to a cold fluid without any physical contact between the fluids. The HBP loop, shown in figure 15, employs 7 heat exchangers including intercoolers, while HBP with heat recovery loop, shown in figure 16, employs 8 heat exchangers. The intercoolers serve to cool down feed gases before further compression, this reduces the specific volume of the gases

and hence, resulting in less work required in next stages of compression. Heat exchanger, Cool 7 shown in figure 15 and 16, cools down the gases so ammonia can be condensed and separated in flash drum. HE-01, heat recovery heat exchanger unit shown in figure 16, heats the feed gases to ammonia reactor by exchanging heat from hot synthesis gas coming out of ammonia reactor.

The amount of heat gained or loosed by the fluid can be calculated using equation 15, while the heat exchanged, Q_{EX} (W), between the fluids can be calculated using equation 18 [70] [71] .

$$\boldsymbol{Q_{EX} = UA_{EX}\Delta T} \quad \textbf{(18)}$$

Where U is the overall heat transfer co-efficient in W m^{-2} $°C^{-1}$, A_{EX} is the heat transfer area in m^2 and ΔT is the log mean temperature difference between hot and cold fluids and can be calculated using equation 19.

$$\boldsymbol{LMTD = \frac{(T_{H,i}-T_{C,o})-(T_{H,o}-T_{C,i})}{ln[\frac{(T_{H,i}-T_{C,o})}{(T_{H,o}-T_{C,i})}]}} \quad \textbf{(19)}$$

Where, T_H and T_C are temperature of the hot and cold fluids respectively, while i and o subscripts represents fluid direction going inside or outside heat exchanger.

The heat transfer coefficient, U, depends upon type(s) of heat transfer process (conduction, convection and radiation), physical properties of fluids, mass flowrates of fluids, type of fabrication material of heat exchange surface and physical arrangement of the heat exchanger. To simplify the approach, all heat exchangers in HBP synthesis loop are floating head shell-in-tube heat exchangers with typical values for U are taken from [71] as shown in table 11.

Table 11: Typical heat transfer coefficient

Cold Fluid	Hot Fluid	U (W m-2 °C-1)
Water	Gases	300
Gases	Gases	50

The intercoolers (cool 1 -6) and cool 7, shown in figure 15 and 16, are assumed to be cooled by water. The cooling water is assumed to enter the heat exchangers in the intercoolers at a temperature of 293.15 K and leaving at 315.15 K. Similarly, the cooling water for synthesis gas cooler, cool 7, enters at 293.15 K, and leaves at 297 K without heat recovery option and at 295 K with heat recovery option. The heat transfer area, A_{EX}, of heat exchanger, shown in table 12, can be calculated using equation 15, 18, 19, the cooling load requirements and temperature of gases (from DWSIM flowsheet).

Note: Heat exchanging efficiency of intercoolers and synthesis gas cooler is assumed to be 90% with a pressure drop of 0.5 bar, while the efficiency of heat recovery unit is assumed to be 85% with a pressure drop of 1 bar.

Table 12: Heat transfer area for heat exchangers

Equipment Name	Type	Q (kW)	LMTD	A_{EX} (m2)
W cool 1	Intercooler	2911	92.99	104
W cool 2	Intercooler	2212	77.96	95
W cool 3	Intercooler	1630	64.43	84
W cool 4	Intercooler	820	43.51	63
W cool 5	Intercooler	554	35.53	52
W cool 6	Intercooler	516	34.22	50
Cool 7	Synthesis gas cooler	23571	96.88	811
HE-01	Heat recovery unit	14473	50.10	5777
Cool 7*	Synthesis gas cooler with heat recovery unit configuration	6437	25.56	839

3.2.2.1 Heat Exchanger Cost Estimation

The cost of heat exchanger is depended on the material of construction and pressure factor. The material selected is stainless steel for feed gases and recycle stream gases as per material compatibility discussed in section 3.2.1.1. Moreover, the section for cooling water can be constructed of carbon steel or stainless steel as stated by Ulrich et. al [64]. Since carbon steel is relatively cheaper than SS, the section of heat exchanger containing cooling water is made from carbon steel. In order to simplify the approach, cooling water in intercoolers and synthesis gas cooler is assumed to flow in the shell side and gases are assumed to flow in the tubes. However, the heat recovery unit is made from SS shell and SS tubes.

The impact of high pressure on heat exchanger cost is estimated by calculating pressure factor, F_P, using equation 3 and table 6. Similarly, the impact of fabrication material on heat exchanger cost estimated by using material factor, F_M, in the appendix A of [61]. The F_M for intercoolers (W cool 1-6) and synthesis gas cooler is 1.8, while F_M for heat recovery unit (HE-01) is 2.75.

The f.o.b costs are calculated using equation 1. F.o.b costs are converted to operating conditions and

base conditions by multiplying with bare module cost factor in equation 5. The bare cost module factor, for both operating condition (F_{BM}) and base condition (F_{BM}^{O}), is calculated using equation 5, F_P, F_M and, B_1 and B_2 from table 7. Finally, the prices are converted to 2019 using the CEPCI index as the prices are in year 2001 from [61]. The capital costs incurred in buying and installing heat exchangers are shown in table 13.

Table 13: Heat exchanger cost estimation

Equipment Name	Pressure (bar)	F_P	F_{BM}	F_{BM}^{o}	A_{EX} (m^2)	Cost in 2019 ($) for operating conditions	Cost in 2019 ($) for base conditions
W cool 1	6.25	1.00	4.62	3.29	104	182041	129677
W cool 2	18.25	1.06	4.79	3.29	95	181794	124815
W cool 3	42.75	1.18	5.15	3.29	84	186132	118927
W cool 4	67.25	1.27	5.43	3.29	63	178361	107975
W cool 5	91.75	1.35	5.68	3.29	52	176937	102534
W cool 6	121.5	1.44	5.94	3.29	50	183508	101584
Cool 7	154	1.53	6.19	3.29	811	1068794	567850
HE-01	157	1.53	8.63	3.29	5777	9117430	3474438
Cool 7*	152	1.52	6.18	3.29	839	1103391	587615

Note: Cool 7* represents HBP loop with heat recovery unit.

3.2.3 Furnace

Indirect fired furnace is used to heat the feed gases to the required temperature. The feed gases are passed through tubes in a fired furnace. This allows separation of process streams and heating streams, which could have impact on product formation. Furnace is used only in SMR-HBP configuration and is assumed to combust natural gas to produce heat for feed gases. The amount of heat gained by the process stream can be calculated using equation 15, while heat produced, Q_C, by combusting natural gas is calculated using equation 20.

$$\boldsymbol{Q_C} = \dot{m}\boldsymbol{LCV} \quad \textbf{(20)}$$

Where ṁ is the mass flowrate of natural gas and LCV (46.5 MJ/kg) is low calorific value of natural gas. Moreover, the efficiency equation, shown below, can be used to relate the amount of heat produced by natural gas and the amount of heat gained. The efficiency, η_F, is for HBP is assumed to be 85%.

$$\eta_F = \frac{Q_{EX}}{Q_C} \quad \textbf{(21)}$$

The heat production, Q_C, requirement from DWSIM flowsheet is 21393 kW for HBP and 3004 kW for HBP with heat recovery.

3.2.3.1 Furnace Cost Estimation

The cost of furnace is depended on the material of construction and pressure factor. The material selected for tubes is stainless steel for feed gases and recycle stream gases as per material compatibility discussed in section 3.2.1.1. Moreover, the section for natural gas and flue gases can be constructed of carbon steel, copper-based alloy, nickel-based alloy or stainless steel as stated by Ulrich et. al [64]. Since carbon steel is relatively cheaper than SS, the shell of furnace is made from carbon steel.

The pressure factor, F_P, is assumed to be 1 for both operating and base conditions. Similarly, the bare module cost factors, both for operating conditions (F_{BM}) and base conditions (F_{BM}^O), are taken from appendix A of Turton et. al [61]. F_{BM} and F_{BM}^O are 2.8 and 2.0 respectively.

F.o.b costs are already discussed in previous sections. The capital costs incurred in buying and installing furnace for operating condition and base condition are $5424687 and $3874777 respectively. Similarly, the capital costs of furnace in HBP with heat recovery unit are $2390270 and $1707336.

3.2.4 Reactor and Separator

The reactor allows conversion of nitrogen and hydrogen into ammonia for specified inlet conditions (temperature, pressure and concentrations of feed gases). Hydrogen is mixed with nitrogen in 3:1 ratio and fed into the reactor. Since the reaction is reversible, the rate of ammonia synthesized is different than the rate at which ammonia is decomposed into nitrogen and hydrogen again. However, at equilibrium, the two rates are equal. The equilibrium constant, K_{EQ}, can be calculated using equation 22, where $[NH_3]$, $[N_2]$ and $[H_2]$ represent the concentrations of respective products and reactant at equilibrium.

$$K_{EQ} = \frac{[NH_3]^2}{[N_2][H_2]^3} \quad \textbf{(22)}$$

The concentrations of reactants and products are known by analysing the yield, conversion and reaction extent. In case, such information is not available, K_{EQ} can be calculated using from thermodynamics from Gibbs free energy, which is the approach of DWSIM software. The Gibbs free energy can be

calculated using equation 23 [72] [73].

$$\Delta \mathbf{G} = \Delta \boldsymbol{G^o} + \boldsymbol{RT\ lnK} = \sum \boldsymbol{n_i G_i^o} + \boldsymbol{RT} \sum \boldsymbol{n_i ln} \frac{\boldsymbol{f_i}}{\boldsymbol{f_i^o}} \quad \textbf{(23)}$$

Where, ΔG^o is the standard state Gibbs free energy, R is the ideal gas constant, T is temperature of system in K, K is the reaction quotient, G_i^o is the standard state Gibbs free energy of a specie i, number of moles of specie i, f_i is fugacity of specie i in the gas mixture and f_i^o is standard state fugacity of specie i. Gibbs free energy, of a system, for reversible reaction becomes minimum at equilibrium for constant temperature and pressure, the minimum Gibbs energy of all components, reactants and products, can be calculated by differentiating equation 23 and setting the derivate to zero. Similarly, ΔG of the system becomes zero at equilibrium and equation 23 can be rewritten and relate K_{EQ} with Gibbs energy in equation 24.

$$\boldsymbol{K_{EQ}} = \boldsymbol{exp}\ (-\frac{\boldsymbol{\Delta G^o}}{\boldsymbol{RT}}) \quad \textbf{(24)}$$

The drum are used to separate the vapor-liquid mixture [64] that is separating ammonia from process gases. If the carryover of liquid droplets is not critical to operation, it is enough to rely on gravity setting separating vessel [71]. The performance of separating vessel can be improved by using demister pads. Demister pads increase separating efficiency and decrease the size of separating vessel.

The size of separating drum, for smooth control of operation, allows 10 minutes for liquid residence time [64] [71]. The settling velocity of liquid droplets calculated using equation 25 is 0.290 m/s, which will help design the separating vessel [71].

$$\boldsymbol{u_t} = \mathbf{0.07}(\frac{\boldsymbol{\rho_l - \rho_v}}{\boldsymbol{\rho_v}})^{\frac{1}{2}} \quad \textbf{(25)}$$

Where ρ_l is liquid density, ρ_v is vapor density and u_t is the settling velocity. If a demister pad is not used, u_t should be multiplied by a factor 0.15 for safety reasons. The diameter for the vessel, assuming vertical vessel, must allow the gases to slow down till the settling velocity of the liquid. The minimum allowable diameter for a vessel, with demister pad, calculated using equation 26 is 0.96m [71].

$$\boldsymbol{D_v} = \sqrt{\frac{\boldsymbol{4V_v}}{\boldsymbol{\pi u_t}}} \quad \textbf{(26)}$$

$$\boldsymbol{L_h} = \frac{\boldsymbol{Volume\ of\ Liquid\ held\ up}}{\boldsymbol{Cross{-}secton\ area\ of\ the\ vessel}} \quad \textbf{(27)}$$

The depth of liquid, L_h, for a 10-min time period is 4.45m calculated using equation 27. The height of the vessel should be enough to allow the separation of liquid from gases, for vertical vessel a minimum height of approximately 1.68m above the liquid level is considered [74]. The final dimensions of the vessel are 5.95m in height with a diameter of 1.5m as the length to diameter ratio for vertical separator should be in the range of 3-5 [64].

3.2.4.1 Reactor, and Separator Cost Estimation

Ammonia reactor and the separator drum are large pressure vessels (discussed in section 3.1.1.2) that process ammonia, hydrogen and nitrogen. In order to avoid failure with catastrophic consequences, the pressure vessel is designed by considering the impact of pressure on the reactor and the drum. Using equation 4, the pressure cost factor, F_P, can be calculated, while material cost factor, F_M, for stainless steel is taken from appendix A of Turton et. al [61]. The dimensions of the reactor are assumed to be 7m tall and 1.4m wide from Morgen et. al [17]. Using equation 5, F_{BM} of the reactor and the drum can be calculated both for operating and base conditions as shown in table 14, while for demister pad made from SS is taken from appendix A of Turton et. al [61].

F.o.b costs are already discussed in previous sections. Finally, the prices are converted to 2019, shown in table 14, using the CEPCI index as the prices are in year 2001 from Turton et. al [61].

Table 14: Reactor and separator drum cost estimation

Equipment	**Pressure (barg)**	**F_P**	**F_M**	**F_{BM}**	**F_{BM}^o**	**Capacity (Units)**	**Cost in 2019 ($) for operating conditions**	**Cost in 2019 ($) for base conditions**
Ammonia Reactor	156	23.6	3.1	135.29	4.07	10.78 m^3	2460373	74015
Separating Vessel	153.5	24.8	3.1	142.10	4.07	10.51 m^3	2542103	72810
Demister Pad	153.5	1	-	1	1	1.77 m^2	3637	3637

Note: The dimensions of reactor are assumed, since the data on kinetics of the reaction and catalyst are unknown. Moreover, the volume of the reactor and separator is assumed to be cylindrical.

3.2.5 Storage Tank System

Ammonia can be stored using two methods [75];

1. Insulated cylindrical storage tanks at ambient pressure and temperature of -33°C that have a capacity up to 50,000 tonnes per vessel.
2. Spherical or cylindrical storage tanks at ambient temperature that have a capacity of 1500 tonnes per vessel

The storage tank are designed to store ammonia for about 30 days [64], so storage capacity required for a 30-day period for 300 tonnes per day plant requires a tank of 9000 tonnes. Since it is a large volume, the capital investment cost for ambient pressure storage are lower than pressure storage [46]. The design pressure is in the range of 1.1 - 1.5 bars, including the static pressure of stored ammonia

[46].

The amount of volume corresponding to a 30-day storage is approximately 13,184 m^3 and adding a 10% freeboard makes the final volume of storage around 14,503 m^3. The optimum height to diameter ratio, to avoid wind overturning and stable for seismic loading, is 0.6 [76]. The diameter and the height of the tank are approximately 31m and 19m respectively. The inner tank is usually surrounded by an outer tank to contain leaked ammonia vapor and liquid [75] [77] . The outer tank is located at a maximum distance of 1.5m from inner tank minimum distance. The height and diameter of the outer tank is 20.5m and 32.5m respectively.

The inner tank stores refrigerated ammonia at -33°C, the refrigeration is provided by recompressing the boil-off from the tank [46]. The recompression is provided by 2 stage reciprocating compressors [46]. The refrigeration provided is depended on the boil-off from the tank, which in turn is depended on the heat flux of the inner tank and latent heat of vaporisation of ammonia [17] [78]. The tank is usually designed to keep the boil-off to be less than 0.04% of the ammonia stored in the tank [17] [78]. Assuming the boil-off of 0.04%, the amount of ammonia vapours entering the refrigeration is 3.6 tons per day for a fully filled ammonia tank. The refrigeration loop shown in figure 17 is developed in DWSIM software as per the approach by Morgan et. al [17], Belapurkar et. al [78] and Webb et. al [79]. The stream data for the loop is shown in stream table A.7 in annex 1.

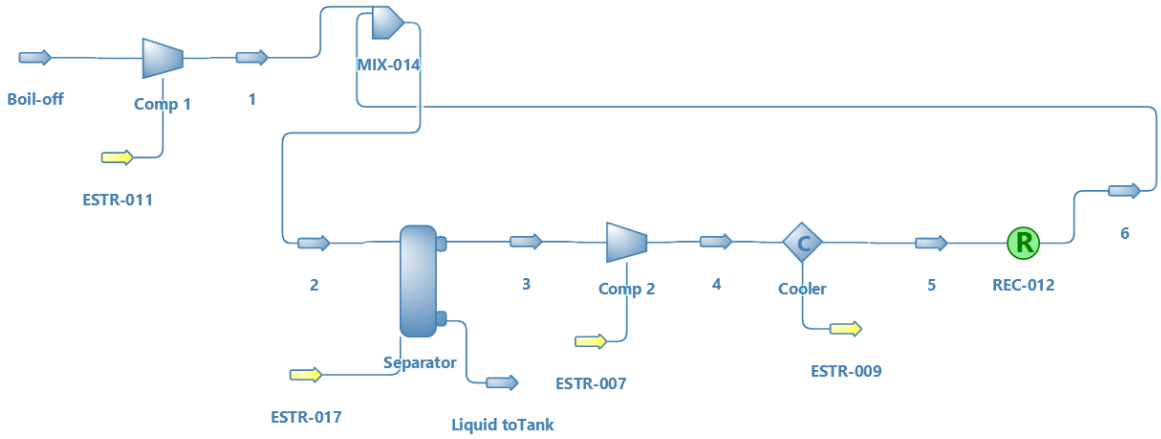

Figure 17: DWSIM flowsheet of compression loop for ammonia storage system

The boil-off is compressed to 3.04 bars and intercooled in a separator by mixing with cold pressurized liquid ammonia. The liquid ammonia is separated and send to the tank, while the vapor are compressed further in the second compressor to 12.67 bars. Ammonia is cooled in a condenser and send to the separator as shown in figure 17. The sizing and selection of equipment are already discussed in section 3.2.1, 3.2.2 and 3.2.4.

Using DWSIM flowsheet, compressor power rating is calculated while equation 16 is used to calculate the electric motor rating. The efficiency of compressors is assumed to 75% and the efficiency of electric motors is assumed to be 95%. Similarly, the separator is designed using equation 25, 26 and 27 with length to diameter ratio in the range of 3 - 5. The final dimensions of the separator are 3.64m in height

and 1m in width. Moreover, the condenser is assumed to be a shell-in tube heat exchanger cooled by chilled water taken at 276 K and heated to 280 K with an efficiency of 90%. The heat exchanger area is calculated using equation 18, equation 19 and heat transfer co-efficient from table 11.

Note: The chill water system has been ignored in the calculations to simplify the approach.

3.2.5.1 Storage Tank Cost Estimation

The cost of equipment depends upon material of fabrication and operating pressure of the equipment. The material compatibility is already discussed for compressor, condensate removal unit and heat exchanger. For the ammonia storage tank, the inner tank is fabricated from SS as discussed earlier, while the outer tank is made of concrete.

The impact of pressure on the cost of storage tank, separator drum and heat exchanger can be calculated using pressure factor. The pressure factor, F_P, can be calculated using equation 4 for separator drum, and equation 3 and table 6 for heat exchangers.

Table 15: Ammonia storage system cost estimation

Equipment	**Pressure (barg)**	**F_P**	**F_M**	**F_{BM}**	**F_{BM}^o**	**Capacity (units)**	**Cost in 2019 ($) for operating conditions**	**Cost in 2019 ($) for base conditions**
Inner Tank	0.5	1	3.1	4.1	2	14,503 m^3	3144224	1533768
Outer Tank	0	1	1.5	2.5	2	17,009 m^3	2183188	1746550
Heat Exchanger (Cooler)	11.67	1.03	1.8	4.7	3.29	7 m^2	157014	109918
Comp 1	2.04	1	-	5.8	2.8	7.8 kW	64031	33022
Comp 2	11.67	1	-	5.8	2.8	14.1 kW	5102	5102
Electric Drive for Comp 1	-	-	-	1.5	1.5	8.4 kW	10190	10190
Electric Drive for Comp 1	-	-	-	1.5	1.5	14.7 kW	23902	11539
Separator Drum	2.04	1	3.1	7.89	4.07	2.86 m^3	47352	22860
Demister Pad	2.04	1	-	1	1	0.79 m^2	2361	2361

The capital costs incurred in buying and installing the units for ammonia storage system in 2019, for operating condition and base condition, are shown in table 15.

Note: The pressure factor for storage tanks is assumed to be 1 and the material factor for concrete outer tank is assumed to be 1.5. Similarly, the material for chilled water in heat exchanger is assumed to be carbon steel. Moreover, the equipment specific constants of equation 5 are assumed unity.

3.2.6 Total Capital Costs for HBP and Ammonia Storage

The capital cost calculation of equipment, discussed in previous section, are used to calculate the grass root cost of different plant configuration; namely HBP, HBP with heat recovery (HBP-HR), Electro HBP (EHBP) and Electro HBP with heat recovery (EHBP-HR). The grass root costs, C_{GR}, is calculated using equation 6 and 7 are shown in table 16. Similarly, the capital cost distribution equipment and cost component wise for different HBP system are shown in figures 18 and 19.

Table 16: Grass root costs of different HBP systems

Process	Cost in 2019 (mil. $) for operating conditions	Cost in 2019 (mil. $) for base conditions	C_{TM} (mil. $)	C_{GR} (mil. $)
HBP	33.49	16.29	39.52	47.67
HBP-HR	39.77	17.71	46.93	55.78
EHBP	28.07	12.42	33.12	39.33
EHBP-HR	37.38	16.00	44.11	52.11
Ammonia Storage System	5.64	3.48	6.65	8.39

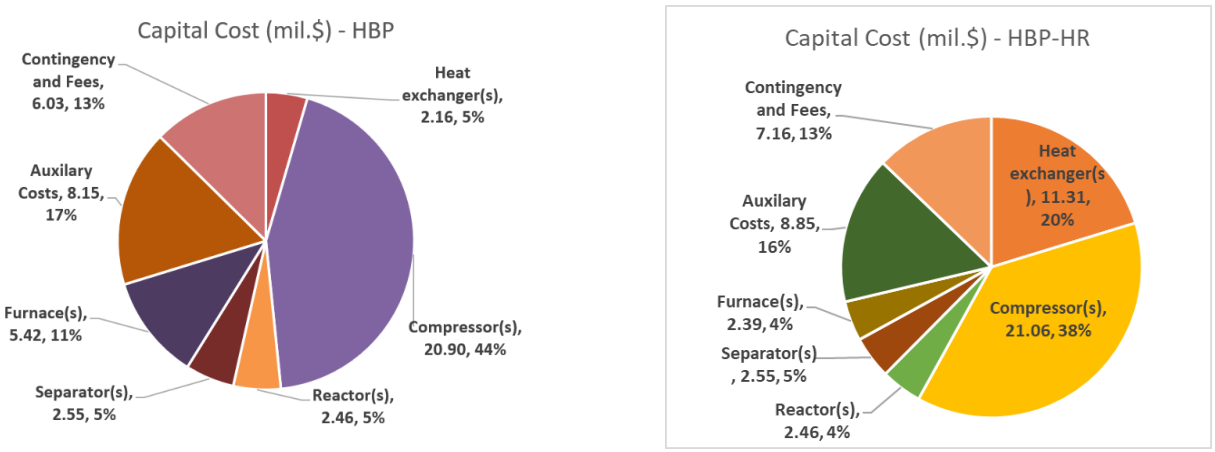

Figure 18: Capital cost distribution of HBP and HBP-HR

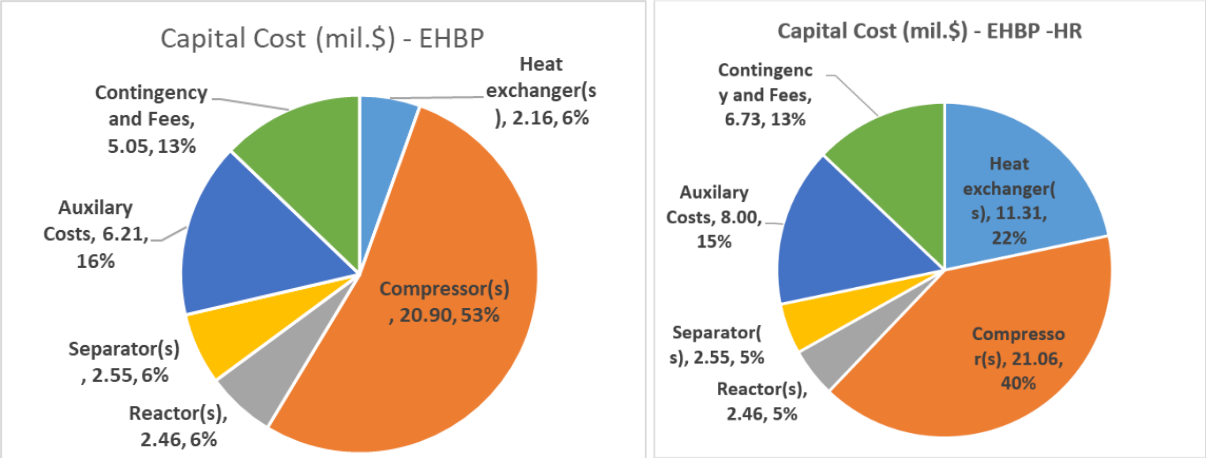

Figure 19: Capital cost distribution of EHBP and EHBP-HR

Note: EHBP is an assumed process where heat input is provided through electric power instead of furnace supplied with natural gas. EHBP will run only in conjunction with electrolyser plants.

3.2.7 Total Manufacturing Costs for HBP and Ammonia Storage

3.2.7.1 Cost of Utilities and Raw Material

The electric power is required to drive the compressors in HBP, ammonia storage system and provide heating load in EHBP loop. Table 17 shows electric consumption for a plant operating 8000 hours/year. The tariff for electric power in Germany is $ 0.21/kWh [80].

Natural gas is required to provide furnace loading in HBP loops only. Table 18 shows cost of natural gas and cost of carbon tax against the required heat load for a plant operating 8000 hours/year. The tariff for natural gas in Germany is $ 0.034 /kWh [81] and cost of carbon emission tax is $ 11.21/ton of CO_2 [82]. The emission factor for natural gas is 54,300 kg/TJ as per InterGovernmental Panel on Climate Change (IPCC) [83]

Table 17: Electricity consumption costs of different HBP systems

Process	Electric Power (kW)	Electric Consumption (kWh/yr)	Electric Utility Cost ($/yr)
HBP	8914	71315864	14976331
HBP-HR	8957	71655065	15047564
EHBP	27099	216790304	0
EHBP-HR	11961	95684265	0
Ammonia Storage System	23	185263	38905

Note: Electric utility cost for ammonia storage system, with Electrolyser systems, will be zero as the system will be using renewable energy generated from onshore wind farm.

Table 18: Natural gas and carbon costs of HBP systems

Utility	HBP	HBP-HR
Heat Load (kW)	21393	3004
Annual Heat Load (kWh/yr)	171146400	24029200
Natural Gas Cost ($/yr)	5818978	816993
Mass of Natural Gas (kg/yr)	13250044	1860325
Mass of Carbon dioxide (kg/yr)	33455698	4697228
Carbon Tax ($/yr)	375038	52656

The water is to provide cooling load. The cooling water requirements can be calculated using equation 15. The hot water from heat exchanger is cooled in a cooling tower and recirculated in the cooling water loop. Since this thesis has not considered cooling tower in the analysis, the amount of water bought daily is assumed to be hourly water consumption in HBP. The annual cost incurred in buying water is shown in table 19, with the tariff for water in Germany as $ 2.23 /m^3 [84].

Table 19: Water consumption costs for different HBP systems

Process	Cooling Water Requirement (kg/hr)	Annual Water Bought (m^3/yr)	Water Utility Cost ($/yr)
HBP	6035901	2203104	4912922
HBP-HR	3756214	1371018	3057370
EHBP	6035901	2203104	4912922
EHBP-HR	3756214	1371018	3057370
Ammonia Storage System	18270	6669	14871

3.2.7.2 Cost of Labour

The operating labour is calculated using equation 10 and 11. Total operators employed on a plant is the product of N_{OL} and number of operators per working operator. The number of operators per working

operator is 4.5, as discussed in section 3.1.2.1. The average annual salary of an operator in Germany is $54,196/yr [85]. The annual cost of labour is shown in table 20 for different ammonia plants.

Table 20: Cost of Labour for different HBP systems

Process	HBP	HBP-HR	EHBP	EHBP-HR	Ammonia Storage System
Compressor	8	8	8	8	2
Heat Exchangers	7	13	7	13	1
Furnace	1	1	0	0	0
Reactor	1	1	1	1	0
N_{OL}	3.19	3.40	3.16	3.37	2.64
Total Operators	15	16	15	16	12
Annual Labour Cost ($/yr)	812940	867136	812940	867136	650352

3.2.7.3 Cost of Manufacturing

The cost of manufacturing is estimated using equation 9 as discussed in detail in section 3.1.2. Depreciation is calculated using a straight-line depreciation model for a project with life of 20 years. The salvage value of equipment at the end of project life is assumed to be 10% of initial capital investment. Table 21 shows cost of manufacturing for different HBP systems.

Table 21: Cost of manufacturing for different HBP systems

Process	HBP	HBP-HR	EHBP	EHBP-HR	Ammonia Storage System
Annual Cost of Water (mil. $/yr)	4.91	3.06	4.91	3.06	0.01
Annual Cost of Electricity (mil. $/yr)	14.98	15.05	-	-	0.04
Annual Cost of NG (mil. $/yr)	5.82	0.82	-	-	-
Annual Carbon Tax (mil. $/yr)	0.38	0.05	-	-	-
Annual Labour Cost (mil. $/yr)	0.81	0.87	0.81	0.87	0.65
Salvage Value (mil. $)	4.77	5.58	3.93	5.21	0.84
Depreciation (mil. $/yr)	2.14	2.51	1.77	2.34	0.38
Miscellaneous (mil. $/yr)	7.95	9.20	6.73	8.66	2.02
Manufacturing Costs (mil. $/yr)	36.99	31.55	14.23	14.93	3.10
					3.06*

Note: *represents manufacturing cost of ammonia storage system when operating on renewable energy.

3.3 Cryogenic Air Distillation

Cryogenic air distillation varies from industry to industry as per requirement of that specific plant. From the process discussed in section 2.2.1, some common equipment include are multi-staged compressor, distillation towers, and heat exchanger. The designs of cryogenic air distillation of industrial scale are propriety and are extensive making it beyond the scope of this thesis, so a preliminary analysis will be based on process simulations based on available literature [40] [43] [44] [86].

The high purity nitrogen is produced from cryogenic air distillation at a rate 246.7 tons per day. Since HBP requires high nitrogen purity, this thesis will not cover the argon distillation. Cryogenic air distillation is modelled using simulation software called DWSIM. The process is simulated for required nitrogen flowrate and purity. Once the plant is sized and simulated, the equipment are sized and economic estimation is carried out as discussed in section 3.1.

Cryogenic air distillation shown in figure 20 takes air at ambient pressure and at a temperature of 298.15 K. The mole fraction of incoming air constitutes of 0.78 of nitrogen, 0.21 of oxygen and 0.01 of argon. The process separates air and produces high purity nitrogen feed for HBP. The process parameters (flowrates, temperature and pressure) are based on following literature [40] [43] [44] [86] and shown in stream tables A.8 - 10 in annex 1. The process, as discussed in detail in section 2.2.1, compresses air using multi-staged intercooled compressors, followed by cooling in heat exchangers, expansion in throttling values and, separation in high pressure (HP) and low pressure (LP) distillation columns.

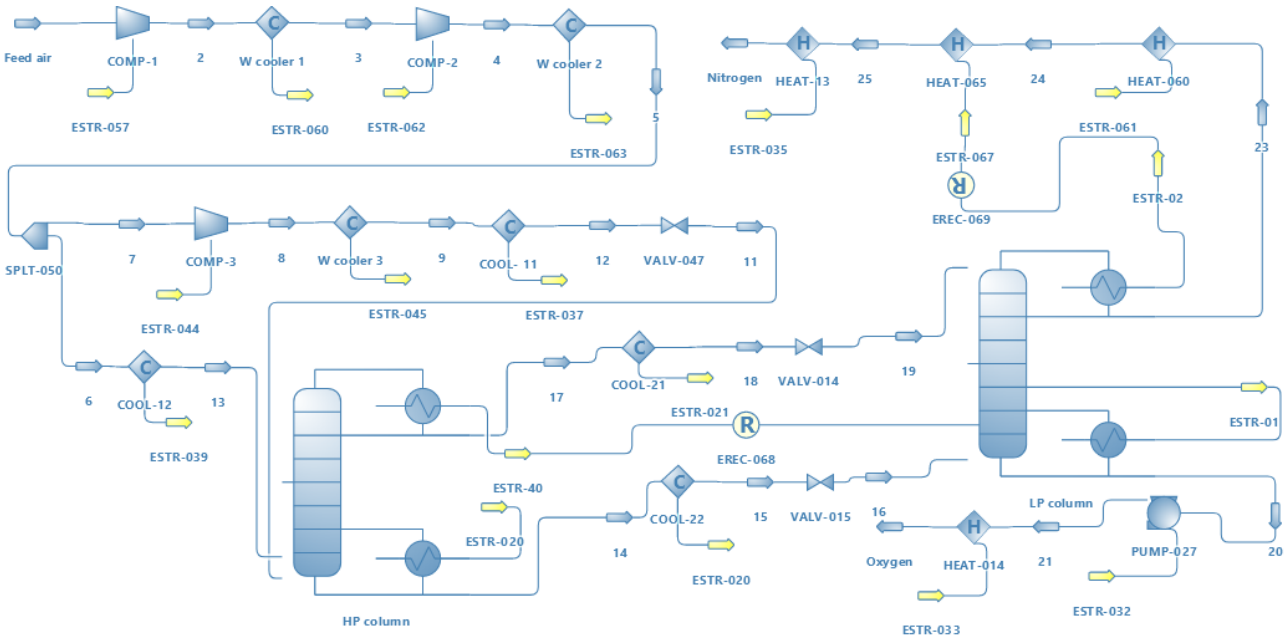

Figure 20: DWSIM flowsheet of air separation via cryogenic air distillation

3.3.1 Distillation Tower

Distillation tower are the most important equipment in cryogenic air separation. The column has trays installed along its height. The tray acts as stages for air separation. The vapor-liquid mixture flows from the hot bottom section to the cold top section resulting in the lighter fractions at the top and the heavier fractions at the bottom of the column.

Table 22: Dimensions of cryogenic distillation columns

Equipment	Number of stages	Number of trays	Height (m)	Diameter (m)	Volume (m^3)
HP column	45	45	25	3	177
LP column	80	80	40	3	283

The number of stages, column height and diameter are based on Morgen et. al [17] and Häring et. al [43] as shown by table 22. This is to simplify the approach of this as the sizing and designs of distillation columns are beyond the scope of this thesis.

3.3.1.1 Distillation Tower Cost Estimation

The cost of distillation towers depends on the working pressure and material of fabrication, while the cost of trays depends on the fabrication material only. The material compatibility is checked from table 4-28 from [64]. Nitrogen and oxygen gas are compatible with carbon steels (CS), SS alloy, aluminium based alloy, copper based alloy or nickel based alloy. However, for safe operation at cryogenic temperatures, SS, aluminium based alloy or copper based alloy are used [87]. In order to simplify the approach, SS will be considered as the fabrication material for both towers and trays.

The impact of pressure can be incorporated by using pressure cost factor, F_P. F_P can be calculated using equation 4 as Turton et. al [61] considers towers as pressure vessels. The material cost factor, F_M, for stainless steel tower is taken from appendix A of Turton et. al [61]. Using equation 5, F_{BM} of the tower can be calculated both for operating and base conditions. The F_{BM} of the taken from appendix A of Turton et. al [61] both for operating and base conditions.

The capital costs for distillation towers are calculated as discussed previously and are shown in table 23.

Table 23: Cost estimation of cryogenic distillation columns

Equipment	Pressure (bar)	F_P	F_M	F_{BM}	F_{BM}^o	Capacity (units)	Cost in 2019 ($) for operating conditions	Cost in 2019 ($) for base conditions
HP column	5.49	2.9	3.1	13.8	4.07	177 m^3	2352822	694863
Sieve Trays (HP)	5.49	-	-	1.8	1	7.07 m^2	566453	314696
Total cost of HP column	-	-	-	-	-	-	2919274	1009559
LP column	1.40	1	3.1	7.9	4.07	283 m^3	2108865	1087567
Sieve Trays (LP)	140	1	-	1.8	1	7.07 m^2	1007027	559459
Total cost of LP column	-	-	-	-	-	-	3115892	1647026

3.3.2 Heat Exchanger

The intercoolers (W cooler 1 - 3), shown in figure 20, are assumed to be cooled by water. The cooling water, for w cooler 1 and 2, is assumed to enter the heat exchangers in the intercoolers at a temperature of 293.15 K and leaving at 300 K. Similarly, the cooling water, for W cooler 3, enters at 293.15 K, and leaves at 296 K.

The intercooling heat exchangers are assumed to be floating head shell-in-tube heat exchangers. The heat transfer area, A_{EX}, of heat exchanger, shown in table 24, can be calculated using equation 15, 18, 19, table 11, the cooling load requirements and temperature of gases (from DWSIM flowsheet).

The cryogenic air separation process uses two other heat exchangers for cooling the incoming air both for HP column and LP column using nitrogen product stream and impure oxygen stream. The heat is assumed to be exchanged between HEAT-060, COOL-21 and COOL-22 in HX-01. A similar assumption is used for heat exchanged between HEAT-13. HEAT-014, COOL-11 and COOL-12 in HX-02.

The multi-stream heat exchanger to cool the incoming feed for the HP column is the main heat exchanger and is a plate-fin heat exchanger [43]. Similarly, the same type of heat exchanger is utilized to cool the incoming feed for LP column and called the sub-cooler [88].The volume, V, of heat exchanger can be calculated for sizing and costing purposes using equation 28.

$$\mathbf{V} = \frac{\boldsymbol{Q}}{\boldsymbol{C}\times\boldsymbol{dT}} \qquad \textbf{(28)}$$

Where, Q is the heat duty of the heat exchanger, C is a constant with a value of 50,000 W K^{-1} m^{-3} and dT is the average temperature difference between the streams exchanging heat [43]. The LMTD approach cannot be used to determine dT here since it is a multi-stream heat exchanger. Typical values of dT are in the range of 3 - 10 K [43]. To simplify the approach, dT is taken as 7K. V is 0.1892 for the sub-cooler (HX-01) and 4.868 for the main heat exchanger (HX-02). Similarly, area of the heat exchanger, A_{EX}, can be determined using equation 29 as shown in table 24.

$$\boldsymbol{A_{EX} = V \times A_P} \quad \textbf{(29)}$$

Where, A_P is the surface density of the fins on the plate heat exchanger and is taken as 1600 m^2/m^3 [88].

Table 24: Heat transfer area for heat exchangers

Equipment Name	Type	Q (kW)	LMTD / dT	A_{EX} (m2)
W cooler 1	Intercooler	1550	45.48	114
W cooler 2	Intercooler	1376	46.50	99
W cooler 3	Intercooler	461.4	27.40	56
HX-01	Sub-cooler	66.24	7	303
HX-02	Main heat exchanger	2906	7	13283

Note: Heat exchanging efficiency of intercoolers is assumed to be 90% with a pressure drop of 0.1 bar.

3.3.2.1 Heat Exchanger Cost Estimation

The cost of heat exchanger is depended on both operating pressure and material of fabrication. The fin plate heat exchanger is not covered by Turton et. al [61], the approach by Haslego et. al [89] l is used in conjunction with Turton et. al [61]. The bare cost of fin plate heat exchanger can be calculated using equation 30 with SS as material of construction, operating at less than 10 bars approximately and have a heat transfer area greater than 18.6 m^2 [89].

$$\mathbf{C = 136\, A_{EX}^{0.6907}} \quad \textbf{(30)}$$

Where, A_{EX} is the heat transfer area in ft^2. Hence, area of the heat exchanger is first converted to appropriate unit before cost estimation.

The installation costs are not considered by equation 30. The pressure factor, F_P, is taken as 1 for pressures less than 19 bars, assuming Turton et. al [61] heat exchanging data for flat plate heat exchanger. Similarly, equipment specific constant B_1 and B_2 are taken as 0.96 and 1.21, and material factor, F_M, is assumed as 1.5.

The intercoolers, on the other hand, are made carbon steel tubes and shell as per material compatibility

discussed in section 3.3.1.1 and section 3.2.2.1. The material factor, F_M, for intercoolers is in the appendix A of Turton et. al [61], while the pressure factor, F_P, is calculated using equation 3 and table 6.

The bare cost module factor, for both operating condition (F_{BM}) and base condition (F_{BM}^O), is calculated using equation 5, F_P, F_M and, B_1 and B_2 from table 7. The capital costs for heat exchangers are calculated as discussed previously and are shown in table 25.

Table 25: Heat exchanger cost estimation

Equipment Name	Pressure (bar)	F_P	F_{BM}	F_{BM}^o	A_{EX} (m^2)	Cost in 2019 ($) for operating conditions	Cost in 2019 ($) for base conditions
W cooler 1	2.68	1	3.29	3.29	114	135116	135116
W cooler 2	5.69	1	3.29	3.29	99	126974	126972
W cooler 3	12.1	1.02	3.33	3.29	56	105753	104476
HX-01	5.49	1	2.76	2.17	303	154656	120938
HX-02	12	1	2.76	2.17	13283	2105694	1646615

Note: CEPCI index for 2002 was 396 [89].

3.3.3 Compressor Cost Estimation

The compressor cost estimation is based on shaft power as discussed in section 3.2.1. The shaft power is calculated using equation 13 and 16, where the isentropic efficiency of COMP-1 is 80%, COMP-2 is 76% and COMP-3 is 75%. Similarly, Electric power to drive electric motor drives can be calculated using equation 17.

The cost of compressor is depended only on material of construction as mentioned in section 3.2.1.1. The material compatibility is checked from table 4-28 from [64]. Nitrogen gas is inert is compatible with carbon steels (CS) till 600°C and stainless steel (SS) till 800°C, while oxygen is not compatible with carbon steels at temperatures higher than 200°C and can damage the equipment. Oxygen is compatible with SS, aluminium based alloy, copper based alloy or nickel based alloy at higher temperatures. Thus, all compressors in this process are assumed to be made from SS as it is relatively cheaper fabrication material compared to other alloys.

After selecting the material and taking power rating of compressors from DWSIM, f.o.b costs are calculated and are converted to operating conditions and base conditions by using equation 5 coupled with appropriate factors in appendix A of [61]. For bare cost module factor made from SS, F_{BM} for compressor is 5.8, and bare cost module operating factor at base condition, F_{BM}^O for compressor is 2.8.

Moreover, bare module cost factor for enclosed electric drives is 1.5 for both conditions. The capital costs for heat exchangers are calculated as discussed previously and are shown in table 26.

Table 26: Capital cost and power rating of compressors and electric motors

Equipment No.	Equipment Type	Rating (kW)	Cost in 2019 ($) for operating conditions	Cost in 2019 ($) for base conditions
Comp 1	Compressor	1451	3321821	1603638
Comp 2	Compressor	1228	2947340	1422854
Comp 3	Compressor	388	1202476	580506
Drive for Comp 1	Electric Motor	1527	289316	289316
Drive for Comp 2	Electric Motor	1293	276251	276251
Drive for Comp 3	Electric Motor	408	172482	172482

3.3.4 Pumping System

The pump is used for internal compression of liquid oxygen. The liquid oxygen is pressurized and evaporated in the main heat exchanger to required temperature and pressure [43]. The power imparted on the fluid by the pump can be calculated using equation 31 [68], where h is the specific enthalpy in kJ/kg, ṁ is the mass flow rate in kg/s, c_p is specific heat capacity in kJ/kgK, T_{01} is the stagnation temperature at inlet conditions in K, T_{02} is the stagnation temperature at outlet conditions in K, γ is the specific weight of oxygen in Nm^{-3}, Q is the volume flow rate in m^3/s and Δh is the required change in elevation.

$$\boldsymbol{W_{fl}} = \dot{m}(\boldsymbol{h_2} - \boldsymbol{h_1}) = \dot{m}\boldsymbol{c_p}(\boldsymbol{T_{02}} - \boldsymbol{T_{01}}) = \boldsymbol{\gamma Q \Delta h} \quad \textbf{(31)}$$

The pump cost estimation as show in table 5 is based on shaft power. The shaft power required by the pump is more than power imparted on the fluid, this is attributed to the irreversibility involved in the process. The shaft power can be calculated from fluid power (calculated in equation 13) using equation 32, where Ƞ is the global efficiency of the pump [68]. The global efficiency for pump is assumed to be 80%.

$$\boldsymbol{W_{sh}} = \frac{\boldsymbol{W_{fl}}}{\eta} \quad \textbf{(32)}$$

Note: A centrifugal pump is assumed for internal compression process.

3.3.4.1 Pump Cost Estimation

The cost of pump is depended on material factor of construction and not on pressure factor as it a pressure changing devices that takes high operating pressures into account. The material of construction for the pump is SS as per material compatibility discussed in section 3.3.2.1. The pressure factor, F_P, is 1. Similarly, the material factor, F_M, is taken from the appendix A of [61]. The F_M for pumps made from SS is 2.4. Similarly, the bare module cost factors, both for operating conditions (F_{BM}) and base conditions (F_{BM}^O), calculated from equation 5 and table 7 are 5.13 and 3.24 respectively. The capital costs for pump are for operating and base conditions are $19369 and $12233.

3.3.5 Total Capital Costs for ASU

The capital cost of ASU that is total module cost, C_{TM}, and the grass root equipment, C_{GR}, calculated from equation 6 and equation 7 are 19.93 and 24.51 million $ respectively with a specific investment cost of 7591 $/kW. Similarly, the capital cost distribution equipment and cost component wise for ASU system is shown in figure 21.

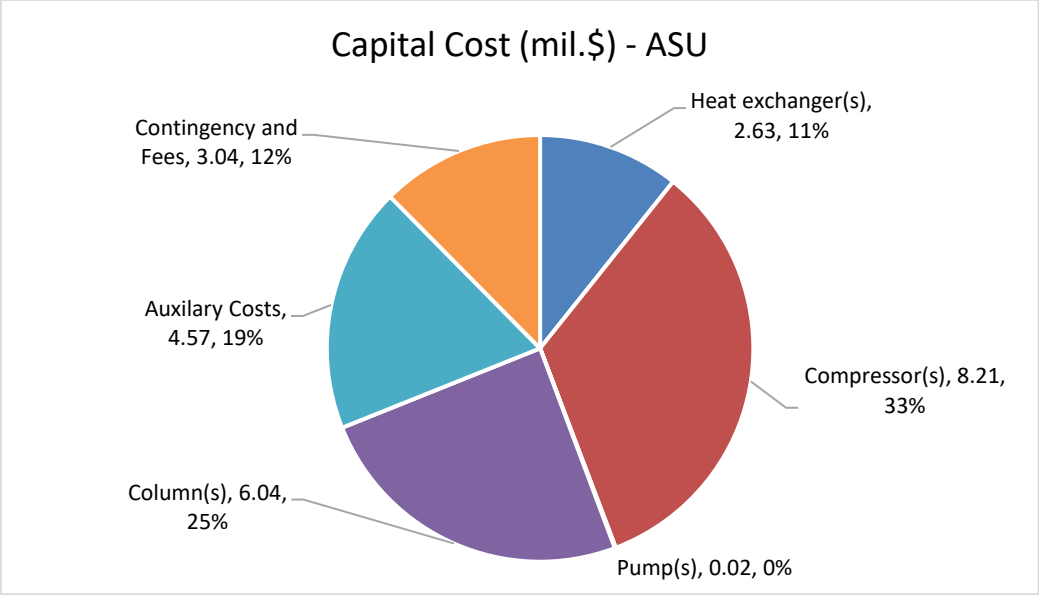

Figure 21: Capital cost distribution of ASU

3.3.6 Manufacturing Costs for ASU

3.3.6.1 Cost of Labour, Utilities and Raw Material

The electric power is required to drive the compressor. The rated electric power of all compressors is 3229 kW that consume 25828623 kWh/yr. This corresponds to electric utility cost $5424011/yr and a specific power of 0.314 kWh/kg of Nitrogen. Furthermore, the daily cooling water consumption is set as 507279 kg/day. This corresponds to annual water consumption of 185157 m^3 and an annual water procurement cost of $412900.

Moreover, the cost of labour is estimated as per approach discussed in section 3.1.2.1. Using equation 11 and 12, N_{NP} for ASU is 10 and N_{OL} is 2.93. Hence, the total number of operators employed are 14 and the annual labour cost is $758744.

Note: The tariffs and approach are the same as used in section 3.2.7

3.3.6.2 Cost of Manufacturing

The annual cost of manufacturing is estimated using equation 9 for ASU is $12.20 million. This accounts for annual miscellaneous costs, shown in table 9, of $4.50 million and annual depreciation of $1.10 million, which is based on a salvage value of $2.45 million of ASU at the end of project life.

Similarly, the annual manufacturing cost of ASU, operating on renewable energy, is $6.77 million with an annual miscellaneous cost of $4.50 million and constant annual depreciation as calculated above.

3.4 SMR

SMR varies from industry to industry as per requirement of that specific plant. From the process discussed in section 2.1.1, some common process equipment include compressor, desulpurization unit, reformer reactor, shift reactors, condensate removal unit, carbon dioxide removal or conversion unit and heat exchanger. The designs of industrial scale SMR unit are extensive making it beyond the scope of this thesis, so a preliminary analysis will be based on process simulations based on available literature [27] [28] [90] [91].

The high purity hydrogen required for HBP is produced from SMR plant at a rate of 53.3 tons per day. SMR plant is modelled using simulation software called DWSIM. The process is simulated for required hydrogen flowrate and purity. Once the plant is sized and simulated, the equipment are sized and economic estimation is carried out as discussed in section 3.1.

Natural gas is reformed to produce hydrogen as shown in figure 22 and 23. The process parameters (flowrates, temperature and pressure) are based on [27] [28] [90] [91] shown in stream tables A.11 – 17 in annex 1. The process, as discussed in detail in section 2.1.1;

- Compresses natural gas
- Removal of hydrogen sulphide in a desulphurization unit
- Mixing with steam
- Production of carbon monoxide and hydrogen in reforming section
- Increase in the production of hydrogen in shift reactors
- Removal of condensate
- Removal of carbon dioxide in a scrubber and methanator
- Removal of remaining condensate before feeding to HBP.

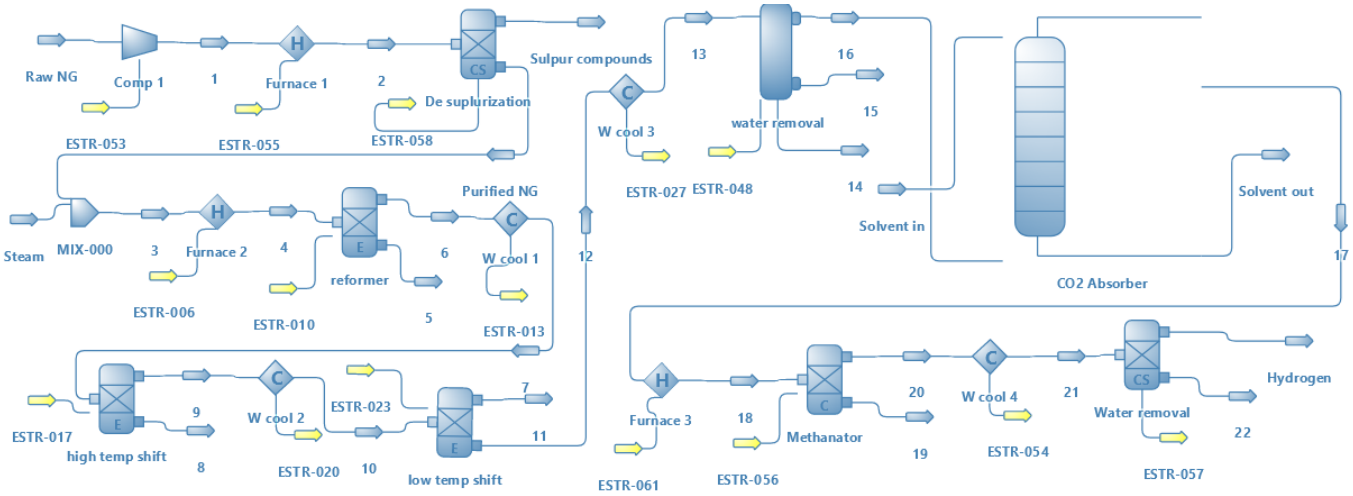

Figure 22: SMR flowsheet generated in DWSIM

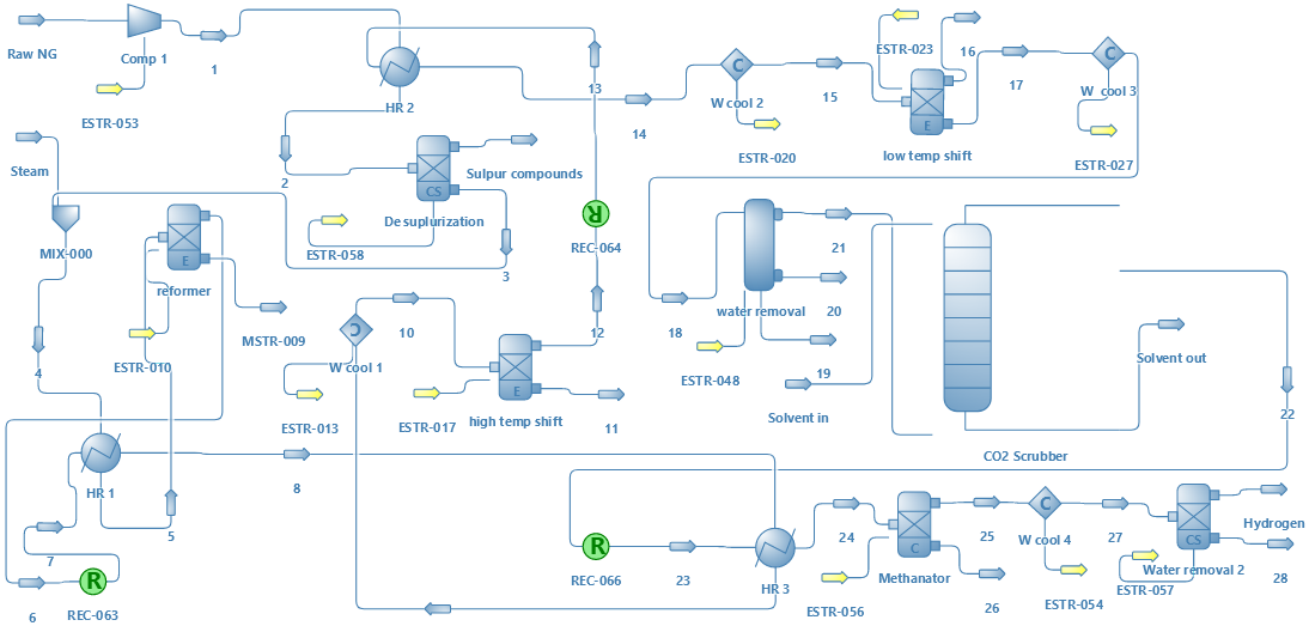

Figure 23: SMR flowsheet with heat recovery generated in DWSIM

The process produces hydrogen with a purity of 97.3% containing traces of methane which is inert in HBP loop. In figure 25, the heat exchangers (HR1, HR2 and HR3) acts as a heat recovery unit and decrease the load on furnace. Although heat recovery is technically feasible, this comparison will help in identifying whether heat recovery is economically feasible or not.

Note: Natural gas is fed at 13.79 bar [92] and is assumed to be containing only methane as a hydrocarbon.

3.4.1 Compressor Cost Estimation

The compressor cost estimation is based on shaft power as discussed in section 3.2.1. The shaft power is calculated using equation 13 and 16, where the isentropic efficiency of Comp 1 is 75%. Similarly, Electric power to drive electric motor drives can be calculated using equation 17.

The cost of compressor is depended only on material of construction as mentioned in section 3.2.1.1. The material compatibility is checked from table 4-28 from [64]. Hydrogen, hydrogen sulphide, water vapours, and methane are compatible with carbon steels (CS) and stainless steel (SS), while carbon dioxide is not compatible with carbon steels at temperatures lower than 200°C and may damage the equipment. Carbon dioxide is compatible with SS, aluminium based alloy, copper based alloy or nickel based alloy at higher temperatures. Since the temperature of natural gas is lower than 200°C during compression stage, the compressor is assumed to be made from carbon steel.

After selecting the material, the power rating of compressor and motor drive are taken from DWSIM flowsheet. The power rating of compressor and motor drive is 242kW and 254kW respectively. Bare cost module factor for compressor and for enclosed electric drives is 2.8 and 1.5 respectively (same for both conditions). The capital costs incurred in buying and installing centrifugal compressors and enclosed electric motors are $388543 and $131793 respectively (same for both operating and base conditions).

3.4.2 Furnace Cost Estimation

Furnace cost estimation is based on heat duty as discussed in section 3.2.3. The heat duty is calculated using equation 15, 20 and 21. The efficiency of furnace, η_F, is for SMR process is assumed to be 85%.

The heat duties, Q_C, for Furnace 1, Furnace 2 and Furnace 3, as per DWSIM flowsheet shown in figure 22, are 1187 kW, 3429 kW and 3297 kW respectively. These heat loads are summed together to procure one common furnace with a load of 7929 kW.

The material compatibility, material factor, pressure factor, base module factor and f.o.b costs are already discussed in section 3.2.3.1. The capital costs incurred in buying and installing furnace in 2019 for operating condition and base condition are $3292836 and $2352026 respectively.

3.4.3 Heat Exchanger Cost Estimation

The heat exchanger (W cool 1 - 4), shown in figure 22 and 23, are assumed to be cool process gases by water. The cooling water, for W cool 1 and 2, is assumed to enter the heat exchangers in the intercoolers at a temperature of 293.15 K and leaving at 323.15 K. Similarly, the cooling water, for W cool 3, enters at 293.15 K, and leaves at 305.15 K and, for W cool 4, the water enters at 293.15 K and leaves at 297 K.

Table 27: Heat transfer area for heat exchangers

Equipment Name	**Q (kW)**	**LMTD**	**A_{EX} (m2)**
W cool 1	11661	586	66
W cool 2	3914	270	48
W cool 3	5668	70	269
W cool 4	3484	73	159
HR 1	2887	365	158
HR 2	1009	157	128
HR 3	2802	577	97
W cool 1*	5187	453	38
W cool 2*	2739	243	38
W cool 3*	5395	70	256
W cool 4*	3483	73	159

The heat recovery units HR 1, HR 2 and HR 3, shown in figure 23, are utilised to recovery waste from high temperature process gas from the outlet of reformer reactor and high temperature shift reactor to heat the process gas entering the desulpurization process, reformer reactor and methanator reactor.
The intercooling heat exchangers are assumed to be floating head shell-in-tube heat exchangers. The heat transfer area, A_{EX}, of heat exchanger, shown in table 27, can be calculated using equation 15, 18, 19, table 11, the cooling load requirements and temperature of gases (from DWSIM flowsheet).

The material compatibility, material factor, pressure factor, base module factor and f.o.b costs are already discussed in section 3.2.2.1. The capital costs incurred in buying and installing heat exchangers in 2019 for operating condition and base condition are shown in table 28.

Note: W cool 1*, W cool 2*, W cool 3* and W cool 4* represents heat exchanger in SMR process heat recovery units. Heat exchanging efficiency of W cool 1 - 4 is assumed to be 90% with a pressure drop of 0.5 bar.

Table 28: Heat exchanger cost estimation

Equipment Name	Pressure (bar)	F_P	F_M	F_{BM}	F_{BM}^o	A_{EX} (m^2)	Cost in 2019 ($) for operating conditions	Cost in 2019 ($) for base conditions
W cool 1	20.5	1.07	1.8	4.83	3.29	66	160716	109505
W cool 2	18.5	1.07	1.8	4.81	3.29	48	147223	100650
W cool 3	18.5	1.06	1.8	4.80	3.29	269	323794	222118
W cool 4	14.5	1.04	1.8	4.73	3.29	159	229877	159901
HR 1	29	1.11	2.75	6.72	3.29	158	325635	159486
HR 2	30	1.12	2.75	6.74	3.29	128	293035	143042
HR 3	19.5	1.07	2.75	6.49	3.29	97	248562	125966
W cool 1*	18.5	1.06	1.8	4.80	3.29	38	140406	96316
W cool 2*	16.5	1.05	1.8	4.76	3.29	38	139439	96316
W cool 3*	15.5	1.04	1.8	4.75	3.29	256	309661	214644
W cool 4*	14.5	1.04	1.8	4.73	3.29	159	229877	159901

3.4.4 Reactor and Separator Cost Estimation

Water condensate is removed twice in the SMR process as shown in figure 22 and 23. Separator drum 1 removes condensate after low temperature shift process and Separator drum 2 removes condensate before feeding hydrogen to HBP. The drums are designed using equation 25, 26 and 27 with length to diameter ratio in the range of 3 - 5. The final dimensions of Separator drum 1 and Separator 2 are shown in table 29.

The desulphurization unit removes hydrogen sulphide from natural gas, while reforming reactor and shift reactors allows conversion of natural gas into hydrogen for specified inlet conditions (temperature, pressure and concentrations of feed gases). Natural gas is mixed with steam in the ratio between 1:2.4, while in industries the ratio ranges from 1:1 to 1:3 [27]. The amount of methane reformed to hydrogen is approximately 98%.

Table 29: Sizing of Desulphurization unit, Separator drums and Reactors

Equipment Name	Diameter (m)	Height (m)	Volume (m3)
Desulphurization unit	1	1	0.79
Separator drum 1	0.97	3.1	2.3
Separator drum 2	0.62	1.9	0.57
Reformer reactor	1	1.3	1.02
HTS reactor	2.2	0.53	2
LTS reactor	2.2	0.53	2
Methanator reactor	2.2	0.53	2

Table 30: Cost estimation of Desulphurization unit, Separator drums and Reactors

Equipment	Pressure (bar)	F_P	F_M	F_{BM}	F_{BM}^o	Capacity, Units	Cost in 2019 ($) for operating conditions	Cost in 2019 ($) for base conditions
Desulphurization Unit	29	3.3	3.1	20.67	4.07	0.79 m^3	103844	20450
Separator Drum 1	18	2.2	3.1	14.39	4.07	2.3 m^3	103643	29319
Demister Pad (Drum 1)	-	-	-	1	1	0.79 m^2	2304	2304
Separator Drum 2	14	1.3	3.1	9.69	4.07	0.57 m^3	36746	15435
Demister Pad (Drum 2)	-	-	-	1	1	0.30 m^2	1825	1825
Reformer Reactor	28	3.2	3.1	20.12	4.07	1.02 m^3	97688	19762
HTS Reactor	20	4.7	3.1	28.58	4.07	2 m^3	192600	27426
LTS Reactor	19	4.5	3.1	27.39	4.07	2 m^3	184570	27426
Methanator Reactor	15	3.6	3.1	22.64	4.07	2 m^3	152569	27426

The reactions taking place in reforming and shift reactors are reversible. DWSIM uses the concept of

minimization of Gibbs free energy to calculate the reaction extent as discussed in section 3.2.4. Since in-depth reaction kinetics are not known, the reforming and high temperature shift reactors are sized by interpolation of low scale and high scale SMR plants by National Renewable Energy Technology [91] and by using Ulrich et. al [64] approach. A similar approach is used in sizing desulphurization unit. The dimensions of reactors are shown in table 29.

Moreover, methanator reactor is used as a conversion reactor in DWSIM with 99.99% conversion of carbon dioxide and carbon monoxide into methane from the process gases to simplify the approach [90].

The material compatibility, material factor, pressure factor, base module factor and f.o.b costs are already discussed in previous sections. The capital costs incurred in buying and installing the units, shown in table 29, in 2019 for operating condition and base condition are shown in table 30.

Note: The size of LTS reactor and Methanator reactor is assumed to be same as that of HTS reactor. Similarly, the volume of the reactors is assumed to cylindrical.

3.4.5 Steam Boiler Unit Cost Estimation

The steam boiler system is employed to provide process steam for reforming purposes and to provide heat duty in carbon dioxide scrubber (section 3.4.6). The steam in the process is at a pressure of 29 bar and temperature of 783.15 K. To simplify the approach, steam system is not included in the DWSIM flowsheet and analysed separately. Moreover, the water is taken at 298.15 K and at ambient pressure inside the boiler system, which is using natural gas as a fuel.

The increase in temperature takes in a steam generator while increase in pressure is provided by pumps. The pump power, to increase the pressure of water to 29 bars, is calculated using equation 31 and equation 32. The pumping system is assumed to have a global efficiency of 80%.

The amount of heat gained by the water to form superheated can be calculated using equation 33, where h_2 is the enthalpy (kJ/kg) of superheated steam at 783.15 K and h_1 is the enthalpy (kJ/kg) of water at 298.15 K.

$$\boldsymbol{Q_W} = \dot{m}(\boldsymbol{h_2} - \boldsymbol{h_1}) \quad \textbf{(33)}$$

The amount of natural gas required to provide boiler heat duty, Q_C, is calculated by using equation 20 and 21, while assuming a boiler efficiency of 85%.

The material for steam generator and pumps is carbon steel as per material compatibility discussed in previous sections. The material factor, F_M, and the pressure factor, F_P, for pumps are taken from the appendix A of [61]. The bare module cost factors, both for operating conditions (F_{BM}) and base conditions (F_{BM}^O), for pumps calculated from equation 5 and table 7. Similarly, for steam generator, F_P is calculated

using equation 3, while F_{BM} and F_{BM}^{O} are taken from the appendix A of [61]. However, there is another factor to take into account for boiler cost estimation, as boiler superheat the steam. The boiler superheat correction factor, F_T, is calculated using equation 34, where ΔT is the amount of superheat in °C [61].

$$F_T = 1 + 0.00184\Delta T + 0.00000335\,(\Delta T^2) \quad \textbf{(34)}$$

The f.o.b costs for pump and boiler are calculated using equation 1. F.o.b costs are converted to operating conditions and base conditions by using equation 5 for pumps and equation 35 for boiler.

$$C_{BM} = C_P^{\circ} F_{BM} F_P F_T \quad \textbf{(35)}$$

Finally, the prices are converted to 2019 using the CEPCI index as the prices are in year 2001 from [61]. The cost factors and capital costs incurred in buying and installing the pumps and boilers, for operating and base conditions are shown in table 32.

Table 32: Cost estimation of Steam Generation System

Equipment	Pressure (bar)	F_T	F_P	F_M	F_{BM}	F_{BM}^{o}	Capacity, Units	N	Cost in 2019 ($) for operating conditions	Cost in 2019 ($) for base conditions
Pumps	30	-	1	1.5	3.92	3.24	28 kW	1	36843	30491
Boilers	29	1.25	1.21	-	2.2	2.2	7714 kW	4	19774203	19774203
Pumps*	30	-	1	1.5	3.92	3.24	28 kW	1	36843	30491
Boilers*	29	1.25	1.21	-	2.2	2.2	7805 kW	4	20002582	20002582

Note: N represents the number of units while * represents system SMR with heat recovery unit.

3.4.6 Carbon Dioxide Scrubber Cost Estimation

The carbon dioxide scrubbers are complex and need to be represented on a model of its own. Since scope of thesis focuses on SMR, the simulation, removing approximately 95% of carbon dioxide, considers carbon dioxide scrubber as a ‘black box’. The standard model, shown in figure 24, for carbon dioxide scrubber is considered for cost estimation purposes by Even Birkelund [93].

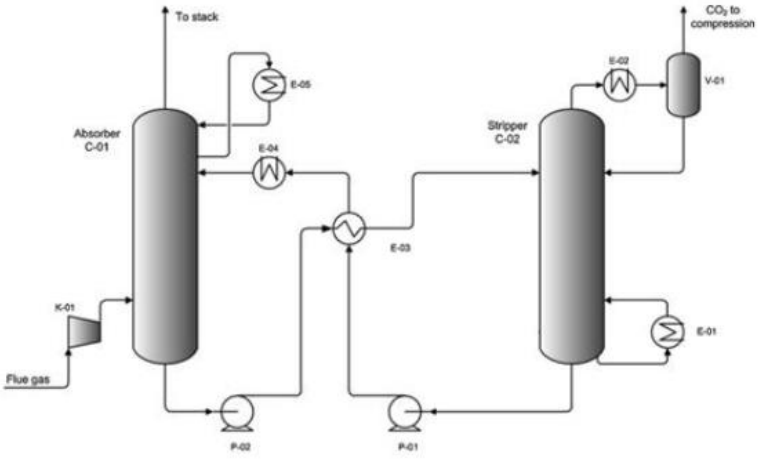

Figure 24: Simplified flowsheet of a standard carbon dioxide scrubber [93]

The scrubber uses monoethanolamine (MEA) as an amine solution to absorb carbon dioxide. The technical and economic details of the standard model [93] are shown in table 33. The capital cost of the scrubber includes the cost of pumps, heat exchangers, absorber column, and stripper column. The model removes kg CO_2 per year is scaled down to kg of CO_2 using equation 36. Moreover, the cost is estimated in 2013, it is inflated to 2019 using CEPCI index as per equation 2 [61].

$$\mathbf{C_2 = C_1 \left[\frac{S_2}{S_1}\right]^{0.6}} \quad \textbf{(36)}$$

Where, C1 and C2 represents the capital cost of the plants, S1 and S2 represents the respective production capacity. Thus, capital costs incurred in buying and installing the scrubber for operating conditions is $22565067. To simplify the approach, the cost for base conditions is assumed to be that of operating conditions.

Table 33: Techno-economic details of a standard CO2 scrubber [93]

Equipment Name	**Standard carbon dioxide scrubber**
Solvent	MEA
Amount of CO_2 removed (ton/year)	1.15×10^6
Boiler Duty (MJ/kg of CO_2 removed)	4.3
Pump Duty (kJ/ kg of CO_2 removed)	3.78
Operating hours (hours/year)	8400
Total Capital Investment 2013 ($)	88283192

3.4.7 Total Capital Costs for SMR

The capital cost of SMR and SMR with heat recovery (SMR-HR) that is total module cost, C_{TM}, and the grass root equipment, C_{GR}, are calculated from equation 6 and equation 7. Table 34 shows C_{TM} and C_{GR} for both units. Similarly, the capital cost distribution equipment and cost component wise for SMR systems are shown in figure 25 and 26.

Table 34: Capital costs of SMR units

Unit Name	C_{TM} (mil. $)	C_{GR} (mil. $)
SMR	56.55	79.56
SMR-HR	53.91	76.05

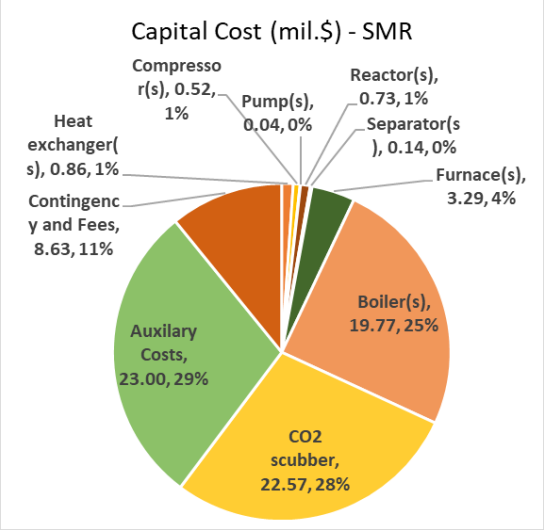

Figure 25: Capital cost distribution of SMR

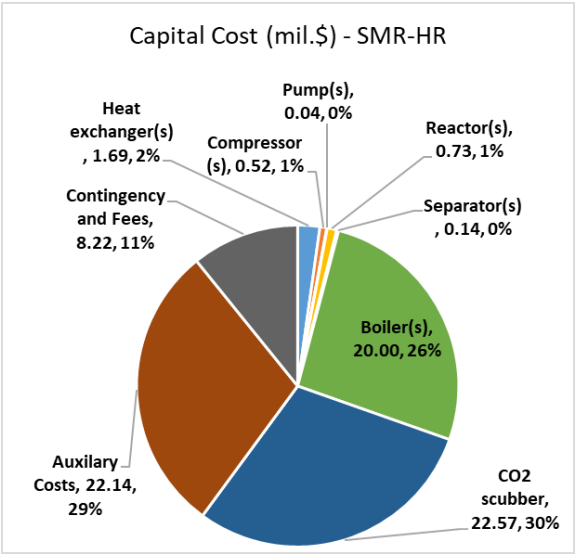

Figure 26: Capital cost distribution of SMR-HR

3.4.8 Manufacturing Cost

The total manufacturing cost, based on the same approach as discussed in section 3.1.2 and used in section 3.2.7, for SMR plants are shown in table 35.

Table 35: Manufacturing costs of SMR units

Process	SMR	SMR-HR
Annual Water Consumption (m^3/yr)	614510	527128
Annual Cost of Water (mil. $/yr)	1.37	1.18
Annual Electricity Consumption (kWh/yr)	2370796	2370796
Annual Cost of Electricity (mil. $/yr)	0.50	0.50
Annual Heat Load (kWh/yr)	510074320	443032000
Annual Cost of Natural Gas (mil. $/yr)	36.31	34.04
Mass of Natural Gas (kg/yr)	82689625	77499252
N_{NP}	16	20
N_{OL}	3.16	3.19
Annual Labour Cost ($/yr)	0.81	0.81
Mass of Carbon dioxide (kg/yr)	99709328	86603895
Carbon Tax (mil. $/yr)	1.12	0.97
Salvage Value (mil. $)	7.96	7.61
Depreciation (mil. $/yr)	3.58	3.42
Miscellaneous Cost (mil. $/yr)	12.60	12.09
Manufacturing Cost (mil. $/yr)	56.30	53.01

Note: Carbon emission from natural gas reformed are usually utilized in the formation of urea in an ammonia plant and hence are not considered in carbon emissions.

3.5 Alkaline Electrolyser System

The alkaline electrolyser system is the most mature electrolytic technology to produce hydrogen. The alkaline electrolyser systems of today are able to produce 485 Nm^3/h of hydrogen with an energy consumption of 4.85 kWh/ Nm^3 of H_2 [26] [94]. The techno-economic details of current electrolyser system are discussed in section 2.1.2. The baseline case selected for the thesis is Norsk Hydro Atmospheric Type No. 5040 (5150 Amp DC), as the techno-economic details conforms to the current alkaline electrolyser shown in table 36.

Table 36: Techno-economical details of baseline case [17] [10] [94] [95]

Equipment	**Norsk Hydro Atmospheric Type No. 5040**
Cell temperature (ºC)	80
Production pressure (bar)	30
Electrical efficiency (% HHV)	73
Conversion efficiency (%)	80
Water requirement (l/hr)	485
Hydrogen Production	485 N m^3/hr; 43.59 kg/hr
Oxygen Production	242.5 N m^3/hr; 346.51 kg/hr
System Power Requirement (kW)	2330
Specific energy consumption	4.8 kWh/ N m^3; 53.5 kWh/kg
Operating Life	7 - 10 years; 60,000 - 90,000 hours
Cost Installed (USD / kW)	1000
Capital Replacement	25% direct installation cost

3.5.1 Mechanical Vapor Compression

The MVC system are complex and need to be represented on a model of its own. Since scope of thesis focuses on the electrolyser system, the model put forward by Morgan et. al [17] is used. The model has a specific power consumption of 22.45 kWh/m^3 of water desalinated. Moreover, the grass root cost, C_{GR}, can be calculated using equation 37 [17] [30].

$$\mathbf{C_{GR}} = (\frac{\mathbf{3}}{\mathbf{200}}\boldsymbol{\dot{m}}_{\mathbf{water}} + \mathbf{4.5}) \times \mathbf{10^6} \quad \textbf{(37)}$$

Where, $\dot{m}_{water}$ represents the distil water flowrate in ton/day.

3.5.2 Total Capital Costs for Alkaline Electrolyser System

The hydrogen required for 300 ton/day ammonia is around 53.3 ton/day, which corresponds to approximately 24887.54 Nm^3/hr or 2220.83 kg/hr. This corresponds to approximately 51 modules of Norsk electrolyser, as shown in table 36, with a water requirement of 24735 kg/hr. The capital cost, C_{GR}, of the electrolyser system can be calculated by incorporating 17% of direct installed capital to account for site preparation, engineering and design, project contingency and permit fees [96]. The table 37 below shows the capital cost estimated for MVC and alkaline electrolyser system.

Table 37: Capital cost estimated for alkaline electrolyser system

Unit Name	**C_{GR} (mil. $)**
MVC	13.40
Alkaline Electrolyser Modules	139.03

3.5.3 Total Manufacturing Costs for Alkaline Electrolyser System

The total manufacturing cost, based on the same approach as previously discussed, for Alkaline electrolyser plant is shown in table 38. The water required for electrolysis and electricity required for desalination and electrolysis are supplied through renewable energy technology.

Moreover, the number of operators required for MVC and Alkaline electrolyser are based on Morgan et. al [17] and Ramsden et. al [95]. However, it is assumed that the wage of a chemical operator is same as that of one operating electrolyser system.

Furthermore, the oxygen is produced is very pure which has a variety of application in industries and is

also used extensively in hospitals and medical facilities. The oxygen can be sold to a local or international supplier. The selling price of oxygen is taken approximately $150/ton [97].

Note: Life of alkaline electrolyser stack is assumed to be 10 years.

Table 38: Manufacturing costs of Alkaline Electrolyser Plant

Process	MVC	Alkaline Electrolyser System
Annual Water Supplied (kg/yr)	197880000	197880000
Annual Electricity Consumption (kWh/yr)	4442406	955681536
N_{NP}	4	-
N_{OL}	2.69	10
Annual Labour Cost (mil. $/yr)	0.70	0.54
Annual Oxygen Production (kg/yr)	-	141376080
Annual Oxygen Revenue (mil. $/yr)	-	21.21
Salvage Value (mil. $)	1.34	13.90
Depreciation (mil. $/yr)	0.6	12.51
Miscellaneous Cost (mil. $/yr)	2.81	20.96
Manufacturing Cost (mil. $/yr)	4.12	12.81

3.6 PEM Electrolyser System

PEM electrolyser system are a commercial technology to produce hydrogen as an alternate to alkaline electrolyser. PEM electrolyser stack of today is able to produce 10 Nm^3/h of hydrogen with an energy consumption of 6.3 kWh/ Nm^3 of H_2 [26] [94]. The techno-economic details of current electrolyser system are discussed in section 2.1.2. A baseline case is selected as PEM modules for this thesis and the techno-economic, shown in table 39, details conforms to the current PEM electrolyser shown in table 1.

Note: The technical data is based on Proton Hogen 380.

Table 39: Techno-economical details of baseline case [10] [94] [98]

Equipment	PEM Electrolyser
Cell temperature (ºC)	60
Production pressure (bar)	14
Electrical efficiency (% HHV)	56
Conversion efficiency (%)	95
Water requirement (l/hr)	8.4
Hydrogen Production	10 N m^3/hr; 0.9 kg/hr
Oxygen Production	5 N m^3/hr; 7.1 kg/hr
System Power Requirement (kW)	63
Specific energy consumption	6.3 kWh/ N m^3; 70.1 kWh/kg
Operating Life	5 – 7 years; 30,000 - 90,000 hours
Cost Uninstalled (USD / kW)	1200
Capital Replacement	25% direct installation cost

3.6.1 Total Capital Costs for PEM Electrolyser System

The hydrogen required for 300 ton/day ammonia is around 53.3 ton/day, which corresponds to approximately 2220.83 kg/hr. This corresponds to approximately 2468 modules of PEM electrolyser, as shown in table 39, with a water requirement of 20723 kg/hr. The capital cost, C_{GR}, of the electrolyser system can be calculated by taking an installation factor of 1.12 and by incorporating 17% of direct installed capital to account for site preparation, engineering and design, project contingency and permit fees [98]. The table 40 below shows the capital cost estimated for MVC and PEM electrolyser system.

Table 40: Capital cost estimated for PEM electrolyser system

Unit Name	C_{GR} (mil. $)
MVC	11.96
PEM Electrolyser Modules	232.85

3.6.2 Total Manufacturing Costs for PEM Electrolyser System

The total manufacturing cost, based on the same approach as previously discussed, for PEM electrolyser plant is shown in table 41.

Table 41: Manufacturing costs of PEM Electrolyser Plant

Process	MVC	PEM Electrolyser System
Annual Water Supplied (kg/yr)	165849600	165849600
Annual Electricity Consumption (kWh/yr)	3723324	1254332016
N_{NP}	4	-
N_{OL}	2.69	10
Annual Labour Cost (mil. $/yr)	0.70	0.54
Annual Oxygen Production (kg/yr)	-	140182400
Annual Oxygen Revenue (mil. $/yr)	-	21.03
Salvage Value (mil. $)	1.20	23.29
Depreciation (mil. $/yr)	0.54	29.94
Miscellaneous Cost (mil. $/yr)	2.60	34.65
Manufacturing Cost (mil. $/yr)	3.85	44.11

Note: The number of operators required for PEM electrolyser are based on Ramsden et. al [98] and the life of PEM stack is assumed to be 7 years.

3.7 Onshore Wind Power

Onshore Wind Power is a commercial technology to produce renewable energy as discussed in section 2.4. Recent studies by Fraunhofer Institute [99] show that the technology have a LCOE of €0.0399/kWh

- €0.0823/kWh in Germany. The analysis was based on wind turbines with a rated capacity of 2 – 4 MW and 1800 – 3200 full load hours (FLH). The techno-economic details of onshore wind in Germany are shown in table 42

Table 42: Techno-economical details of onshore wind [99]

Equipment	Onshore Wind
LCOE (€/kWh)	0.0399 - 0.0823
FLH (hrs)	1800 – 3200
Capital Expenditure (€/kW)	1500 – 2000
Operation Expenditure Direct (€/kW)	30
Operation Expenditure Variable (€/kWh)	0.005

Note: The currency conversion rate from euro to dollar is taken as 1.12.

3.7.1 Capital and Operating Costs for Onshore Wind Farms

The electricity generated using the wind far is used to drive air separation units, electrolyser stacks and HBP loop. LCOE is calculated using equation 38.

$$LCOE = \frac{I_o + \sum_{t=1}^{n} \frac{A_t}{(1+i)^t}}{M} \quad \textbf{(38)}$$

Where, I_O is the capital investment, A_t are the operating costs, n is the project life (20 years), i is the discount factor taken as 3% [100] and M is overall energy production from the farm over the entire life of the project.

To simplify the approach, the tecno-economic data as per studies conducted by Fraunhofer Institute [99] is used. The coastal areas of Germany have wind speed is around 7.3 m/s at a hub height of 120m. The FLH are 3200 hours and the capital expenditures are €1900/kWh. Table 43 shows the capital and operating expenditures of wind farms to supply different ammonia plants.

The electric power produced from wind farms is used to power electrolyser system, ASU, MVC, ammonia storage system and EHBP(-HR). Power consumed by each unit is shown in figures 27 and 28

Table 43: Capital and operating cost of wind farms

Equipment	Wind Farm 1	Wind Farm 2	Wind Farm 3	Wind Farm 4
Power Production (kWh/yr)	1202928132	1081822094	1500859529	1379753491
Wind Farm Rated Power (kW)	375915	338069	469019	431173
LCOE (€/kW)	0.0404	0.0404	0.0404	0.0404
Capital Costs (mil. $)	799.95	719.41	998.07	917.54
Operating Costs (mil. $/yr)	19.37	17.42	24.16	22.21
Process Units	Alkaline Electrolyser, MVC, ASU, EHBP, Ammonia Storage System	Alkaline Electrolyser, MVC, ASU, EHBP-HR, Ammonia Storage System	PEM Electrolyser, MVC, ASU, EHBP, Ammonia Storage System	PEM Electrolyser, MVC, ASU, EHBP-HR, Ammonia Storage System

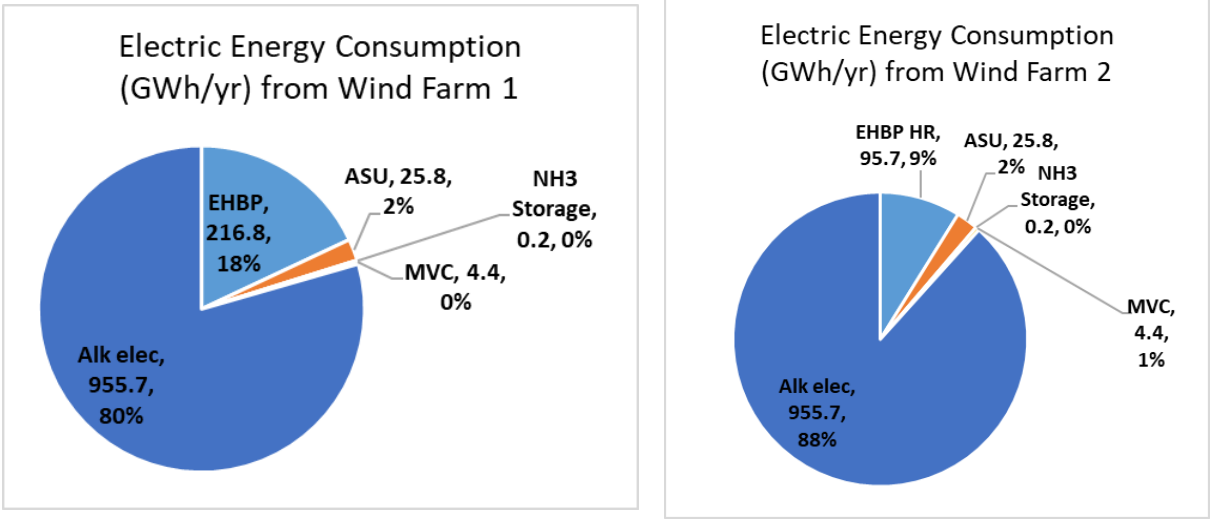

Figure 27: Electric power consumption by processes/units powered by Wind Farms 1 and 2

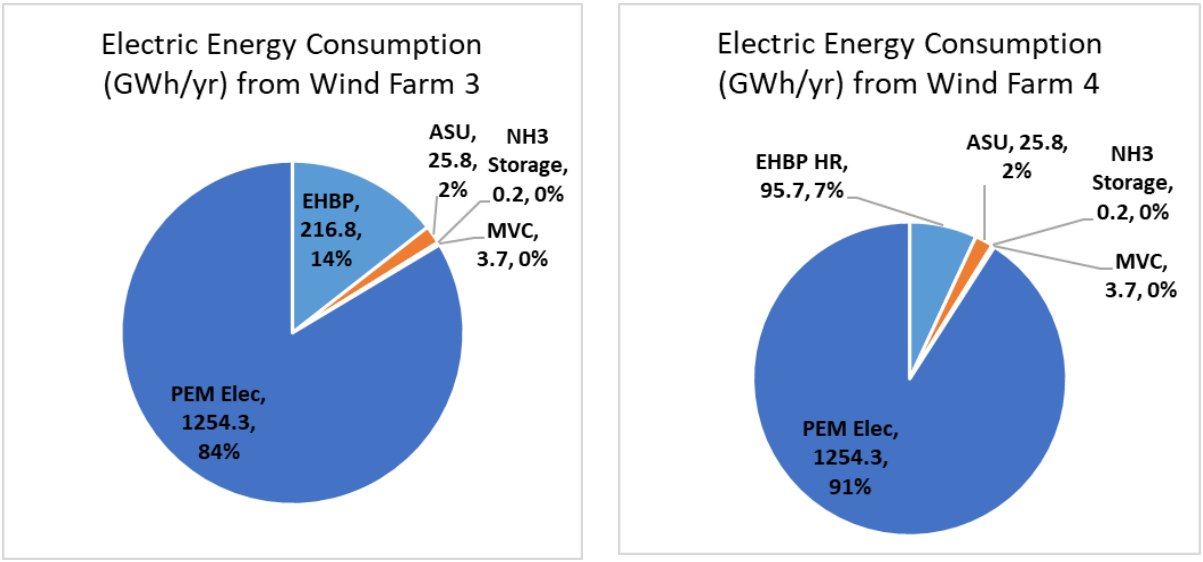

Figure 28: Electric power consumption by processes/units powered by Wind Farms 3 and 4

The figure 27 show that a major portion of energy produced from wind farms 1 and 2 is consumed by alkaline electrolyser, that is around 955.7 GWh/yr. This is followed by EHBP, which makes up 18% (216.8 GWh/yr) of power produced from wind farm 1. The rest 2% of power produced from wind farm 1 and 2 is used to drive ASU, MVC and ammonia storage system. Moreover, it can be noticed that by using a heat recovery unit the power consumed by EHBP reduces from 216.8 GWh/yr to 95.7 GWh/yr.

Similarly, figure 28 show that major portion of power produced by wind 3 and 4 is consumed by PEM electrolyser, that is around 1254.3 GWh/yr. It can also be noticed that PEM electrolyser consume 298.6 GWh/yr more power than alkaline electrolyser.

3.8 Levelized Cost of Ammonia

The levelized cost is an effective tool for comparing different production methods. LCOA helps in identifying different methods on the basis of investment required for producing a ton of ammonia. LCOA can be calculated using equation 39.

$$LCOA = \frac{I_o + \sum_{t=1}^{n} \frac{A_t}{(1+i)^t}}{A_M} \quad (39)$$

Where, A_M represents the amount of ammonia produced in tons for the entire project life. The other expressions are same as that in equation 38.

The capital and manufacturing costs of each unit are discussed in previous section and are shown in figures A.1-8 in annex 1. However, a holistic approach to compare the capital cost, manufacturing cost

and LCOA is shown in figure 29.

Table 44 shows LCOA for different methods, energy consumption per ton of ammonia and natural gas consumption per ton of ammonia.

Table 44: LCOA of different ammonia plants

Plant	LCOA ($/$t_{NH3}$)	Energy Requirements (kWh/t_{NH3})	Gas Consumption (GJ/t_{NH3})	Process Units
Ammonia Plant 1	883 761*	7809	44.6	SMR, ASU, HBP, Ammonia Storage System
Ammonia Plant 2	798 684*	5671	36.9	SMR-HR, ASU, HBP-HR, Ammonia Storage System
Ammonia Plant 3	961	12029	0.0	Alkaline Electrolyser, MVC, ASU, EHBP, Ammonia Storage System, Wind Farm 1
Ammonia Plant 4	917	10818	0.0	Alkaline Electrolyser, MVC, ASU, EHBP-HR, Ammonia Storage System, Wind Farm 2
Ammonia Plant 5	1366	15009	0.0	PEM Electrolyser, MVC, ASU, EHBP, Ammonia Storage System, Wind Farm 3
Ammonia Plant 6	1323	13798	0.0	PEM Electrolyser, MVC, ASU, EHBP-HR, Ammonia Storage System, Wind Farm 4

*represents LCOA without ammonia storage system, ASU and carbon tax.

Note: The levelized cost of hydrogen from SMR and SMR-HR plants are \$2.52/kg of H_2 and \$2.38/kg of H_2 respectively. This can be calculated using the same approach as discussed in section 3.8.

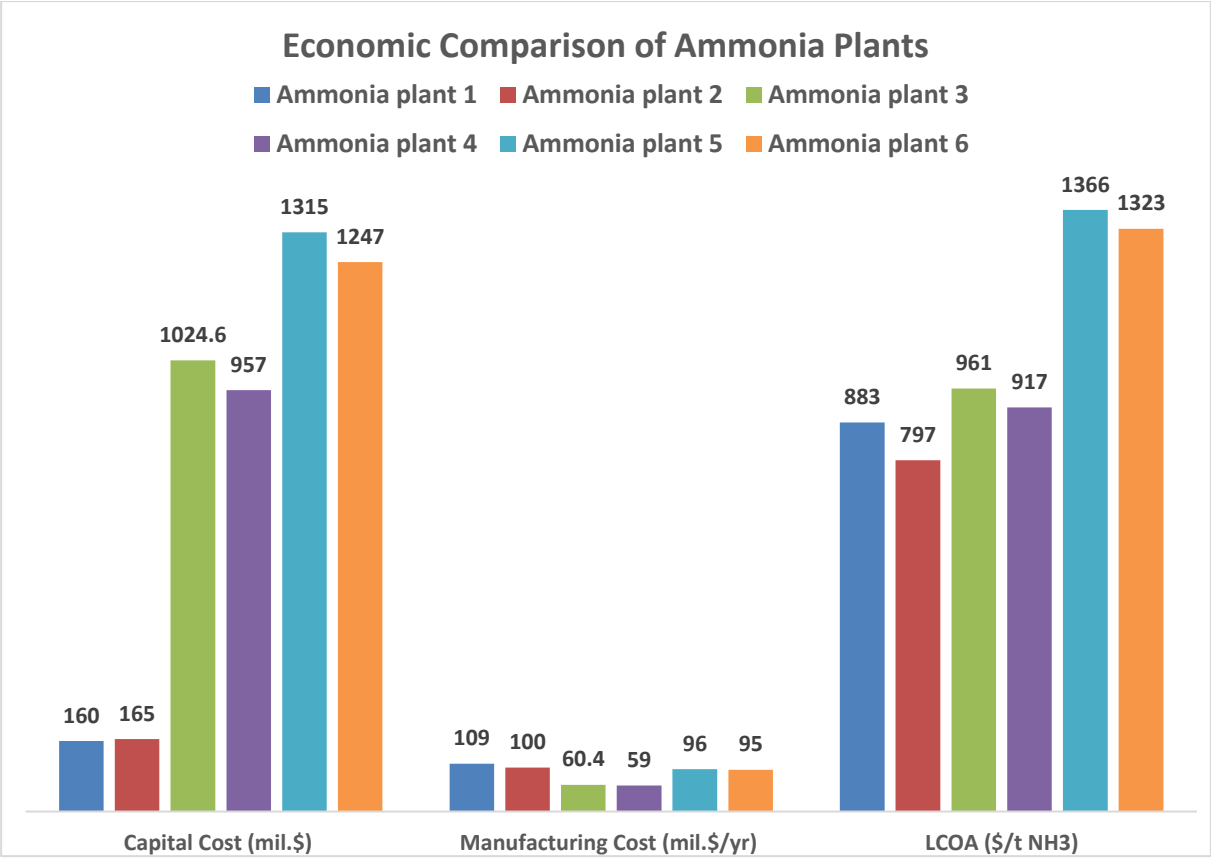

Figure 29: cost and LCOA comparison of different ammonia plants

3.9 Future of Green Ammonia Production

The research and development of water electrolyser will aid in increasing the efficiency of the stacks, size of the stack and life of the stack. Table 45 shows techno-economic data of Alkaline and PEM electrolysers in 2030 as per a study conducted by E4tech [31].

The capital and manufacturing cost of electrolyser system are calculated, as discussed in section 3.5 and 3.6, and are shown in section A.3.1 of annex 1. Moreover, the onshore wind farm power rating, capital cost and manufacturing cost, shown in section A.3.2 of annex 1, are based on studies conducted by Fraunhofer Institute [99]. The work by Fraunhofer Institute shows that the LCOE of onshore wind will be approximately €0.035/ kWh in Germany by 2030 [99].

Moreover, there is a predicted increase by the year 2030 in the cost of carbon tax (€30/ metric ton of carbon), natural gas (€0.0322/kWh) and electric tariffs (€ 0.0422/kWh) [9] [82] [99]. This in turn can have a significant impact on the production of ammonia through SMR-HBP. LCOA of ammonia plants in 2030, shown in table 44, can be recalculated using equation 39 and are shown in table 46.

Table 45: Commercial water electrolyser in 2030 [31]

Equipment	PEM Electrolyser	Alkaline Electrolyser
Cell temperature (ºC)	70	75
Production pressure (bar)	30	30
Electrical efficiency (% LHV)	71	66
System Power Requirement (kW)	6400	6700
Specific energy consumption (kWh/kg)	47	50
Project Life (years)	20	20
Capital Expenditure (€ / kW)	580	760
Operational Expenditure (€/ kW/year)	9	12

Table 46: LCOA of different ammonia plants in 2030

Plant	LCOA ($/t$_{NH3}$)	Process Units
Ammonia Plant 1	916	SMR, ASU, HBP, Ammonia Storage System
	787*	
Ammonia Plant 2	819	SMR-HR, ASU, HBP-HR, Ammonia Storage System
	714*	
Ammonia Plant 3	709	Alkaline Electrolyser, MVC, ASU, EHBP, Ammonia Storage System
Ammonia Plant 4	673	Alkaline Electrolyser, MVC, ASU, EHBP-HR, Ammonia Storage System
Ammonia Plant 5	670	PEM Electrolyser, MVC, ASU, EHBP, Ammonia Storage System
Ammonia Plant 6	635	PEM Electrolyser, MVC, ASU, EHBP-HR, Ammonia Storage System

*represents LCOA without ammonia storage system, and ASU.

Note: Manufacturing cost, salvage value and capital costs of all other units are assumed to be constant. Similarly, the discount factor is assumed to be constant at 3%. The conversion factor for euro to dollar is takes as 1.12. However, the selling cost for oxygen is not considered as future cost for oxygen is not under study.

4. Discussion and Conclusion

4.1 Summary

In this thesis, a preliminary cost estimation of 300 tonne per day ammonia plants is conducted that were built from “ground zero”. The thesis studies the technical and economic feasibility of producing ammonia powered by onshore wind and compare it with conventional ammonia synthesis process (using SMR and HBP). Ammonia production systems were thoroughly reviewed and process of HBP, ASU, SMR and ammonia storage system were simulated on DWSIM based on that literature. Similarly, techno-economic data, for alkaline and PEM electrolyser system to produce hydrogen for ammonia synthesis, is based on case studies by National Renewable Energy Laboratory. Moreover, techno-economic data on onshore wind is based on case studies by Fraunhofer Institute. Finally, levelized cost concept is used to model and compare the conventional ammonia synthesis with green ammonia synthesis.

The results of work are summarized below.

- LCOA from SMR-HBP configurations are $883/ton of ammonia and $798/ton of ammonia.
- While LCOA using onshore wind farm to power alkaline electrolyser, ASU and EHBP are $961/ton of ammonia and $917/ton of ammonia with heat recovery unit. Similarly, LCOA using onshore wind farm to power PEM electrolyser, ASU and EHBP are $1366/ton of ammonia and $1323/ton of ammonia with heat recovery unit.
- LCOA from alkaline and PEM electrolyser are higher due to higher capital costs of the electrolyser modules and, also due high electrical consumption by both electrolyser systems, higher capital costs of onshore wind farms.

The current economies show that SMR-HBP will continue to dominate ammonia synthesis market. This is can be attributed to the fact that SMR-HBP have a lower energy requirement and less capital intensive when compared to green ammonia plants. Moreover, scale and production capacity of plants are big compared to the current feasibility studies, current demonstration plants or green ammonia plants in the past. However, the research and development in water electrolyser technologies can shift the market towards the green ammonia in the future [31] [47].

The research in alkaline electrolyser is directed towards improving the performance of catalytic/electrode materials [31] [101]. The concept of porous electrodes adhered to diaphragm helps in reducing the distance and energy consumption. This zero-gap configuration results in avoiding bubbles and non-conductive film over the electrodes (which increases the energy consumption and gas transport through the diaphragm) [31] [101]. These advanced concepts results in increasing the current density of the electrolyser by up to 2 A/cm^2 and pressures up to 350 bar [101].

Similarly, PEM electrolyser systems need to be built from inexpensive materials having longer life and efficiencies comparable to that of alkaline electrolyser [31]. The existing challenge is directed towards the replacement of platinum group metals with non-noble electrocatalysts and the replacement of noble

catalyst in oxygen evolution reaction [31] [101]. Moreover, both water electrolyser systems need to be scaled up so they can gain economies of scale and be comparable to commercial SMR plants.

Furthermore, this transition from brown to green ammonia will also be depended upon a significant increase in carbon tax from \$11.21/ ton CO_2 to \$30/ton CO_2 (or more). However, the success of carbon capture and storage (CCS) both technically and economically can extend the time-period of this transition. The research is directed towards improving the performance of sorbents and chemicals, and removing the factors impeding the scaling up of CCS plant from lab scale to pilot scale. However, the barrier of safety plays a pivotal role in implementation CCS on a large scale [102].

Considering the reduction in capital costs (less than \$500/kW) and energy consumption of electrolyser (less than 4.5 kWh/kg of H_2), followed by a significant increase in carbon tax in the future (more than \$50/ton of CO_2), green ammonia can be more economically feasible in the future as shown by results below;

- LCOA in 2030 from SMR-HBP configurations are \$916/ton of ammonia and \$819/ton of ammonia .
- LCOA in 2030 using onshore wind to power alkaline electrolyser, ASU and EHBP, are \$709/ton of ammonia and \$673/ton of ammonia with heat recovery unit.
- LCOA in 2030 using onshore wind to power PEM electrolyser, ASU and EHBP, are \$670/ton of ammonia and \$635/ton of ammonia with heat recovery unit.

4.2 Recommendations

This thesis is can be improved by;

- The ammonia reactor, reformer reactor, shift reactors and methanator reactor should be based on chemical kinetics in presence of catalyst similar to that based on commercial and industrial scale.
- ASU, SMR and HBP systems are quite complex with different configuration of the equipment and different operating conditions. The thesis approximates the process based on data provided by the literature and only incorporates the major equipment in the process. The auxiliary equipment costs are taken as a fraction of the major equipment cost to simplify the cost estimation. However, a detailed economic and technical model should be developed as per industrial standards.
- All processes and systems are considered individually and in a steady state. Since ammonia synthesis process is complex, the system should be studied dynamically as it depended upon other process to produce hydrogen and nitrogen. A holistic approach should be used to model the system instead of an individualistic one. This can aid in heat and power integration to improve the system efficiency.
- Similarly, there are no connections to the grid for onshore wind farm powering the green ammonia plants. In reality, power is given to and taken from the grid for constant production of ammonia. Alternate scenario would be production of ammonia when power is produced from onshore wind farm. In that case, ramp up and ramp down of processes and system should be considered.

- The models have not been validated, however, recently the successful operation of a demonstration plant in Oxford show that wind energy can be used to power electrolyser stacks, ASU, and HBP to produce ammonia.
- The scale of chemical plant is small compared to existing ammonia plants that operate at a production capacity of 3000 tonnes/day. To keep the comparison fair and in balance, one approach is to calculate LCOA of SMR-HBP plant producing 3000 tonne/day ammonia and compare it with LCOA of 300 tonne/day ammonia plant operating on onshore wind and water electrolyser.
- Another factor to consider while doing LCOA calculation in the future is to include the projected economies of CCS technology. This approach can portray a clear picture whether green ammonia or brown ammonia will dominate the market.

Annex 1. Stream Data, Future Cost Estimation and Cost Distribution

Annex 1 is divided into three section. Section A.1 shows stream data of processes simulated using DWSIM chemical process software. The flowsheets in shown in figures 15,16,17, 22, 24 and 25 for HBP, HBP-HR, Ammonia storage system, ASU, SMR and SMR-HR processes. The stream data includes thermodynamic properties and mass flowrate for each stream as shown in Table A.1-17.

Section A.2 will include figures showing capital cost and manufacturing cost distribution of ammonia plants 1-6 as shown in table 44. Moreover, section A.2 shows the capital and manufacturing costs estimation of onshore wind farm, alkaline electrolyser and PEM electrolyser based on case studies by E4tech [31] and by Fraunhofer Institute [99].

A.1 Stream Tables

Table A.1: Stream data for HBP (part 1)

Stream Properties	Nitrogen	Hydrogen	feed	1	2	3	4	5	6	7
Temperature (K)	299.82	299.82	299.796	539.366	320	486.474	320	442.088	320	381.102
Pressure (Pa)	101300	101300	101300	625000	575000	1.83E+06	1.78E+06	4.28E+06	4.23E+06	6.73E+06
Mass Flow (kg/s)	0.616898	2.85532	3.47222	3.47222	3.47222	3.47222	3.47222	3.47222	3.47222	3.47222
Molar Flow (mol/s)	306.019	101.495	407.514	407.514	407.514	407.514	407.514	407.514	407.514	407.514
Mixture Specific Enthalpy (kJ/kg)	23.6121	1.45022	5.38767	827.829	73.1828	644.869	71.6214	491.288	68.8732	279.164
Mixture Molar Enthalpy (kJ/kmol)	47.5993	40.7987	45.9056	7053.51	623.554	5494.61	610.25	4186.02	586.834	2378.61
Molar Flow (Mixture) / Ammonia (mol/s)	0	0	0	0	0	0	0	0	0	0
Mass Flow (Mixture) / Ammonia (kg/s)	0	0	0	0	0	0	0	0	0	0
Molar Flow (Mixture) / Nitrogen (mol/s)	0	100.48	100.48	100.48	100.48	100.48	100.48	100.48	100.48	100.48
Mass Flow (Mixture) / Nitrogen (kg/s)	0	2.81478	2.81478	2.81478	2.81478	2.81478	2.81478	2.81478	2.81478	2.81478
Molar Flow (Mixture) / Hydrogen (mol/s)	306.019	0	306.019	306.019	306.019	306.019	306.019	306.019	306.019	306.019
Mass Flow (Mixture) / Hydrogen (kg/s)	0.616898	0	0.616898	0.616898	0.616898	0.616898	0.616898	0.616898	0.616898	0.616898
Molar Flow (Mixture) / Argon (mol/s)	0	1.01495	1.01495	1.01495	1.01495	1.01495	1.01495	1.01495	1.01495	1.01495
Mass Flow (Mixture) / Argon (kg/s)	0	0.0405451	0.0405451	0.0405451	0.0405451	0.0405451	0.0405451	0.0405451	0.0405451	0.0405451

Table A.2: Stream data for HBP (part 2)

Stream Properties	8	9	10	11	12	Pressurized feed	13	14	15	16
Temperature (K)	320	361.067	320	357.97	320	353.239	313.8	698.15	698.15	300
Pressure (Pa)	6.68E+06	9.18E+06	9.13E+06	1.23E+07	1.22E+07	1.58E+07	1.58E+07	1.57E+07	1.55E+07	1.55E+07
Mass Flow (kg/s)	3.47222	3.47222	3.47222	3.47222	3.47222	3.47222	11.5421	11.5421	11.5421	11.5421
Molar Flow (mol/s)	407.514	407.514	407.514	407.514	407.514	407.514	1510.36	1510.36	1309.41	1309.41
Mixture Specific Enthalpy (kJ/kg)	66.6801	208.672	65.0007	197.318	63.5585	180.631	21.5263	1597.01	1456.3	-381.699
Mixture Molar Enthalpy (kJ/kmol)	568.148	1777.99	553.839	1681.25	541.55	1539.07	164.502	12204.2	12836.9	-3364.56
Molar Flow (Mixture) / Ammonia (mol/s)	0	0	0	0	0	0	128.736	128.736	329.685	329.685
Mass Flow (Mixture) / Ammonia (kg/s)	0	0	0	0	0	0	2.19244	2.19244	5.6147	5.6147
Molar Flow (Mixture) / Nitrogen (mol/s)	100.48	100.48	100.48	100.48	100.48	100.48	216.7	216.7	116.226	116.226
Mass Flow (Mixture) / Nitrogen (kg/s)	2.81478	2.81478	2.81478	2.81478	2.81478	2.81478	6.07051	6.07051	3.25588	3.25588
Molar Flow (Mixture) / Hydrogen (mol/s)	306.019	306.019	306.019	306.019	306.019	306.019	1140.39	1140.39	838.962	838.962
Mass Flow (Mixture) / Hydrogen (kg/s)	0.616898	0.616898	0.616898	0.616898	0.616898	0.616898	2.29888	2.29888	1.69125	1.69125
Molar Flow (Mixture) / Argon (mol/s)	1.01495	1.01495	1.01495	1.01495	1.01495	1.01495	24.5377	24.5377	24.5377	24.5377
Mass Flow (Mixture) / Argon (kg/s)	0.0405451	0.0405451	0.0405451	0.0405451	0.0405451	0.0405451	0.980231	0.980231	0.980231	0.980231

Table A.3: Stream data for HBP (part 3)

Stream Properties	Ammonia	Unreac gases	recycle stream	Purge	17	recycle feed	MSTR-029	MSTR-049
Temperature (K)	298.15	298.15	298.15	298.15	300.669	300.669	698.15	298.15
Pressure (Pa)	1.55E+07	1.55E+07	1.55E+07	1.55E+07	1.58E+07	1.58E+07	1.55E+07	1.55E+07
Mass Flow (kg/s)	3.47513	8.06692	7.98625	0.0806692	7.98625	7.98625	2.56E-15	3.47513
Molar Flow (mol/s)	205.938	1103.47	1092.44	11.0347	1092.44	1092.44	∞	205.938
Mixture Specific Enthalpy (kJ/kg)	-1201.72	-57.1837	-57.1837	-57.1837	-46.9511	-46.9511	0	-1201.72
Mixture Molar Enthalpy (kJ/kmol)	-20278.6	-418.041	-418.041	-418.041	-343.236	-343.236	0	-20278.6
Molar Flow (Mixture) / Ammonia (mol/s)	200.878	128.806	127.518	1.28806	127.518	127.518	NaN	200.878
Mass Flow (Mixture) / Ammonia (kg/s)	3.42106	2.19364	2.1717	0.0219364	2.1717	2.1717	0	3.42106
Molar Flow (Mixture) / Nitrogen (mol/s)	0.36501	115.861	114.702	1.15861	114.702	114.702	NaN	0.36501
Mass Flow (Mixture) / Nitrogen (kg/s)	0.0102252	3.24565	3.2132	0.0324565	3.2132	3.2132	0	0.0102252
Molar Flow (Mixture) / Hydrogen (mol/s)	3.78875	835.173	826.822	8.35173	826.822	826.822	NaN	3.78875
Mass Flow (Mixture) / Hydrogen (kg/s)	0.00763767	1.68361	1.66677	0.0168361	1.66677	1.66677	0	0.00763767
Molar Flow (Mixture) / Argon (mol/s)	0.906384	23.6313	23.395	0.236313	23.395	23.395	NaN	0.906384
Mass Flow (Mixture) / Argon (kg/s)	0.0362082	0.944023	0.934582	0.00944023	0.934582	0.934582	0	0.0362082

Table A.4: Stream data for HBP with heat recovery (part 1)

Stream Properties	Nitrogen	Hydrogen	Feed	1	2	3	4	5	6	7
Temperature (K)	299.82	299.82	299.796	539.366	320	486.474	320	442.088	320	381.102
Pressure (Pa)	101300	101300	101300	625000	575000	1.83E+06	1.78E+06	4.28E+06	4.23E+06	6.73E+06
Mass Flow (kg/s)	0.616898	2.85532	3.47222	3.47222	3.47222	3.47222	3.47222	3.47222	3.47222	3.47222
Molar Flow (mol/s)	306.019	101.495	407.514	407.514	407.514	407.514	407.514	407.514	407.514	407.514
Mixture Specific Enthalpy (kJ/kg)	23.6121	1.45022	5.38767	827.829	73.1828	644.869	71.6214	491.288	68.8732	279.164
Mixture Molar Enthalpy (kJ/kmol)	47.5993	40.7987	45.9056	7053.51	623.554	5494.61	610.25	4186.02	586.834	2378.61
Molar Flow (Mixture) / Ammonia (mol/s)	0	0	0	0	0	0	0	0	0	0
Mass Flow (Mixture) / Ammonia (kg/s)	0	0	0	0	0	0	0	0	0	0
Molar Flow (Mixture) / Nitrogen (mol/s)	0	100.48	100.48	100.48	100.48	100.48	100.48	100.48	100.48	100.48
Mass Flow (Mixture) / Nitrogen (kg/s)	0	2.81478	2.81478	2.81478	2.81478	2.81478	2.81478	2.81478	2.81478	2.81478
Molar Flow (Mixture) / Hydrogen (mol/s)	306.019	0	306.019	306.019	306.019	306.019	306.019	306.019	306.019	306.019
Mass Flow (Mixture) / Hydrogen (kg/s)	0.616898	0	0.616898	0.616898	0.616898	0.616898	0.616898	0.616898	0.616898	0.616898
Molar Flow (Mixture) / Argon (mol/s)	0	1.01495	1.01495	1.01495	1.01495	1.01495	1.01495	1.01495	1.01495	1.01495
Mass Flow (Mixture) / Argon (kg/s)	0	0.0405451	0.0405451	0.0405451	0.0405451	0.0405451	0.0405451	0.0405451	0.0405451	0.0405451

Table A.5: Stream data for HBP with heat recovery (part 2)

Stream Properties	8	9	10	11	12	Pressurized feed	13	18	14	15
Temperature (K)	320	361.067	320	357.97	320	353.239	315.591	638.485	695	695
Pressure (Pa)	6.68E+06	9.18E+06	9.13E+06	1.23E+07	1.22E+07	1.58E+07	1.58E+07	1.57E+07	1.56E+07	1.54E+07
Mass Flow (kg/s)	3.47222	3.47222	3.47222	3.47222	3.47222	3.47222	11.1103	11.1103	11.1103	11.1103
Molar Flow (mol/s)	407.514	407.514	407.514	407.514	407.514	407.514	1433.06	1433.06	1433.06	1233.55
Mixture Specific Enthalpy (kJ/kg)	66.6801	208.672	65.0007	197.318	63.5585	180.631	28.5438	1331.17	1560.97	1416.33
Mixture Molar Enthalpy (kJ/kmol)	568.148	1777.99	553.839	1681.25	541.55	1539.07	221.295	10320.4	12101.9	12756.5
Molar Flow (Mixture) / Ammonia (mol/s)	0	0	0	0	0	0	120.581	120.581	120.581	320.091
Mass Flow (Mixture) / Ammonia (kg/s)	0	0	0	0	0	0	2.05355	2.05355	2.05355	5.45131
Molar Flow (Mixture) / Nitrogen (mol/s)	100.48	100.48	100.48	100.48	100.48	100.48	213.589	213.589	213.589	113.834
Mass Flow (Mixture) / Nitrogen (kg/s)	2.81478	2.81478	2.81478	2.81478	2.81478	2.81478	5.98336	5.98336	5.98336	3.18888
Molar Flow (Mixture) / Hydrogen (mol/s)	306.019	306.019	306.019	306.019	306.019	306.019	1076.27	1076.27	1076.27	777
Mass Flow (Mixture) / Hydrogen (kg/s)	0.616898	0.616898	0.616898	0.616898	0.616898	0.616898	2.16962	2.16962	2.16962	1.56634
Molar Flow (Mixture) / Argon (mol/s)	1.01495	1.01495	1.01495	1.01495	1.01495	1.01495	22.6225	22.6225	22.6225	22.6225
Mass Flow (Mixture) / Argon (kg/s)	0.0405451	0.0405451	0.0405451	0.0405451	0.0405451	0.0405451	0.903725	0.903725	0.903725	0.903725

Table A.6: Stream data for HBP with heat recovery (part 3)

Stream Properties	19	20	16	Ammonia	Unreac gases	recycle stream	Purge	17	recycle feed	MSTR-029	MSTR-049
Temperature (K)	695	359.783	300	298.15	298.15	298.15	298.15	302.146	302.146	695	298.15
Pressure (Pa)	1.54E+07	1.53E+07	1.53E+07	1.53E+07	1.53E+07	1.53E+07	1.53E+07	1.58E+07	1.58E+07	1.54E+07	1.53E+07
Mass Flow (kg/s)	11.1103	11.2205	11.2205	3.47978	7.74074	7.66333	0.0774074	7.66333	7.66333	0	3.47978
Molar Flow (mol/s)	1233.55	1243.48	1243.48	206.175	1037.31	1026.94	10.3731	1026.94	1026.94	0	206.175
Mixture Specific Enthalpy (kJ/kg)	1416.33	124.13	-392.128	-1202.38	-56.4741	-56.4741	-56.4741	-40.5684	-40.5684	0	-1202.38
Mixture Molar Enthalpy (kJ/kmol)	12756.5	1120.08	-3538.35	-20293.6	-421.428	-421.428	-421.428	-302.735	-302.735	0	-20293.6
Molar Flow (Mixture) / Ammonia (mol/s)	320.091	323.172	323.172	201.202	121.971	120.751	1.21971	120.751	120.751	0	201.202
Mass Flow (Mixture) / Ammonia (kg/s)	5.45131	5.50379	5.50379	3.42657	2.07722	2.05645	0.0207722	2.05645	2.05645	0	3.42657
Molar Flow (Mixture) / Nitrogen (mol/s)	113.834	115.593	115.593	0.381889	115.211	114.059	1.15211	114.059	114.059	0	0.381889
Mass Flow (Mixture) / Nitrogen (kg/s)	3.18888	3.23815	3.23815	0.010698	3.22745	3.19518	0.0322745	3.19518	3.19518	0	0.0106998
Molar Flow (Mixture) / Hydrogen (mol/s)	777	782.142	782.142	3.71496	778.427	770.643	7.78427	770.643	770.643	0	3.71496
Mass Flow (Mixture) / Hydrogen (kg/s)	1.56634	1.5767	1.5767	0.00748892	1.56922	1.55352	0.0156922	1.55352	1.55352	0	0.00748892
Molar Flow (Mixture) / Argon (mol/s)	22.6225	22.5761	22.5761	0.876799	21.6994	21.4824	0.216994	21.4824	21.4824	0	0.876799
Mass Flow (Mixture) / Argon (kg/s)	0.903725	0.901872	0.901872	0.0350264	0.866846	0.858177	0.00866846	0.858177	0.858177	0	0.0350264

Table A.7: Stream data for ammonia storage system

Stream Properties	Boil-off	1	2	3	4	5	6	Liquid toTank
Temperature (K)	247.07	337.725	264.299	264.299	401.151	283.65	283.65	264.299
Pressure (Pa)	108000	304000	304000	304000	1.27E+06	1.22E+06	1.22E+06	304000
Molar Flow (Mixture) / Ammonia (mol/s)	2.46616	2.46616	5.43244	2.96628	2.96628	2.96628	2.96628	2.46616
Mass Flow (Mixture) / Ammonia (kg/s)	0.042	0.042	0.0925174	0.0505173	0.0505173	0.0505173	0.0505173	0.042
Mixture Specific Enthalpy (kJ/kg)	-109.896	75.6787	-683.47	-82.3774	197.138	-1314.62	-1314.62	-1406.46
Mixture Specific Entropy (kJ/[kg.K])	-0.429784	-0.287909	-3.08887	-0.815221	-0.634327	-5.49417	-5.49417	-5.8236
Mixture Molar Enthalpy (kJ/kmol)	-1871.59	1288.85	-11639.8	-1402.93	3357.36	-22388.7	-22388.7	-23952.7
Mixture Molar Entropy (kJ/[kmol.K])	-7.31945	-4.90324	-52.6051	-13.8836	-10.8029	-93.5685	-93.5685	-99.1789
Vapor Phase Mass Flow (kg/s)	0.042	0.042	0.0505173	0.0505173	0.0505173	0	0	0
Vapor Phase Molar Flow (mol/s)	2.46616	2.46616	2.96628	2.96628	2.96628	0	0	0
Liquid Phase (Mixture) Mass Flow (kg/s)	0	0	0.042	0	0	0.0505173	0.0505173	0.042
Liquid Phase (Mixture) Molar Flow (mol/s)	0	0	2.46616	0	0	2.96628	2.96628	2.46616

Table A.8: Stream data for cryogenic air distillation (part 1)

Stream Properties	25	13	20	15	11	18	19	23	16	14
Temperature (K)	78.9408	109.045	91.3462	92.55	97.9008	87.45	79.6467	79.6467	84.279	100.157
Pressure (Pa)	123000	549000	140000	539000	549000	525000	133000	133000	140000	549000
Mass Flow (kg/s)	2.85793	8.228	1.01402	1.92524	3.872	1.94669	1.94669	2.85793	1.92524	1.92524
Molar Flow (mol/s)	102.02	284.021	31.6358	64.1651	133.657	69.4914	69.4914	102.02	64.1651	64.1651
Mixture Specific Enthalpy (kJ/kg)	-426.171	-197.698	-393.676	-394.629	-326.495	-408.898	-408.898	-424.783	-394.629	-380.013
Mixture Molar Enthalpy (kJ/kmol)	-11938.5	-5727.24	-12618.5	-11840.6	-9458.45	-11454.6	-11454.6	-11899.6	-11840.6	-11402.1
Vapor Phase Mass Flow (kg/s)	0	8.228	1.83E-07	0	1.32493	0	0.158728	0	0.150505	0
Liquid Phase (Mixture) Mass Flow (kg/s)	2.85793	0	1.01402	1.92524	2.54707	1.94669	1.78796	2.85793	1.77474	1.92524
Mass Flow (Mixture) / Argon (kg/s)	1.72E-09	0.113461	0.0533859	0.0533698	0.0533933	7.73E-09	7.73E-09	1.72E-09	0.0533698	0.0533698
Mass Flow (Mixture) / Nitrogen (kg/s)	2.85793	6.20599	0.0626197	0.974125	2.92047	1.94669	1.94669	2.85793	0.974125	0.974125
Mass Flow (Mixture) / Oxygen (kg/s)	9.58E-14	1.90855	0.898018	0.897746	0.898141	7.55E-13	7.55E-13	9.58E-14	0.897746	0.897746

Table A.9: Stream data for cryogenic air distillation (part 2)

Stream Properties	17	24	Nitrogen	21	Oxygen	9	6	7	8	12
Temperature (K)	94.8237	78.9408	299.92	91.4902	297	297.85	303.15	303.15	402.526	109.35
Pressure (Pa)	535000	123000	113000	480000	470000	1.20E+06	559000	559000	1.21E+06	1.19E+06
Mass Flow (kg/s)	1.94669	2.85793	2.85793	1.01402	1.01402	3.872	8.228	3.872	3.872	3.872
Molar Flow (mol/s)	69.4914	102.02	102.02	31.6358	31.6358	133.657	284.021	133.657	133.657	133.657
Mixture Specific Enthalpy (kJ/kg)	-393.046	-426.171	1.53446	-393.291	-2.41503	-3.62231	3.51776	3.51776	103.626	-326.495
Mixture Molar Enthalpy (kJ/kmol)	-11010.6	-11938.5	42.9855	-12606.2	-77.409	-104.937	101.908	101.908	3002.01	-9458.45
Vapor Phase Mass Flow (kg/s)	0	0	2.85793	0	1.01402	3.872	8.228	3.872	3.872	0.863449
Liquid Phase (Mixture) Mass Flow (kg/s)	1.94669	2.85793	0	1.01402	0	0	0	0	0	3.00855
Mass Flow (Mixture) / Argon (kg/s)	7.73E-09	1.72E-09	1.72E-09	0.0533859	0.0533859	0.0533933	0.113461	0.0533933	0.0533933	0.0533933
Mass Flow (Mixture) / Nitrogen (kg/s)	1.94669	2.85793	2.85793	0.0626197	0.0626197	2.92047	6.20599	2.92047	2.92047	2.92047
Mass Flow (Mixture) / Oxygen (kg/s)	7.55E-13	9.58E-14	9.58E-14	0.898018	0.898018	0.898141	1.90855	0.898141	0.898141	0.898141

Table A.10: Stream data for cryogenic air distillation (part 3)

Stream Properties	5	Feed air	2	3	4
Temperature (K)	303.15	298.15	416.973	303.15	403.84
Pressure (Pa)	559000	101300	268000	258000	569000
Mass Flow (kg/s)	12.1	12.1	12.1	12.1	12.1
Molar Flow (mol/s)	417.678	417.678	417.678	417.678	417.678
Mixture Specific Enthalpy (kJ/kg)	3.51776	-0.283991	119.619	4.32581	105.84
Mixture Molar Enthalpy (kJ/kmol)	101.908	-8.22713	3465.32	125.317	3066.15
Vapor Phase Mass Flow (kg/s)	12.1	12.1	12.1	12.1	12.1
Liquid Phase (Mixture) Mass Flow (kg/s)	0	0	0	0	0
Mass Flow (Mixture) / Argon (kg/s)	0.166854	0.166854	0.166854	0.166854	0.166854
Mass Flow (Mixture) / Nitrogen (kg/s)	9.12645	9.12645	9.12645	9.12645	9.12645
Mass Flow (Mixture) / Oxygen (kg/s)	2.80669	2.80669	2.80669	2.80669	2.80669

Table A.11: Stream data for SMR (part 1)

Stream Properties	18	22	Hydrogen	21	19	Purified NG	Sulpur compounds	2	1	14
Temperature (K)	573.15	300	300	300	573.15	616.483	616.483	616.483	374.185	310.928
Pressure (Pa)	1.50E+06	1.40E+06	1.40E+06	1.40E+06	1.45E+06	2.90E+06	2.90E+06	2.90E+06	3.00E+06	1.60E+06
Mass Flow (kg/s)	0.956555	0.203732	0.752823	0.956555	0	1.48787	0.0121274	1.5	1.5	0
Molar Flow (mol/s)	338.85	11.3088	314.257	325.566	0	88.2489	0.355842	88.6047	88.6047	0
Mixture Specific Enthalpy (kJ/kg)	2875.18	-2527.48	19.3863	-488.831	0	822.478	327.531	818.499	145.874	0
Mixture Molar Enthalpy (kJ/kmol)	8116.47	-45533.2	46.4411	-1436.25	0	13866.9	11162.5	13856.5	2469.51	0
Molar Flow (Mixture) / Hydrogen (mol/s)	329.537	0	305.75	305.75	0	0.177921	0	0.177921	0.177921	0
Mass Flow (Mixture) / Hydrogen (kg/s)	0.664307	0	0.616356	0.616356	0	0.000358668	0	0.000358668	0.000358668	0
Molar Flow (Mixture) / Carbon monoxide (mol/s)	2.78253	0	0	0	0	0	0	0	0	0
Mass Flow (Mixture) / Carbon monoxide (kg/s)	0.077939	0	0	0	0	0	0	0	0	0
Molar Flow (Mixture) / Carbon dioxide (mol/s)	3.85976	0	0	0	0	2.66882	0	2.66882	2.66882	0
Mass Flow (Mixture) / Carbon dioxide (kg/s)	0.169866	0	0	0	0	0.117453	0	0.117453	0.117453	0
Molar Flow (Mixture) / Methane (mol/s)	1.86434	0	8.50663	8.50663	0	85.402	0	85.4022	85.4022	0
Mass Flow (Mixture) / Methane (kg/s)	0.0299086	0	0.136467	0.136467	0	1.37006	0	1.37006	1.37006	0

Table A.12: Stream data for SMR (part 2)

Stream Properties	16	15	Raw NG	20	13	11	12	10	9	8
Temperature (K)	310.928	310.928	298.15	573.15	310.928	485.93	485.93	477.594	700.93	700.93
Pressure (Pa)	1.60E+06	1.60E+06	1.38E+06	1.45E+06	1.80E+06	1.85E+06	1.85E+06	1.90E+06	1.95E+06	1.95E+06
Mass Flow (kg/s)	4.47076	0.98047	1.5	0.956555	5.45123	-1.21E-15	5.45123	5.45123	5.45123	0
Molar Flow (mol/s)	420.855	54.3094	88.6047	325.566	475.165	-∞	475.165	475.165	475.165	0
Mixture Specific Enthalpy (kJ/kg)	30.0013	-2469.1	-15.2397	2788.83	-421.477	0	514.379	484.193	1130.45	0
Mixture Molar Enthalpy (kJ/kmol)	318.705	-44575.7	-257.995	8193.95	-4835.31	0	5901.12	5554.81	12968.9	0
Molar Flow (Mixture) / Hydrogen (mol/s)	331.204	0.000339677	0.177921	305.75	331.204	NaN	331.204	308.316	308.316	0
Mass Flow (Mixture) / Hydrogen (kg/s)	0.667668	6.85E-07	0.000358668	0.616356	0.667668	0	0.667668	0.621529	0.621529	0
Molar Flow (Mixture) / Carbon monoxide (mol/s)	2.80542	1.11E-06	0	0	2.80542	NaN	2.80542	25.6936	25.6936	0
Mass Flow (Mixture) / Carbon monoxide (kg/s)	0.0785801	3.10E-08	0	0	0.0785802	0	0.0785802	0.719681	0.719681	0
Molar Flow (Mixture) / Carbon dioxide (mol/s)	83.2415	0.0798991	2.66882	0	83.3214	NaN	83.3214	60.4332	60.4332	0
Mass Flow (Mixture) / Carbon dioxide (kg/s)	3.66342	0.00351632	0.117453	0	3.66693	0	3.66693	2.65963	2.65963	0
Molar Flow (Mixture) / Methane (mol/s)	1.94417	5.50E-06	85.4022	8.50663	1.94417	NaN	1.94417	1.94417	1.94417	0
Mass Flow (Mixture) / Methane (kg/s)	0.0311892	8.83E-08	1.37006	0.136467	0.0311893	0	0.0311893	0.0311893	0.0311893	0

Table A.13: Stream data for SMR (part 3)

Stream Properties	7	5	6	4	Steam	3	Solvent in	Solvent out	17
Temperature (K)	623.15	1273.15	1273.15	922.039	783.15	721.274	293.15	295.492	294.669
Pressure (Pa)	2.00E+06	2.05E+06	2.05E+06	2.80E+06	2.90E+06	2.90E+06	1.60E+06	1.60E+06	1.60E+06
Mass Flow (kg/s)	5.45123	0	5.45123	5.45123	3.96336	5.45123	185	188.514	0.956555
Molar Flow (mol/s)	475.165	0	475.165	308.249	220	308.249	2697.24	2779.24	338.85
Mixture Specific Enthalpy (kJ/kg)	873.178	0	2798.49	1431.78	925.056	897.058	-1051.13	-1030.55	-54.125
Mixture Molar Enthalpy (kJ/kmol)	10017.4	0	32105.1	25320.3	16665.1	15864	-72095.7	-69901.6	-152.792
Molar Flow (Mixture) / Hydrogen (mol/s)	250.552	0	250.552	0.177921	0	0.177921	0	1.66724	329.537
Mass Flow (Mixture) / Hydrogen (kg/s)	0.505082	0	0.505082	0.000358668	0	0.000358668	0	0.00336095	0.664307
Molar Flow (Mixture) / Carbon monoxide (mol/s)	83.458	0	83.458	0	0	0	0	0.0228935	2.78253
Mass Flow (Mixture) / Carbon monoxide (kg/s)	2.33767	0	2.33767	0	0	0	0	0.00064125	0.077939
Molar Flow (Mixture) / Carbon dioxide (mol/s)	2.66882	0	2.66882	2.66882	0	2.66882	0	79.3817	3.85976
Mass Flow (Mixture) / Carbon dioxide (kg/s)	0.117453	0	0.117453	0.117453	0	0.117453	0	3.49355	0.169866
Molar Flow (Mixture) / Methane (mol/s)	1.94417	0	1.94417	85.4022	0	85.4022	0	0.0798321	1.86434
Mass Flow (Mixture) / Methane (kg/s)	0.0311893	0	0.0311893	1.37006	0	1.37006	0	0.0012807	0.0299086

Table A.14: Stream data for SMR-HR (part 1)

Stream Properties	9	28	Hydrogen	27	26	3	Sulpur compounds	14	2	1
Temperature (K)	925.371	300	300	300	573.15	616.483	616.483	636.86	616.483	374.185
Pressure (Pa)	1.85E+06	1.40E+06	1.40E+06	1.40E+06	1.45E+06	2.90E+06	2.90E+06	1.65E+06	2.90E+06	3.00E+06
Mass Flow (kg/s)	5.36116	0.203622	0.752758	0.95638	0	1.48787	0.0121274	5.36116	1.5	1.5
Molar Flow (mol/s)	469.952	11.3027	314.281	325.584	0	88.2489	0.355842	469.952	88.6047	88.6047
Mass Flow (Mixture) / Hydrogen (kg/s)	0.504438	0	0.616422	0.616422	0	0.000358668	0	0.619027	0.0003586688	0.000358668
Mass Flow (Mixture) / Carbon monoxide (kg/s)	2.33468	0	0	0	0	0	0	0.742492	0	0
Mass Flow (Mixture) / Carbon dioxide (kg/s)	0.117453	0	0	0	0	0.117453	0	2.6191	0.117453	0.117453
Mass Flow (Mixture) / Methane (kg/s)	0.0328994	0	0.136336	0.136336	0	1.37006	0	0.0328994	1.37006	1.37006
Mass Flow (Mixture) / Water (kg/s)	2.37169	0.203622	0	0.203622	0	0	0	1.34764	0	0
Mass Flow (Mixture) / Hydrogen sulfide (kg/s)	0	0	0	0	0	0	0.0121274	0	0.0121274	0.0121274
Mass Flow (Mixture) / Oxygen (kg/s)	0	0	0	0	0	0	0	0	0	0
Mass Flow (Mixture) / Nitrogen (kg/s)	0	0	0	0	0	0	0	0	0	0

Table A.15: Stream data for SMR-HR (part 2)

Stream Properties	7	19	21	20	Raw NG	25	18	16	17	15
Temperature (K)	1273.15	310.928	310.928	310.928	298.15	573.15	310.928	485.93	485.93	477.594
Pressure (Pa)	2.05E+06	1.60E+06	1.60E+06	1.60E+06	1.38E+06	1.45E+06	1.50E+06	1.55E+06	1.55E+06	1.60E+06
Mass Flow (kg/s)	5.36116	0	4.46324	0.897913	1.5	0.95638	5.36116	0	5.36116	5.36116
Molar Flow (mol/s)	469.952	0	420.215	49.7367	88.6047	325.584	469.952	0	469.952	469.952
Mass Flow (Mixture) / Hydrogen (kg/s)	0.504438	0	0.666368	6.27E-07	0.000358668	0.616422	0.666368	0	0.666368	0.619027
Mass Flow (Mixture) / Carbon monoxide (kg/s)	2.33468	0	0.0847002	3.07E-08	0	0	0.0847003	0	0.0847003	0.742492
Mass Flow (Mixture) / Carbon dioxide (kg/s)	0.117453	0	3.64941	0.00321275	0.117453	0	3.65262	0	3.65262	2.6191
Mass Flow (Mixture) / Methane (kg/s)	0.0328994	0	0.0328993	8.54E-08	1.37006	0.136336	0.0328994	0	0.0328994	0.0328994
Mass Flow (Mixture) / Water (kg/s)	2.37169	0	0.0298653	0.894699	0	0.203622	0.924565	0	0.924565	1.34764
Mass Flow (Mixture) / Hydrogen sulfide (kg/s)	0	0	0	0	0.0121274	0	0	0	0	0
Mass Flow (Mixture) / Oxygen (kg/s)	0	0	0	0	0	0	0	0	0	0
Mass Flow (Mixture) / Nitrogen (kg/s)	0	0	0	0	0	0	0	0	0	0

Table A.16: Stream data for SMR-HR (part 3)

Stream Properties	12	11	10	MSTR-009	6	23	Steam	4	Solvent in	Solvent out
Temperature (K)	700.93	700.93	623.15	1273.15	1273.15	294.665	783.15	720.386	293.15	295.486
Pressure (Pa)	1.75E+06	1.75E+06	1.80E+06	2.05E+06	2.05E+06	1.60E+06	2.90E+06	2.90E+06	1.60E+06	1.60E+06
Mass Flow (kg/s)	5.36116	0	5.36116	0	5.36116	0.957855	3.87329	5.36116	185	188.505
Molar Flow (mol/s)	469.952	0	469.952	0	469.952	338.408	215	303.249	2697.24	2779.04
Mass Flow (Mixture) / Hydrogen (kg/s)	0.619027	0	0.504438	0	0.504438	0.663009	0	0.0003586 68	0	0.00335888
Mass Flow (Mixture) / Carbon monoxide (kg/s)	0.742492	0	2.33468	0	2.33468	0.0840082	0	0	0	0.000692132
Mass Flow (Mixture) / Carbon dioxide (kg/s)	2.6191	0	0.117453	0	0.117453	0.164778	0	0.117453	0	3.48464
Mass Flow (Mixture) / Methane (kg/s)	0.0328994	0	0.0328994	0	0.0328994	0.0315465	0	1.37006	0	0.00135285
Mass Flow (Mixture) / Water (kg/s)	1.34764	0	2.37169	0	2.37169	0.0145131	3.87329	3.87329	24.2957	24.3111
Mass Flow (Mixture) / Hydrogen sulfide (kg/s)	0	0	0	0	0	0	0	0	0	0
Mass Flow (Mixture) / Oxygen (kg/s)	0	0	0	0	0	0	0	0	0	0
Mass Flow (Mixture) / Nitrogen (kg/s)	0	0	0	0	0	0	0	0	0	0

Table A.17: Stream data for SMR-HR (part 4)

Stream Properties	22	13	8	5	24
Temperature (K)	294.665	700.93	1099.46	922.082	573.15
Pressure (Pa)	1.60E+06	1.75E+06	1.95E+06	2.80E+06	1.50E+06
Mass Flow (kg/s)	0.957855	5.36116	5.36116	5.36116	0.95638
Molar Flow (mol/s)	338.408	469.952	469.952	303.249	338.852
Mass Flow (Mixture) / Hydrogen (kg/s)	0.663009	0.619027	0.504438	0.0003586668	0.664327
Mass Flow (Mixture) / Carbon monoxide (kg/s)	0.0840082	0.742492	2.33468	0	0.0776526
Mass Flow (Mixture) / Carbon dioxide (kg/s)	0.164778	2.6191	0.117453	0.117453	0.169957
Mass Flow (Mixture) / Methane (kg/s)	0.0315465	0.0328994	0.0328994	1.37006	0.0299086
Mass Flow (Mixture) / Water (kg/s)	0.0145131	1.34764	2.37169	3.87329	0.0145344
Mass Flow (Mixture) / Hydrogen sulfide (kg/s)	0	0	0	0	0
Mass Flow (Mixture) / Oxygen (kg/s)	0	0	0	0	0
Mass Flow (Mixture) / Nitrogen (kg/s)	0	0	0	0	0

A.2 Figures of Ammonia Plants 1-6

Ammonia plant comprises of different processes and unit. Each process/unit contributes to the capital costs and manufacturing cost of respective plants. The capital cost and manufacturing cost of each process/plant for ammonia plants 1-6 are shown in figures A.1- A.6. In the case of ammonia plant 1 and 2, manufacturing costs are dependent on utilities cost, carbon tax and raw material cost as shown in figures A.7 and A.8.

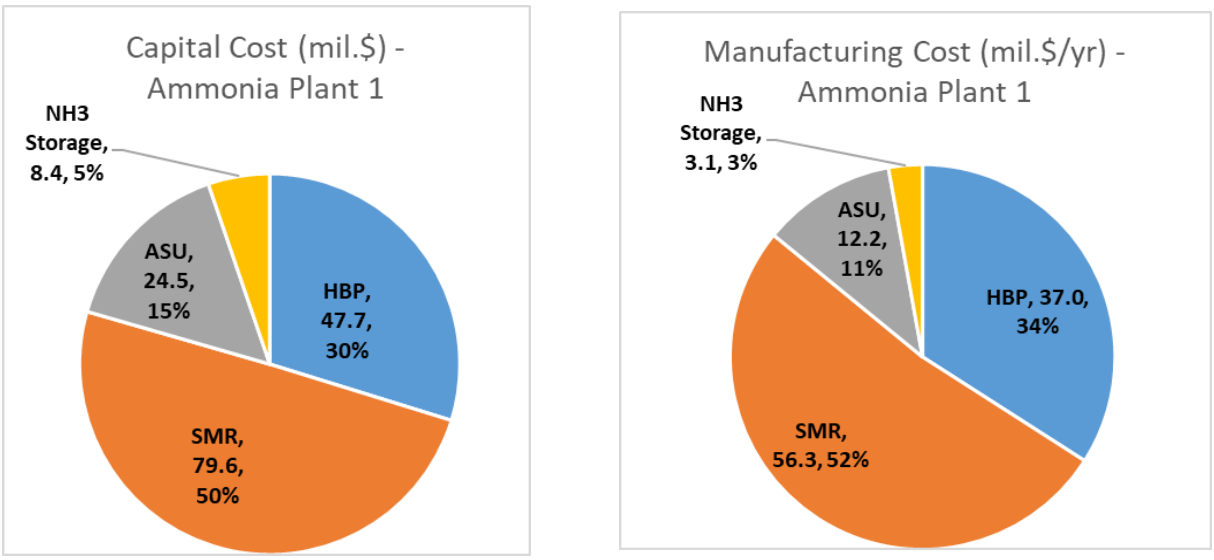

Figure A.1: Capital and Manufacturing costs distribution of Ammonia Plant 1

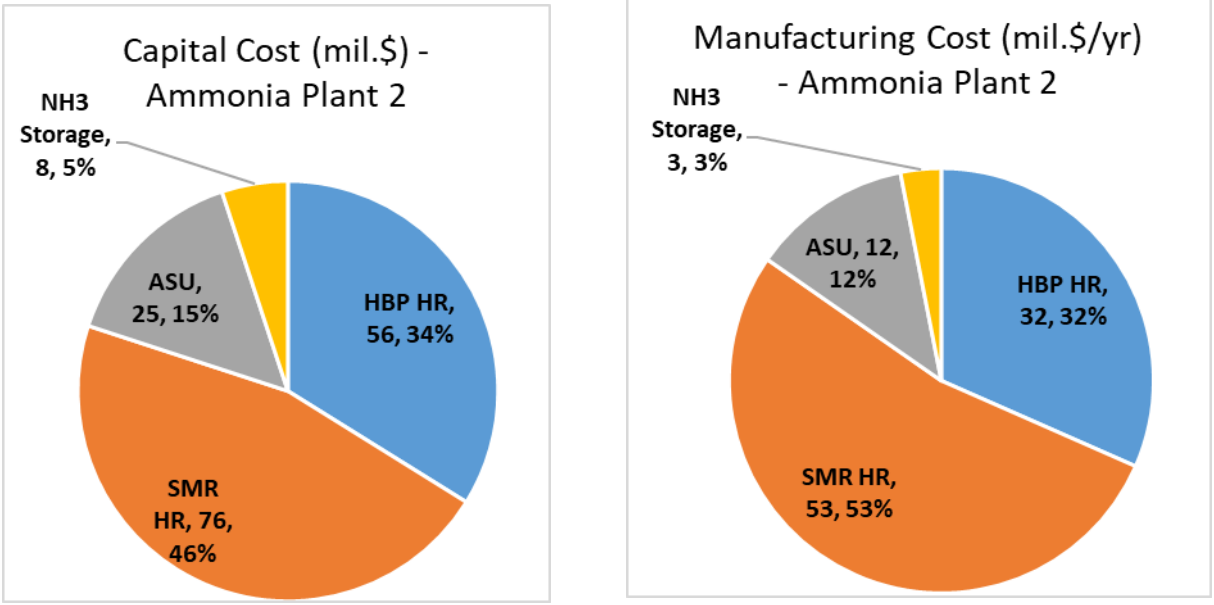

Figure A.2: Capital and Manufacturing costs distribution of Ammonia Plant 2

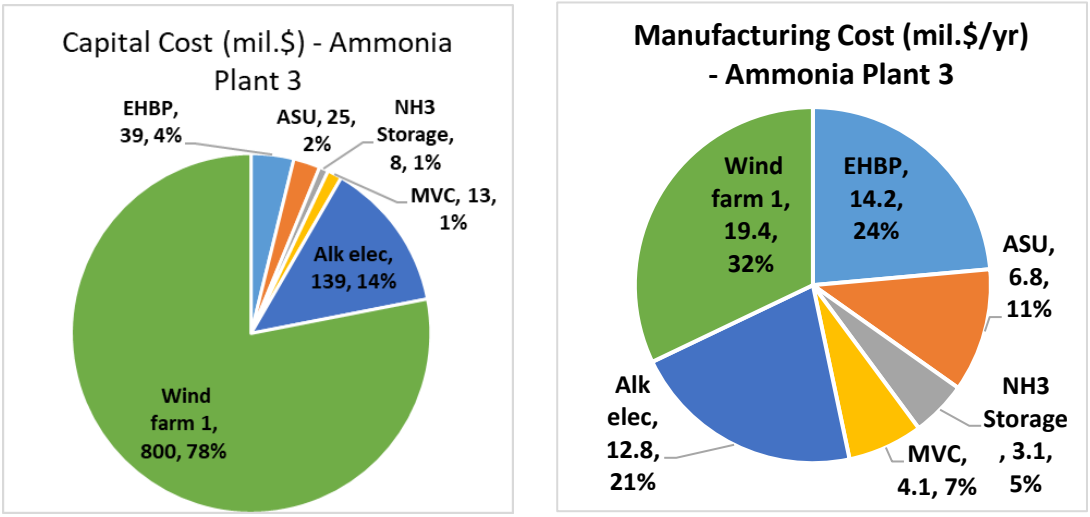

Figure A.3: Capital and Manufacturing costs distribution of Ammonia Plant 3

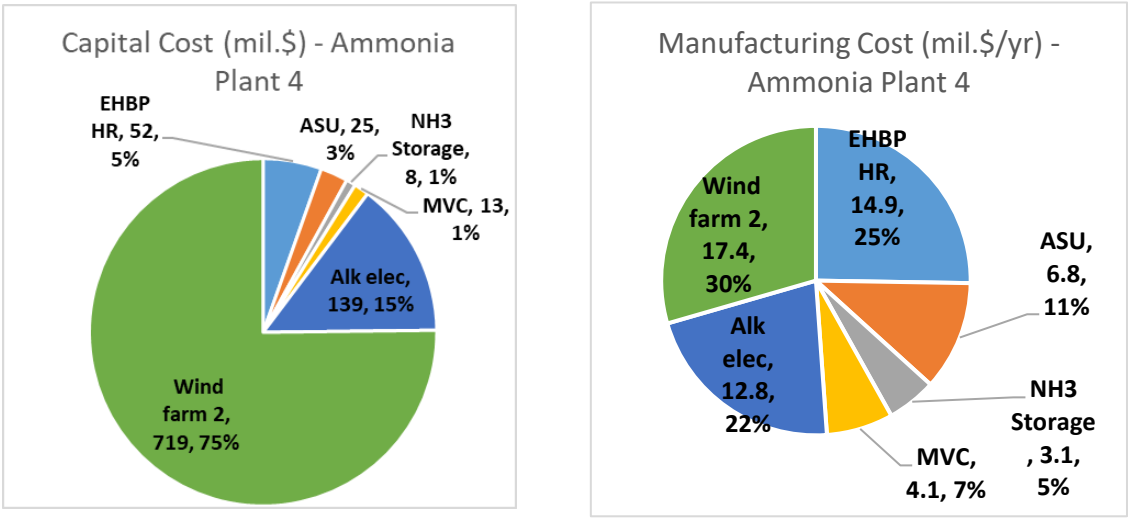

Figure A.4: Capital and Manufacturing costs distribution of Ammonia Plant 4

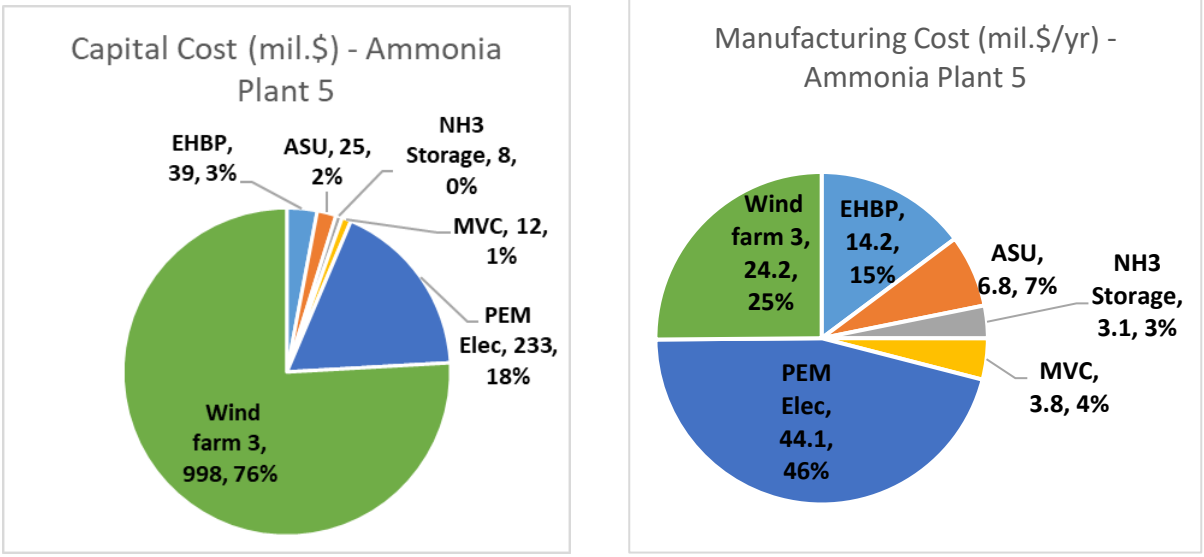

Figure A.5: Capital and Manufacturing costs distribution of Ammonia Plant 5

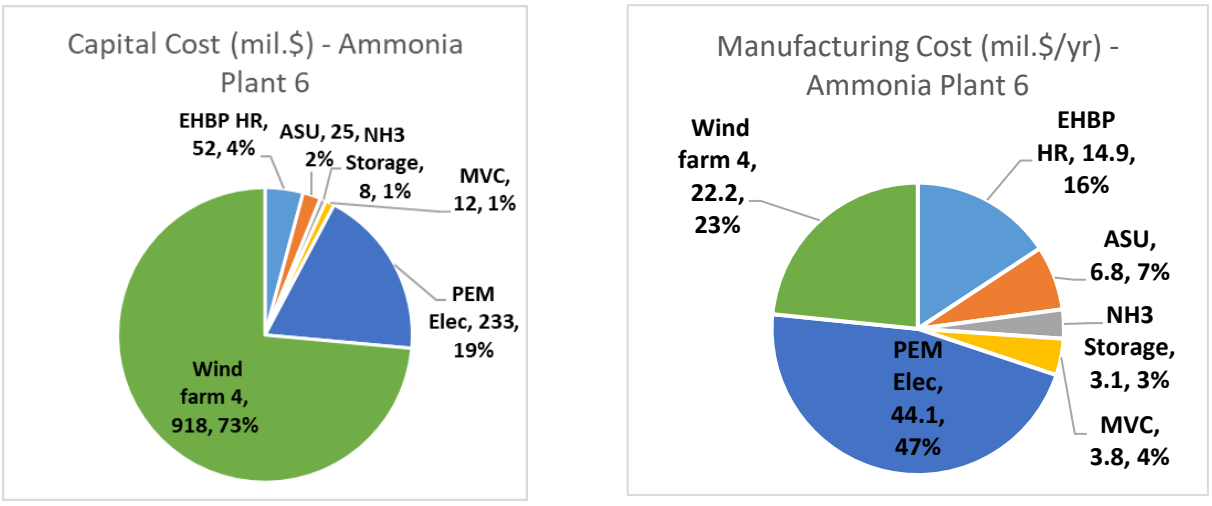

Figure A.6: Capital and Manufacturing costs distribution of Ammonia Plant 6

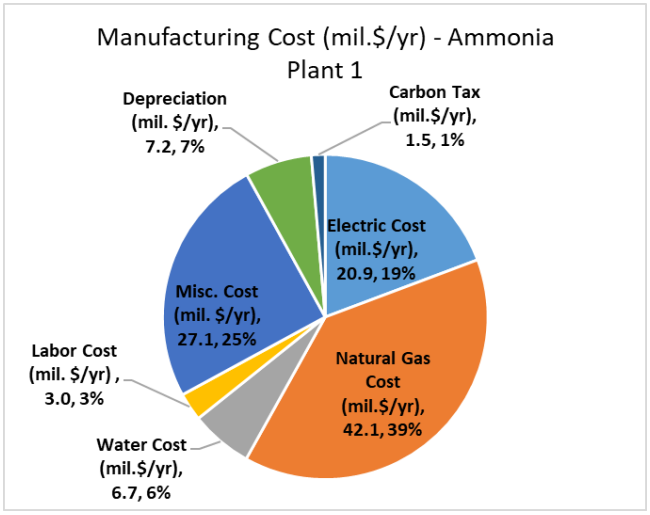

Figure A.7: Manufacturing cost items of Ammonia Plant 1

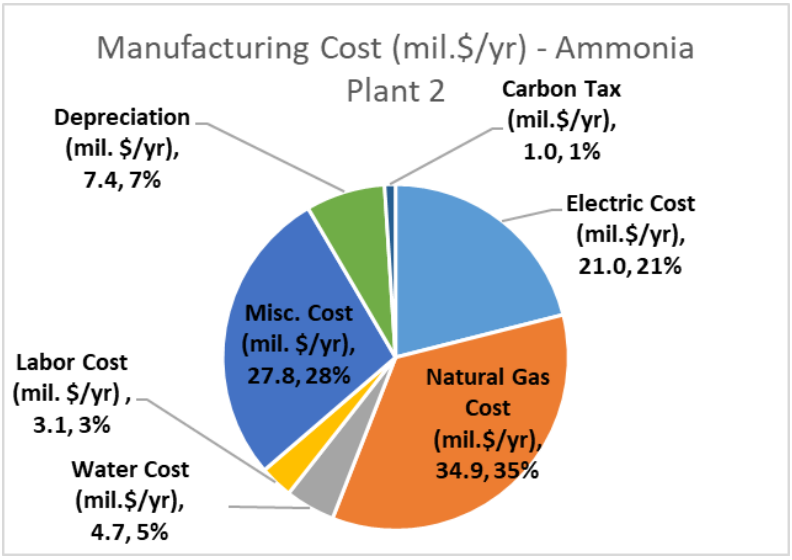

Figure A.8: Manufacturing cost items of Ammonia Plant 2

A.3 Future Cost Estimation of Onshore Wind and Electrolyser Systems

A.3.1 Capital and Manufacturing Costs for Electrolyser System

The hydrogen required for 300 ton/day ammonia is around 53.3 ton/day, which corresponds to approximately 2220.83 kg/hr. Based on the data provided in table 45, the capital and manufacturing costs of alkaline and PEM electrolyser plants in 2030 are shown in table A.18.

Table A.18: Capital and Manufacturing cost estimated for electrolyser systems

Equipment	Alkaline Electrolyser	PEM Electrolyser
Number of Modules	17	16
Capital Costs (mil. $)	73.99	88.85
Annual Electricity Consumption (kWh/yr)	888333333	835033333
Manufacturing Cost (mil. $/yr)	1.12	1.40

A.3.2 Capital and Operating Costs for Onshore Wind

Onshore Wind Power is a commercial technology to produce renewable energy as discussed in section 2.4. Recent studies by Fraunhofer Institute [99] show that the technology have a LCOE of €0.035/kWh in Germany by 2020. Assuming FLH of 3200, direct operating costs at €30/kW and variable operating costs at €0.005/kWh, the capital and operating expenditures of wind farms powering green ammonia plants are shown in table A.19.

Table A.19: Capital and operating cost of wind farms

Equipment	Wind Farm 1	Wind Farm 2	Wind Farm 3	Wind Farm 4
Power Production (kWh/yr)	1135579929	1014473891	1081560847	960454808
Wind Farm Rated Power (kW)	354869	317023	337988	300142
Capital Costs (mil. $)	616.05	550.35	586.75	521.05
Operating Costs (mil. $/yr)	18.28	16.33	17.41	15.46
Process Units	Alkaline Electrolyser, MVC, ASU, EHBP, Ammonia Storage System	Alkaline Electrolyser, MVC, ASU, EHBP-HR, Ammonia Storage System	PEM Electrolyser, MVC, ASU, EHBP, Ammonia Storage System	PEM Electrolyser, MVC, ASU, EHBP-HR, Ammonia Storage System

References

[1] N. A. a. M. A. Ghulam Habib, The kinetic study of ammonia synthesis, Scholar's Press, 2018.

[2] H. X. ,. M. O.-J. W. D. a. P. B. A Valera-Medina, "Ammonia for power," *Progress in Energy and Combustion Science,* no. 69, pp. 63-102, 2018.

[3] Yara, "Yara Fertilizer Handbook 2017," 2017.

[4] T. Brown, "What drives new investments in low-carbon ammonia production? One million tons per day demand," 2018. [Online]. Available: https://ammoniaindustry.com/what-drives-new-investments-in-low-carbon-ammonia/.

[5] N. R. Q. C. S. S. J. H. K. A. K. A. Ahmed Afif, "Ammonia-fed fuel cells: a comprehensive review," *Renewable and Sustainable Energy Reviews,* pp. 822-835, 2016.

[6] A. Y. a. I. Dincer, "A review on clean ammonia as a potential fuel for power generators," *Renewable and Sustainable Energy Reviews,* pp. 96-108, 2019.

[7] D. A. Kramer, "Mineral Commodity Profiles - Nitrogen," U.S. Department of the Interior, 2004.

[8] M. R. H. a. I. K. P. Mehdi Ghommem, "Influence of natural and anthropogenic carbon dioxide sequestration on global warming," *Ecological Modelling,* pp. 1-7, 2012.

[9] I. f. S. P. Technology, "Power to Ammonia," 2016.

[10] I. E. A. (IEA), "The future of hydrogen," Japan, 2019.

[11] T. Brown, "Green ammonia pilot plants now running, in Oxford and Fukushima," 2018. [Online]. Available: https://ammoniaindustry.com/green-ammonia-pilot-plants-now-running-in-oxford-and-fukushima/.

[12] G. Ondrey, "World's first successful ammonia synthesis using renewable hydrogen and power," 2018. [Online]. Available: https://www.chemengonline.com/worlds-first-successful-ammonia-synthesis-using-renewable-hydrogen-and-power/.

[13] S. B. a. A. K. S.Giddey, "Review of electrochemical ammonia production technologies and

materials," *Internation journal of hydrogen energy,* pp. 14576-14594, 2013.

[14] J. M. ,. a. J. M. Eric Morgan, "Wind-powered ammonia fuel production for remote islands: a case study," *Renewable Energy,* pp. 51-61, 2014.

[15] R. B.-A. a. I. W. Richard Nayak-Luke, ""“Green” Ammonia: Impact of Renewable Energy Intermittency on Plant Sizing and Levelized Cost of Ammonia," *Industrial and Engineering Chemical Research ,* pp. 14607-14616, 2018.

[16] J. R. Bartels, "A feasibility study of implementing an Ammonia Economy," Iowa State University, 2008.

[17] E. R. Morgan, "Techno-Economic Feasibility Study of Ammonia Plants Powered by Offshore Wind," University of Massachusetts Amherst, 2013.

[18] H. Song, "DEVELOPING A FRAMEWORK FOR AMMONIA ENERGY CARRIER SUPPLY CHAIN," 2018.

[19] A. S. a. M. Martín, "Optimal renewable production of ammonia from water and air," *Journal of Cleaner Production,* 2017.

[20] T. G. a. K. Christiansen, "Hydrogen by water electrolysis as basis for small scale ammonia production. A comparison with hydrocarbon based technologies.," *International journal of hydrogen energy,* pp. 247-257, 1982.

[21] Thyssenkrupp, "Ammonia Plants," [Online]. Available: https://www.thyssenkrupp-industrial-solutions.com/en/products-and-services/fertilizer-plants/ammonia-plants-by-uhde.

[22] T. Brown, "Power to Ammonia: alternative synthesis technologies," 2017. [Online]. Available: https://ammoniaindustry.com/power-to-ammonia-alternative-synthesis-technologies/.

[23] P. E. International, "Renewables cover 42% of German power consumption," 2019. [Online]. Available: https://www.powerengineeringint.com/2019/11/02/renewables-cover-42-of-power-german-consumption/.

[24] A. P. Pavlos Nikolaidis, "A comparative overview of hydrogen production processes," *Renewable and Sustainable Energy Reviews,* pp. 597-611, 2017.

[25] M. B. P. N. K. O. Jeffrey R. Bartels, "An economic survey of hydrogen production from conventional and alternative energy sources," *International Journal of Hydrogen Energy,* pp. 8371-8384, 2010.

[26] K. Verfondern, "Nuclear Energy for Hydrogen Production," Forschungszentrums Jülich GmbH, 2007.

[27] P. M. a. A. K. Dalai, Sustainable Utilization of Natural Resources, CRC Press, 2017.

[28] E. F. M. Association, "Production of Ammonia," 2000.

[29] G. D. M. F. P. G. J. M. L. E. T. A. Y. L. Y. S. Z. René Bañares-Alcántara, "Analysis of Islanded Ammonia-based Energy Storage Systems," University of Oxford, 2014.

[30] F. v. L. R.E. Stoll, "Hydrogen - what are the costs?," 2000.

[31] A. C. D. H. F. L. B. M. E. S. Luca Bertuccioli, "Study on development of water electrolysis in EU," E4tech, 2014.

[32] A. A. J. N. a. S. F. O. Schmidt, "Future cost and performance of water electrolysis:An expert elicitation study," *International journal of hydrogen energy,* pp. 30470-30492, 2017.

[33] H. W. H. L. N. Z. Dmitri Bessarabov, PEM Electrolysis for Hydrogen Production, CRC Press, 2016.

[34] A. Godula-Jopek, Hydrogen Production by Electrolysis, Wiley-VCH, 2014.

[35] M. S. D. B. A. Z. U.F. Vogt, "Novel Developments in Alkaline Water Electrolysis," in *8th International Symposium Hydrogen & Energy*, 2014.

[36] D. L. F. J. M. D. S. Marcelo Carmo, "A comprehensive review on PEM water electrolysis," *International Journal of Hydrogen Energy,* pp. 4901-4934, 2013.

[37] K. Meier, "Hydrogen production with sea water electrolysis using Norwegian offshore wind energy potentials," *International Journal of Energy and Environmental Engineering,* no. 5, 2014.

[38] H. M. E. C. Lucio Rizzuti, Solar Desalination for the 21st century, Springer, 2006.

[39] H. M. E. Hisham T. El-Dessouky, Fundamentals of Salt Water Desalination, Elsevier, 2002.

[40] D. K. Bhunya, "Simulation Study of Cryogenic Air Separation Unit Using Aspen Hysys At Rourkela Steel Plant," National Institute of Technology Rourkela.

[41] F. G. Kerry, Industrial Gas Handbook, CRC Press, 2007.

[42] N. Downie, Industrial Gases, Kluwer Academic Publisher, 2002.

[43] H.-W. Häring, Industrial Gases Processing, Wiley VCH, 2008.

[44] T. L. Group, "Air separation plants".

[45] W. F. Castle, "Air separation and liquefaction: recent developments and prospects for the beginning of the new millennium," *International Journal of Refrigeration,* pp. 158-172, 2002.

[46] M. Appl, Ammonia, Wiley VCH, 2006.

[47] D. J. a. Y. v. Delft, "Power to Ammonia," ECN, 2017.

[48] B. Leighty, "Alaska's Solid State Ammonia Synthesis Pilot Plant (SSAS-PP) Demonstration System for Renewable Energy (RE) Firming Storage, Transmission, and Export.," 2013.

[49] "How does the Haber process feed the world?," [Online]. Available: http://haber-boschprocess.blogspot.com/2013/03/what-is-haber-bosch-process.html.

[50] I. G. E. V. A. V. M. S. V. Kyriakou, "Progress in the Electrochemical Synthesis of Ammonia," *Catalysis Today,* pp. 2-13, 2017.

[51] P. A. Lynn, Onshore and Offshore Wind Energy, John Wiley & Sons Ltd, 2012.

[52] A. W. E. Association, "Basics of Wind Energy," [Online]. Available: https://www.awea.org/wind-101/basics-of-wind-energy.

[53] G. R. Energy, "What is wind energy?," [Online]. Available: https://www.ge.com/renewableenergy/wind-energy/what-is-wind-energy.

[54] L. S. o. E. a. P. Science, "What are the pros and cons of onshore wind energy?," 2018. [Online]. Available: http://www.lse.ac.uk/GranthamInstitute/faqs/what-are-the-pros-and-cons-of-onshore-wind-energy/.

[55] M. Arshad, "Clean and sustainable energy technologies," in *Clean Energy for Sustainable Development*, Academic Press, 2017, pp. 73-89.

[56] Engie, "Wind energy," [Online]. Available: https://www.engie.com/en/activities/renewable-energies/wind-energy.

[57] S. B. a. N. Hicks, "Onshore wind energy: what are the pros and cons?," 2012. [Online]. Available:

https://www.theguardian.com/environment/2012/sep/25/climate-change-windpower.

[58] S. Gamesa, "Onshore wind energy for a cleaner planet," [Online]. Available: https://www.siemensgamesa.com/products-and-services/onshore.

[59] Drawdown, "Onshore Wind Turbines," [Online]. Available: https://www.drawdown.org/solutions/onshore-wind-turbines.

[60] I. R. E. Agency, "Renewable Capacity Statistics 2019," 2019.

[61] R. C. B. W. B. W. J. A. S. Richard Turton, Analysis, Synthesis, and Design of Chemical Processes, Prentice Hall PTR, 2009.

[62] Y. F. a. G. P. Rangaiah, "Evaluating Capital Cost Estimating Programs," 2011.

[63] S. Jenkins, "2019 CHEMICAL ENGINEERING PLANT COST INDEX ANNUAL AVERAGE," Chemical Engineering, essential for the CPI professional , March 2020. [Online]. Available: https://www.chemengonline.com/2019-chemical-engineering-plant-cost-index-annual-average/.

[64] G. D. Ulrich, A Guide to Chemical Engineering Process Design and Economics, John Wiley and sons, 1984.

[65] S. S. Antonio Araujo, "Control structure design for the ammonia synthesis process," *Computers and Chemical Engineering,* pp. 2920-2932, 2008.

[66] R. E. B. ,. K. S. H. K. Ueno, "Compressor Efficiency Definitions," 2003.

[67] M. A. B. Y. A. Cengel, Thermodynamics: An Engineering Approach, 4th edition, McGraw Hill.

[68] D. F. Y. T. H. O. W. W. H. B. R. Munson, Fundamentals of Fluid Mechanics, 6th edition, John Wiley and Sons, 2009.

[69] "Compressor Calculations and Formulas," Lewis Systems and Service Company, [Online]. Available: https://www.lewissystemsinc.com/formulas/.

[70] Y. A. Cengel, Heat transfer: a practical approach, McGraw Hill, 2002.

[71] R. K. Sinnott, Chemical Engineering Design, 4th Edition, Elsevier Butterworth-Heinemann, 2005.

[72] Y. Lwin, "Chemical Equilibrium by Gibbs Energy," *Internation Journal of Engineering Education,* pp. 335-339, 2000.

[73] LibreTexts, "Equilibrium Results when Gibbs Energy is Minimized," 2019. [Online]. Available: https://chem.libretexts.org/Bookshelves/Physical_and_Theoretical_Chemistry_Textbook_Maps/Map%3A_Physical_Chemistry_(McQuarrie_and_Simon)/26%3A_Chemical_Equilibrium/26.01%3A_Equilibrium_Results_when_Gibbs_Energy_is_Minimized.

[74] W. R. P. J. R. F. S. M. W. James R. Couper, Chemical Process Equipment, Elsevier, 2005.

[75] A. P. A. P. C. E. J. V. S. L. J. M. H. M. v. S. Yasmina Bennani, "Power-to-Ammonia: Rethinking the role of ammonia – from a value product to a flexible energy carrier (FlexNH3)," Netherlands Enterprise Agency (RVO), 2016.

[76] M. N. S. a. M. E. Hady, "STORAGE TANKS - SELECTION OF TYPE, DESIGN CODE AND TANK SIZING," *The Transactions of Egyptians Society of Chemical Engineers,* vol. 30, pp. 201-225, 2004.

[77] B. G. Bob Long, Guide to Storage Tanks and Equipment, Wiley and Sons, 2004.

[78] V. Belapurkar, "Cheresources," [Online]. Available: https://www.cheresources.com/refnh3tanks.shtml.

[79] D. Webb, "LARGE SCALE AMMONIA STORAGE AND HANDLING," CF Industries.

[80] E. Koptyug, "Industrial electricity prices including tax in Germany 1998-2020," 2020. [Online]. Available: https://www.statista.com/statistics/1050448/industrial-electricity-prices-including-tax-germany/.

[81] eurostat, "Natural gas price statistics," 2020. [Online]. Available: https://ec.europa.eu/eurostat/statistics-explained/index.php/Natural_gas_price_statistics#Natural_gas_prices_for_non-household_consumers.

[82] J. Thurau, "Germany plans price hike for CO2 emissions," 2019. [Online]. Available: https://www.dw.com/en/germany-doubles-co2-emissions-pricing-cop25/a-51696203.

[83] K. K. a. T. P. Amit Garg, "IPCC Guidelines for National Greenhouse Gas Inventories," IPCC, 2006.

[84] C. M. Consultants, "Comparison of European Water Prices," Berlin, 2018.

[85] "Chemical Operator Salary," [Online]. Available: https://www.salaryexpert.com/salary/job/chemical-operator/germany.

[86] M. M. H. A. R. O. P. M. A. Armin Ebrahimi, "Energetic, exergetic and economic assessment of oxygen production from two columns cryogenic air separation unit," *Energy,* pp. 1298-1316, 2015.

[87] W. P. S. K. S. W. M. D. H. Castle-Smith, "Safe design and operation of a cryogenic air separation unit," *Process Safety Progress,* vol. 20, no. 4, pp. 269-279, 2004.

[88] T. L. Group, "Aluminium Plate-Fin Heat Exchangers".

[89] G. P. Christopher Haslego, "Compact heat exchangers - Part 1: Designing plate-and-frame heat exchangers," *Chemical Engineering Progress,* pp. 32-37, 2002.

[90] R. D. D. John C. Molburg, "Hydrogen from Steam-Methane Reforming with CO2 Capture," in *20th Annual International Pittsburgh Coal Conference*, Pittsburgh, USA, September 2003.

[91] N. R. E. Laboratory, "Equipment Design and Cost Estimation for Small Modular Biomass Systems, Synthesis Gas Cleanup, and Oxygen Separation Equipment," San Francisco, California, 2006.

[92] "Pipeline Basics & Specifics About Natural Gas Pipelines," Pipeline Safety Trust, 2015.

[93] E. S. Birkelund, "CO2 Absorption and Desorption Simulation with Aspen HYSYS," University of Tromso, 2013.

[94] J. Ivy, "Summary of Electrolytic Hydrogen Production," National Renewable Energy Laboratory, 2004.

[95] T. Ramsden, "Hydogen Production from Central Grid Electrolysis," National Renewable Energy Laboratory, 2005.

[96] G. S. a. T. Ramsden, "Wind Electrolysis: Hydrogen Cost Optimization," National Renewable Energy Laboratory, 2011.

[97] M. R. L. M. D. Bellotti, "Economic feasbility of menthanol synthesis as a method for CO2 reduction and energy storage," in *10th International Conference on Applied Energy*, 2018.

[98] W. C. J. M. G. S. T. R. Brian James, "PEM Electrolysis H2A Production Case Study Documentation," U.S. Department of Energy, 2013.

[99] S. S. V. J. H.-T. N. T. S. CHRISTOPH KOST, "LEVELIZED COST OF ELECTRICITY RENEWABLE ENERGY TECHNOLOGIES," FRAUNHOFER INSTITUTE FOR SOLAR

ENERGY SYSTEMS ISE, 2018.

[100] B. V. M. I. R. S. Kenneth Hansen, "Full energy system transition towards 100% renewable energy in Germany in 2050," *Renewable and Sustainable Energy Reviews,* pp. 1-13, 2019.

[101] V. D. P. S.A.Grigoriev, "Current status, research trends, and challenges in water electrolysis science and technology," *International Journal of hydrogen energy,* vol. 45, pp. 26036-26058, 2020.

[102] F. M. M. A.-F. M. S. J.C.M. Pires, "Recent developments on carbon capture and storage: An overview," *chemical engineering research and design,* pp. 1446-1460, 2011.

[103] L. S. C Egenhofer, "Compostion and Drives of Energy Prices and costs in Energy Intensive Industries: The Case of the Chemical Industry - Ammonia," Centre for European Policy Studies, 2014.

[104] J. A. M. Aikaterini Boulamanti, "Production costs of the chemical industry in the EU and other countries: Ammonia, methanol and light olefins," *Renewable and Sustainable Energy Reviews,* pp. 1205 - 1212, 2017.

[105] P. W. M. B. T. H. Alexander Tremel, "Techno-economic analysis for the synthesis of liquid and gaseous fuels based on hydrogen production via electrolysis," *International Journal of Hydrogen Energy,* pp. 11457-11464, 2015.